7/25/68

DEUTERON DISINTEGRATION BY PIONS, PHOTONS, AND NEUTRINOS BELOW 450 MeV

A THESIS

Presented to

The Faculty of the Graduate Division

by

William Michael Wynn

In Partial Fulfillment

of the Requirements for the Degree

Doctor of Philosophy in the School of Physics

Georgia Institute of Technology

April, 1971

DEUTERON DISINTEGRATION BY PIONS, PHOTONS,

AND NEUTRINOS BELOW 450 MeV

Approved:

Chairman

Date approved by Chairman: 4/15/72

Dedication

To Diane,

for the years

of patience and understanding

ACKNOWLEDGMENTS

I wish to express a special debt of gratitude to Dr. R. M. Ahrens for his guidance and patience in the preparation of this thesis. I also wish to thank Drs. H. R. Biritz and M. B. Sledd for their services as members of the reading committee. Finally, I would like to express my appreciation to Dr. C. P. Frahm for his influence, as both friend and tutor, during my graduate career.

TABLE OF CONTENTS

TABLE OF CONTENTS

TABLE OF CONTENTS (Concluded)

LIST OF TABLES

LIST OF TABLES (Concluded)

LIST OF ILLUSTRATIONS

LIST OF ILLUSTRATIONS (Continued)

Figure | Page

SUMMARY

Since the mid 1950's, increasing refinements in nucleon structure measurements, and the necessity of using deuterium as a source of target neutrons has caused an increasing interest in relativistic analyses of processes involving the deuteron. The most widely used technique in this area has been dispersion theory. The main purposes in this approach have been to obtain an accurate description of deuteron structure, as it appears in electron scattering and electro-disintegration, in order to allow an unambiguous determination of neutron form factors, and a significant amount of work has been done which seeks to describe other disintegration processes. Unfortunately because of the approximation techniques used, dispersion treatments of these processes have produced useful results only at low to moderate energies for the incident particle, and fail to account for a prominent peak in the total cross section for both pion and photon disintegration of the deuteron.

In 1955, Austern developed a simple heuristic model based on the assumed dominance of the $\Delta^{\frac{3}{2},\frac{3}{2}}$ nucleon resonance in pion and photon induced disintegration, and used the model to determine simple cross section ratios in the vicinity of the resonant peak. In 1966, Barshay gave a relativistic formulation of the Austern model which contained a cut-off parameter in the divergent closed-loop Feynman integral, chosen to fit the photodisintegration total cross section data in the vicinity of the resonant peak. He used the formalism to make a conjecture on the possibility of

failure of time reversal invariance in the process $\gamma + d \rightarrow n + p$. Neither Austern nor Barshay attempted to formulate a complete, relativistic expression for the deuteron disintegration cross section. Austern's analysis was nonrelativistic and neglected background terms. Barshay's treatment neglects background terms, and although he starts from a relativistic Feynman amplitude, his analysis is performed in terms of Pauli spin matrices.

The first systematic attempt to represent deuteron disintegration over a wide range of energies, including the resonance region, was made by George in 1967. George's treatment uses Barshay's relativistic formulation of the Austern model, modified by a Δ-N pion-exchange form factor developed by Ferrari and Selleri, improved values for the $\Delta\pi N$ and $\Delta\gamma N$ coupling constants, and a Δ propagator developed by Mohan and Agarwal. For the background terms, George introduces nucleon-pole and deuteron-pole amplitudes. The nucleon-pole amplitudes involve two vertex functions; the deuteron-two-nucleon (dNN) vertex function with one nucleon off the mass shell, and the $N\pi N$ or $N\gamma N$ vertex function with one nucleon off the mass shell. The deuteron-pole amplitude is pure isoscalar and thus appears only in photodisintegration. It also involves two vertex functions; the dNN vertex function with both nucleons on the mass shell and the deuteron off the mass shell, and the $d\gamma d$ vertex function with one deuteron off the mass shell.

In George's work, and in ours, it is assumed that the $N\gamma N$ and $N\pi N$ vertex functions do not deviate appreciably from their values with both nucleons on the mass shell. This is just the assumption that nucleon structure is not important at the energies we consider, other than that implied by the Austern model. Thus the $N\gamma N$ vertex is specified in terms of the Dirac and Pauli coupling constants, and the $N\pi N$ vertex in terms of the pion-nucleon coupling constant. The deuteron, however, is a very loosely bound structure on the energy scale considered, and it is expected that the dNN vertex function will be a very sensitive function of off-shell momenta.

In George's calculation, the simpler case of pion disintegration is considered first, both because the analysis is simpler, and because the experimental data is considerably better than that for photodisintegration. As mentioned above, only the nucleon-pole amplitudes occur in the background for this process. Since the dNN vertex function in these amplitudes involves one off-shell nucleon, its rigorous description requires the specification of four functions of the (invariant) square of the off-shell nucleon momentum, called "invariant" functions. In transition amplitudes, the contribution of two of these functions, H and I, relative to the contribution from the other two, F and G, vanishes in the limit that the off-shell nucleon approaches the mass shell. This does not mean that H and I vanish on the mass shell, just their relative importance in the transition amplitude. Indeed, we show in this work that H and I are both non-zero on the mass shell. In the following, we will designate the mass-shell limits of the vertex invariants by F_o, G_o, H_o, and I_o.

The mass-shell invariants F_o and G_o have been specified in terms of the physical parameters of the deuteron, including the binding energy, the asymptotic d-to-s admixture ratio ρ, and the triplet effective range r_e. The specification of the mass-shell invariants H_o and I_o constitutes one of the principal contributions of this work.

Having no means of specifying H and I, and not knowing the precise forms for G and F, George attempted to specify the dNN vertex function in terms of F_o and G_o, multiplied by a form factor introduced by Lebellac. The form factor corresponds to the assumption of a single simple Hulthén wave function to describe both the s- and d-state of the deuteron. With this background amplitude, George found that, if the physical values of F_o and G_o were used (corresponding to ρ = three percent), the background contribution to the pion disintegration total cross section completely obscures the resonant peak. George's approach was to modify F_o and G_o by making a parametric adjustment of ρ down to a value of 0.6 percent. With this value of ρ in the background amplitudes, and a cut-off parameter in the resonant amplitude close to the value found by Barshay, George succeeded in obtaining a reasonably good fit to both the total and differential pion disintegration cross sections.

With an adequate description of pion disintegration, George sought to use the same parameters in the nucleon-pole and resonance amplitudes in photodisintegration. As we have remarked previously, the isoscalar deuteron-pole amplitude involves both the $d\gamma d$ and dNN vertex functions with an off-shell deuteron. With the deuteron off-shell, these vertex functions are quite complex, and, in general, unknown. George's procedure was to evaluate these vertex functions with the deuteron on the mass shell, and to use the value ρ = .6 percent in this amplitude as well. There is really no reason to expect that this procedure adequately represents the deuteron-pole-term, and examination shows that the resulting cross sections deviate only a few percent from those obtained by neglecting the deuteron-pole amplitude altogether. Once the deuteron-pole vertex functions are restricted to the mass shell, some such procedure for damping the deuteron-pole amplitude must be adopted; otherwise, it leads to a divergent cross section at high energies. Using this technique, George purports to obtain a reasonably good fit to the photodisintegration total cross section, but with a severe lack of agreement with the differential cross section data.

When the present work was initiated, our purpose was twofold: first, the parametric adjustment of ρ to the extremely small value of 0.6 percent is unphysical. Estimates of ρ taken from deuteron magnetic moment measurements indicate that ρ is of the order of three or four percent, and the uncertainties in the data are not so large as to permit significant deviations below this value. We felt that the necessity of adjusting ρ to such a small value is symptomatic of large errors being introduced, either by neglecting H and I, or using incorrect forms for F and G, or both, and we sought a more physical method of treating the dNN vertex function. Second, we intended to use the pion and photodisintegration amplitudes obtained from George's model (with our more physical dNN vertex function) to construct the amplitudes and cross section for neutrino disintegration of the deuteron, and thus make a prediction for the contribution of the Δ resonance to this process. The connection between pion and photodisintegration and the weak process of neutrino disintegration is based on the conserved vector current (CVC) hypothesis directly relating first order electromagnetic processes to the weak vector amplitude for a similar process and the formal field-theoretic Partially-Conserved Axial-Vector Current (PCAC) hypothesis, indirectly relating pion processes to the weak axial-vector amplitude for a similar process. Remarkably, we have found that the execution of the second part of our program has a fundamental influence on the first, in that the PCAC hypothesis imposes a consistency condition on the dNN vertex function, which in turn, suggests a second condition on the vertex function which seems to be borne out by the limited experimental data.

The first step in our program was to repeat George's calculations for pion and photodisintegration, using his dNN vertex function, both to check his results, and to provide a check on the complicated algebraic manipulations and spin sums which must be performed. In pion disintegration, we found some minor algebraic errors in the resonant amplitude, which, when corrected, give a total cross section which is superior to George's published curve at high energies. In photodisintegration, the analysis of the resonant amplitude is far more complex than in pion disintegration. This is because the amplitude itself is more complex, and the algebraic reduction of the amplitude to standard form is very complex. In George's work, the reduction of this amplitude was done by means of a symbol manipulation program developed by Hearn. Lacking facilities to implement this program, we had hoped to use George's published amplitudes directly. However, when we attempted to reproduce George's published cross sections, we obtained results which were totally unreasonable. Consequently, we have performed the reduction of the photodisintegration resonant amplitude by means of a hand calculation, and the resulting invariant coefficients are markedly different from those published by George.

Having resolved George's calculational errors, we proceed to examine the dNN vertex function with one nucleon off the mass shell. The method we use here is based on a technique developed by Gross, which appears to have escaped the attention of other authors. Gross' technique is to develop an approximate Bethe-Salpeter amplitude for the deuteron, and to decompose this amplitude into two amplitudes, one of which reduces to the nonrelativistic deuteron wave function near the mass shell, the other being associated with antiparticle contributions to relativistic deuteron processes. The two amplitudes are expressible as combinations of the dNN vertex invariants F, G, H, and I, and these may be related to phenomenological deuteron s- and d-state wave functions, provided some means of estimating the antiparticle amplitude is available.

Gross' method for determining F, G, H, and I is to argue that the antiparticle amplitude may be made to vanish identically, provided that the non-relativistic deuteron wave function is expressed in terms of phenomenological s- and d-wave functions, since antiparticle contributions should already be incorporated by virtue of the fact that the wave functions are chosen to fit experimental data. This prescription leads to the requirement that one of the invariant functions, H, must vanish identically. Gross then indicates that this requirement is unphysical, since independent estimates indicate that H is non-zero.

We have followed the prescription outlined by Gross, but we have adopted a different, and we believe, a more fundamental method of treating the antiparticle amplitude. In our application of PCAC to neutrino disintegration of the deuteron, we obtain a consistency condition on the dNN vertex function, which requires that the mass-shell values of F and H be related by $F_o = 2H_o$. Returning to examine the antiparticle amplitude in the deuteron Bethe-Salpeter amplitude, we find that the lowest order term in this amplitude (in terms of $\vec{r}^2/m^2$ where $\vec{r}$ is the relative nucleon momentum) is $F_o - 2H_o - G_o + 2I_o$. In view of the relation between F_o and H_o, we are then lead to modify Gross' argument to the requirement that the antiparticle amplitude vanish in lowest order. We then obtain the symmetric relation $G_o = 2I_o$, and we do not have the inconsistent requirement that H vanish.

Comparing our vertex invariants to those obtained using Gross' procedure, we find that F and G are virtually the same, while H and I appear to be significantly different. However, it is known that, near the mass shell, F and G are related by $G \cong 25F$ (for a d-to-s ratio of three percent). As a consequence of this relation, our prescription for the invariants is quantitatively nearly the same as that given by Gross, and the two methods lead to predictions for cross sections which differ by no more than a few percent.

With a prescription relating the dNN vertex invariants to deuteron s- and d-state wave functions, we select phenomenological wave functions of the form given by Hulthén and Sugawara. With a cutoff parameter in the pion resonant amplitude corresponding to the value used by George, we construct the total and differential cross sections for pion disintegration, using phenomenological wave functions corresponding to d-to-s ratios of three, four, and five percent. Each of these gives cross sections which fit the experimental data as well or better than George's method, with the best result occuring for a d-to-s ratio of five percent.

Having obtained an excellent fit to the pion disintegration total and differential cross sections using the phenomenological method, we estimate the importance of the invariants H and I. If H is omitted, the resulting cross section differs by only a few percent. This is approximately the difference between Gross' identification procedure and ours. However, if I is omitted, the cross section changes quite significantly, indicating the importance of this invariant in the dNN vertex function, and suggesting that our relation $G_o = 2I_o$ is correct, since it produces agreement with experiment where any significantly different prescription will not.

With pion disintegration of the deuteron accounted for, we attempt to test the generality of our prescription for the dNN vertex function by applying it to photodisintegration. In doing so, we encounter significant difficulties. In photodisintegration, we encounter two additional amplitudes which are potentially important in the energy range below 450 MeV. The first of these is the deuteron-pole amplitude. This amplitude involves the dγd vertex function with an off-shell deuteron, and the dNN vertex function with an off-shell deuteron, neither of which is known. In the limit that the deuteron is on the mass shell, this amplitude can be constructed, and it is known to be unimportant at low energies. If the on-shell form is retained at higher energies, it leads to a divergent cross section. Consequently, it is clear that the above-mentioned vertex functions must contain momentum dependence which damps the deuteron-pole amplitude at higher energies. The second additional amplitude is the exchange-current amplitude, and corresponds to the coupling of the photon to a charged pion exchanged between the outgoing nucleons. This amplitude involves the dNN vertex function with both nucleons off the mass shell, as well as a closed momentum loop. Consequently, its analysis is quite difficult. In this work, we outline a method for calculating this amplitude, but we do not attempt to carry it through.

With essentially no knowledge of amplitudes whose relative importance is unknown, it seems questionable to attempt any quantitative calculations for photodisintegration. However, by calculating cross sections using only the nucleon-pole and resonance amplitudes, and using the pion disintegration parameters as a guide, we can at least get an idea as to the nature and magnitude of the contribution from these amplitudes. Using the parameters of pion disintegration, we find that George's prescription produces a total cross section which is much too low below the resonant peak. Then, using the phenomenological dNN vertex function, we find that d-to-s ratios of three, four, and five percent produce successively better estimates of the total cross section. In all of these calculations, it is found that the resonant mass must be adjusted to locate the peak properly (1190 MeV as compared to 1210 MeV for pion disintegration), and that the cross section is too large at the peak. Using a d-to-s ratio of five percent, we adjust the resonant width from the pion disintegration value of 120 MeV to 143 MeV, and obtain quite good agreement with the total cross section.

With the total cross section reproduced, we examine the differential cross section. We remark that, contrary to George's reported result, we find the differential cross section to be peaked at 90 degrees center-of-mass scattering angle, as originally reported by Austern. To describe our conclusions, we digress for a moment on the isospin structure of the photodisintegration amplitude. In first-order electromagnetic processes involving two nucleons, the amplitude may be decomposed into isoscalar and isovector parts. The isoscalar amplitude is symmetric and the isovector amplitude antisymmetric in the space and spin variables of the two nucleons. Consequently, either a pure isoscalar or a pure isovector amplitude will lead to a differential cross section which, for our process, is symmetric about 90 degrees center-of-mass scattering angle, and a mixed amplitude would be expected to show asymmetry in the center of mass system. For photodisintegration, the resonant amplitude is pure isovector, and the nucleon-pole amplitude is nearly pure isovector. Thus, as expected, our calculated differential cross sections are very nearly symmetric in the center-of-mass scattering angle. The experimental cross section, however, while symmetric near the resonant peak (the choice of a pure $I = \frac{3}{2}$ Δ resonance model is based on this fact), shows a significant asymmetry both below and above the peak. Thus, while the omitted amplitudes appear to have little influence on the total cross section, they are obviously important for a correct differential cross section. Significant in this connection is the fact that the deuteron-pole amplitude is pure isoscalar.

With photodisintegration described as well as our model permits, we next consider the problem of neutrino disintegration of the deuteron. Using the CVC hypothesis, the weak vector amplitude is obtained directly from the isovector part of the photodisintegration amplitude. Since we consider only the neutrino disintegration cross section integrated over outgoing nucleon moments, the deficiency in the photodisintegration differential cross section should not be important, but this is not an important point as we will find that the weak vector amplitude does not contribute significantly to the process we consider: $\nu + d \rightarrow \ell + p + p$ with a forward-scattered lepton.

We construct the weak axial-vector amplitude using the PCAC hypothesis in a technique suggested by Adler. The PCAC hypothesis states that for momentum transfers satisfying $m_\pi^2 \geqq q^2 \geqq -m_\pi^2$, the divergence of the axial-vector current is proportional to the pion field. This may be used in an indirect fashion to relate the weak axial-vector amplitude to the amplitude for pion disintegration, which we have successfully described with a presumably physically correct model for the dNN vertex function. In applying PCAC to neutrino disintegration, it is found that a consistency condition occurs which requires that a linear combination of F_o, H_o, and the zero-momentum limit of the non-pole part of the pion disintegration amplitude vanish. We assume that the Austern model resonant amplitude, extrapolated off the pion mass shell, correctly describes the non-pole part of the pion disintegration amplitude in the zero-momentum limit, and we find that this amplitude vanishes. This leaves the consistency condition $F_o = 2H_o$, which was discussed above.

Having constructed the neutrino disintegration amplitude, we construct the cross section for forward scattering of the outgoing lepton, differential in lepton energy, and integrated over outgoing nucleon moments. The kinematical restrictions our theory places on the process limit us to neutrino energies above 600 MeV and energy transfers in the range 0-450 MeV. This general type of process (where a general hadronic system replaces the two outgoing nucleons) has been considered by Adler. He has shown that, if the mass of the outgoing lepton is negligible, then the cross section is proportional to the square of the matrix element of the divergence of the weak current. Consequently, if the vector current is conserved (which we assume) then the vector contribution vanishes, and the cross section depends only on the divergence of the axial-vector current.

In our process, the minimum outgoing lepton total energy is 150 MeV. Thus, if the outgoing lepton is an electron (m_e = 105.7 MeV) the rest energy is a significant fraction of the total energy, and the importance of the vector current must be determined directly. We have calculated the cross section for neutrino energies of 600, 800, 1000 MeV and 3, 6, and 10 BeV for both outgoing electron and muon. As expected, the vector contribution with an outgoing electron is vanishingly small, and surprisingly, the vector contribution with an outgoing muon does not exceed a few percent of the axial-vector cross section at 600 MeV, diminishing in importance at higher energies.

The cross section we obtain depends importantly only on the axial vector current. It is not clear that, for an outgoing muon, it depends only on the divergence of the axial-vector current, as would be expected for a zero-mass lepton, from Adler's theorem. All we can conclude here is that the vector part is unimportant. Since the calculation of the axial-vector amplitude is based on the successful treatment of pion disintegration, the rather well established CVC hypothesis, and the less well-established PCAC hypothesis, it is clear that it should provide a test of PCAC (this has already been pointed out by Adler in connection with the general process). We find that the calculated cross section displays a characteristic resonant peak which becomes more pronounced at higher neutrino energies, and thus provides a sharp characteristic to be sought for experimentally. However, experimental data for this process are not yet available. Even for total cross sections for neutrino processes, available neutrino beam intensities and the weakness of the process combine to allow only very crude experimental data, and the refinements necessary for measurements differential in both lepton energy and direction are in the future.

CHAPTER I

INTRODUCTION

In this work we examine strong, electromagnetic, and weak deuteron disintegration processes for energy transfers in the range 0 MeV to 450 MeV. The methods of nonrelativistic Schrodinger theory and relativistic dispersion theory, successful below 150 MeV, are not applicable in the energy region under consideration, and we use a variety of techniques, including the Austern Model,[1,2] the relativistic perturbation approach used by George,[3] and the phenomenological representation of deuteron structure given by Gross,[4] as well as the Conserved Vector Current (CVC) hypothesis,[5,25] and the Partially-Conserved Axial-Vector Current (PCAC) hypothesis.[6,7,8,9]

General Features of Deuteron Disintegration

We begin by examining the general deuteron disintegration process depicted in Figure 1. Throughout this work we will use the notation and conventions of Bjorken and Drell,[10] as well as their Feynman rules for the construction of perturbation theory amplitudes.

Pion Probe

For an incoming pion, the disintegration amplitude takes the form

$$T = g_{N\pi} \chi\, U^{\mu}\, \bar{u}(p_1)\, M_{\mu}\, C\, \bar{u}^{T}(p_2)\,. \tag{I-1}$$

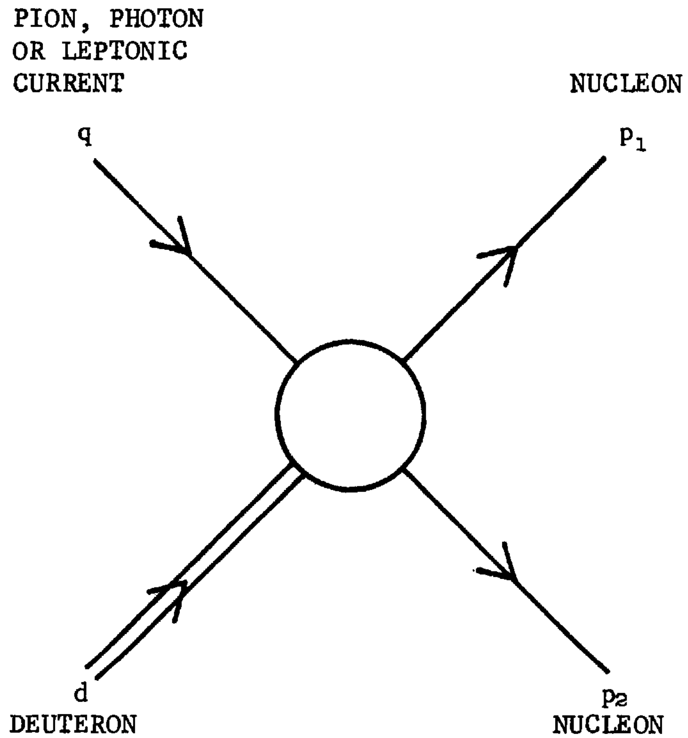

Figure 1. General Deuteron Disintegration Process

Here, $g_{N\pi}$ is the pion-nucleon ($\pi^o p$) coupling constant whose value is given by $g_{N\pi}^2/4\pi \cong 14.6$. χ is a pseudoscalar phase factor included to reflect the pseudoscalar character of the pion. U is the deuteron polarization vector with the properties[11]

$$U^2 = -1 \,, \tag{I-2}$$

$$\sum_{\lambda} U_\alpha(d,\lambda)\, U_\beta(d,\lambda) = -g_{\alpha\beta} + \frac{d_\alpha d_\beta}{M_d^2} \,, \tag{I-3}$$

and

$$U \cdot d = 0 \,, \tag{I-4}$$

where a given polarization state is labeled by λ, d is the deuteron four-momentum, and M_d is the deuteron mass. $u(p_1)$ and $u(p_2)$ are the Dirac polarization spinors of the outgoing nucleons, C is the charge-conjugation matrix $i\gamma_2\gamma_o$, and M_β is a 4×4 matrix containing the dynamical details of the disintegration process. The superscript T denotes matrix transposition.

The matrix M_β can depend only on the independent momenta associated with the disintegration process, or the Dirac gamma matrices. To determine the possible forms composing M_β we note that parity invariance of the strong interaction requires that $U^\beta M_\beta$ combine with χ to form a Lorentz scalar. Consequently, M_β must transform like a Lorentz axial vector. This implies that M_β is formed from all independent Lorentz four-vectors that can be constructed from the momenta and the gamma matrices, and each such term is multiplied by the factor $\gamma_5 = i\gamma_o\gamma_1\gamma_2\gamma_3$. There is a number of conditions which limit the number of independent terms from which M_β

may be constructed. First, momentum conservation implies that only three of the momenta are independent. For these, we choose the combinations

$$q \;,\; k = \frac{P_1 - P_2}{2} \quad \text{and} \quad Q = \frac{P_1 + P_2}{2} \tag{I-5}$$

Second, equation (I-4), together with momentum conservation, implies that $U \cdot q = 2U \cdot Q$, and we will delete Q_β from the possible forms. Finally, the Dirac equation $(\not{p} - m)\, u\,(p) = 0$ may be used to reduce factors of $\not{Q}$ and $\not{k}$ to constants, and the relation $\not{q}\not{q} = q^2$, and the anticommutation relation for the gamma matrices may be used to limit M_β to terms linear in $\not{q}$. With these considerations, the possible forms composing M_β are

$$\gamma_5 q_\beta,\ \gamma_5 k_\beta,\ \gamma_5 \gamma_\beta,\ \gamma_5 \not{q} q_\beta,\ \gamma_5 \not{q} k_\beta,\ \text{and}\ \gamma_5 \not{q} \gamma_\beta\ .$$

In the following we will use the normalized combination[3] given in Table 1. The variable ϵ_i gives the symmetry of the quantities $\bar{u}(P_1)\, I^{\pi}_{i\beta}\, C\, \bar{u}^T\,(P_2)$ under interchange of the outgoing nucleons, and will be important in subsequent analysis.

Electromagnetic and Weak Probe

The electromagnetic and weak disintegration amplitudes have the form

$$T = \mathcal{B}\, W^\alpha U^\beta\, \bar{u}(P_1)\, M_{\alpha\beta}\, C\, \bar{u}^T(P_2)\,. \tag{I-6}$$

For photodisintegration, $W^\alpha = \epsilon^\alpha$, the photon polarization vector, and $\mathcal{B} = e$, the electronic charge, whose value is given by $e^2/4\pi = 1/137$. For weak disintegration, in particular neutrino disintegration with an out-

Table 1. Invariant Amplitudes in Pion Disintegration

i	$I^{\pi}_{i\beta}$	ϵ_i
1	$(1/2m)\,\gamma_5\, q_\beta$	-
2	$(1/m)\,\gamma_5\, k_\beta$	+
3	$\gamma_5\,\gamma_\beta$	-
4	$(1/2m)\,\gamma_5\,[\not{q}, \gamma_\beta]$	+
5	$(1/2m^2)\,\gamma_5\,\not{q}\, q_\beta$	-
6	$(1/m^2)\,\gamma_5\,\not{q}\, k_\beta$	+

going muon, $W^{\alpha} = \mathcal{L}^{\alpha} = \bar{u}(\nu)\gamma^{\alpha}(1 - \gamma_5)u(\mu)$ and $\mathcal{G} = G/\sqrt{2}$ where $G = 1.015 \times 10^{-5}$ in units of the squared nucleon Compton wavelength.

The amplitude T transforms as a Lorentz scalar in the case of photodisintegration, and as a combination of Lorentz scalar and pseudoscalar in neutrino disintegration. Consequently $M_{\alpha\beta}$ will be composed of Lorentz tensors or pseudotensors constructed from the momenta listed in equation (I-5), and the Dirac gamma matrices. The pseudotensor forms may be constructed from the tensor forms by multiplying by γ_5. In Table 2 we give a preliminary list of the 52 possible amplitudes which may be constructed by imposing the restrictions given in the discussion of pion disintegration. Some of these amplitudes do not have definite symmetry under interchange of the nucleons, but this will be remedied in subsequent specialized discussion.

Photodisintegration. Imposing the Lorentz condition $\epsilon^{\alpha} q_{\alpha} = 0$, we can eliminate entries containing q_{α} from Table 2. The remaining amplitudes are then combined to give amplitudes of definite symmetry, which are listed in Table 3. The amplitudes in Table 3 correspond to those given by Lebellac, et al.[12], except for over-all sign. In the last entry, $\epsilon^{\mu\nu\rho\sigma}$ is the completely antisymmetric tensor whose value is + 1 if $\mu\nu\rho\sigma$ is an even permutation of 0123, - 1 for an odd permutation, and zero otherwise. The relation between N_{20} and terms of the form given in Table 2 is easily shown to be given by

$$i\gamma_5 \epsilon^{\mu\nu\rho\sigma} g_{\mu\alpha} g_{\nu\beta} \gamma_{\rho} q_{\sigma} = \gamma_{\alpha}\gamma_{\beta}\not{q} + q_{\alpha}\gamma_{\beta} - \gamma_{\alpha} q_{\beta} - g_{\alpha\beta}\not{q} . \qquad \text{(I-7)}$$

The amplitudes given in Table 3 are not the simplest set for

Table 2. Simple Tensor and Pseudotensor Amplitudes

i	$A_{i\alpha\beta}$	i	$A_{i\alpha\beta}$
1	$(\gamma_5)\ g_{\alpha\beta}$	14	$(\gamma_5)\ K_\alpha K_\beta \not q$
2	$(\gamma_5)\ K_\alpha q_\beta$	15	$(\gamma_5)\ \gamma_\alpha q_\beta \not q$
3	$(\gamma_5)\ Q_\alpha q_\beta$	16	$(\gamma_5)\ \gamma_\alpha K_\beta \not q$
4	$(\gamma_5)\ K_\alpha K_\beta$	17	$(\gamma_5)\ K_\alpha \gamma_\beta \not q$
5	$(\gamma_5)\ Q_\alpha K_\beta$	18	$(\gamma_5)\ Q_\alpha \gamma_\beta \not q$
6	$(\gamma_5)\ K_\alpha \gamma_\beta$	19	$(\gamma_5)\ \gamma_\alpha \gamma_\beta$
7	$(\gamma_5)\ Q_\alpha \gamma_\beta$	20	$(\gamma_5)\ \gamma_\alpha \gamma_\beta \not q$
8	$(\gamma_5)\ g_{\alpha\beta} \not q$	21	$(\gamma_5)\ q_\alpha q_\beta$
9	$(\gamma_5)\ \gamma_\alpha q_\beta$	22	$(\gamma_5)\ q_\alpha K_\beta$
10	$(\gamma_5)\ Q_\alpha q_\beta \not q$	23	$(\gamma_5)\ q_\alpha \gamma_\beta$
11	$(\gamma_5)\ K_\alpha q_\beta \not q$	24	$(\gamma_5)\ q_\alpha q_\beta \not q$
12	$(\gamma_5)\ \gamma_\alpha K_\beta$	25	$(\gamma_5)\ q_\alpha K_\beta \not q$
13	$(\gamma_5)\ Q_\alpha K_\beta \not q$	26	$(\gamma_5)\ q_\alpha \gamma_\beta \not q$

Table 3. Basic Amplitudes for Photodisintegration

i	$N_{i\,\alpha\beta}$	ε_i
1	$g_{\alpha\beta}$	-
2	$k_\alpha q_\beta$	+
3	$Q_\alpha q_\beta$	-
4	$k_\alpha k_\beta$	-
5	$Q_\alpha k_\beta$	+
6	$k_\alpha \gamma_\beta$	-
7	$Q_\alpha \gamma_\beta$	+
8	$g_{\alpha\beta} \not{q}$	+
9	$\gamma_\alpha q_\beta$	+
10	$Q_\alpha q_\beta \not{q}$	+
11	$k_\alpha q_\beta \not{q}$	-
12	$\gamma_\alpha k_\beta$	-
13	$Q_\alpha k_\beta \not{q}$	-
14	$k_\alpha k_\beta \not{q}$	+
15	$[\not{q}, \gamma_\alpha] q_\beta$	+
16	$[\not{q}, \gamma_\alpha] k_\beta$	-
17	$[\not{q}, \gamma_\beta] k_\alpha$	-
18	$[\not{q}, \gamma_\beta] Q_\alpha$	+
19	$[\gamma_\alpha, \gamma_\beta]$	+
20	$i \gamma_5 \epsilon^{\mu\nu\rho\sigma} g_{\mu\alpha} g_{\nu\beta} \gamma_\rho q_\sigma$	-

photodisintegration. Sakita[13] has shown that the N_i satisfy two complicated internal constraints, and, imposing the requirement of gauge invariance,

$$q^{\alpha} M_{\alpha\beta} = 0 \tag{I-8}$$

leads to six additional constraints, leaving only twelve independent amplitudes. These amplitudes are listed in Table 4.

Neutrino disintegration. In the case of weak disintegration of the deuteron, the variable q is given by $q = p_\nu - p_\mu$, and $M_{\alpha\beta}$ is composed of two parts:

$$M_{\alpha\beta} = M^{V}_{\alpha\beta} + M^{A}_{\alpha\beta} \tag{I-9}$$

where the superscripts V and A refer to the Lorentz vector (V) and axial-vector (A) parts of $U^{\beta} M_{\alpha\beta}$. The composition of the vector part $M^{V}_{\alpha\beta}$ follows directly from the CVC hypothesis, and consists of the gauge invariant amplitudes listed in Table 4. The composition of $M^{A}_{\alpha\beta}$ is considerably more complicated, and in this work, we will use combinations of the amplitudes listed in Table 1 having definite exchange symmetry. These are listed in Table 5.

Invariant Coefficients

The previous discussion establishes the basic Lorentz invariant amplitudes that we will use to construct the transition amplitudes for the various disintegration processes. The transition amplitudes are obtained as linear combinations of these invariant amplitudes with invariant coefficients which are functions of the independent Lorentz scalars which

Table 4. Normalized Gauge-Invariant Amplitudes for Photodisintegration

i	$I^{r}_{i\alpha\beta}$	ε_i
1	$(1/2m^2)\,(k_\alpha q_\beta - g_{\alpha\beta}\, q\cdot k)$	+
2	$(1/2m^2)\,(g_{\alpha\beta}\, q\cdot Q - Q_\alpha q_\beta)$	-
3	$(1/m^4)\,(k_\alpha\, q\cdot Q - Q_\alpha\, q\cdot k)\, k_\beta$	-
4	$(1/m^3)\,(k_\alpha\, q\cdot Q - Q_\alpha\, q\cdot k)\, \gamma_\beta$	-
5	$(1/2m)\,(g_{\alpha\beta}\, \not{q} - \gamma_\alpha q_\beta)$	+
6	$(1/2m^3)\left[(Q_\alpha \not{q} - q\cdot Q\, \gamma_\alpha) q_\beta - 2\,(k_\alpha \not{q} - q\cdot k\, \gamma_\alpha)\, k_\beta\right]$	+
7	$(1/2m^3)\left[(k_\alpha \not{q} - q\cdot k\, \gamma_\alpha) q_\beta + 2\,(Q_\alpha \not{q} - q\cdot Q\, \gamma_\alpha)\, k_\beta\right]$	-
8	$(1/4m^2)\,[\gamma_\alpha, \not{q}]\, q_\beta$	+
9	$(1/2m^2)\,[\gamma_\alpha, \not{q}]\, k_\beta$	-
10	$(1/2m^2)\left\{[\gamma_\beta, \gamma_\alpha]\, q\cdot k - [\gamma_\beta, \not{q}]\, k_\alpha + 2\,(Q_\alpha q_\beta - g_{\alpha\beta}\, q\cdot Q)\right\}$	-
11	$(1/2m^2)\left\{[\gamma_\beta, \gamma_\alpha]\, q\cdot Q - [\gamma_\beta, \not{q}]\, Q_\alpha + 2\,(k_\alpha q_\beta - g_{\alpha\beta}\, q\cdot k)\right\}$	+
12	$(i/2m)\, \gamma_5\, \epsilon^{\mu\nu\rho\sigma}\, \gamma_\rho\, g_{\mu\alpha}\, g_{\nu\beta}\, q_\sigma$	-

Table 5. Basic Axial-Vector Amplitudes

i	$I^{A}_{i\alpha\beta}$	ε_i	i	$I^{A}_{i\alpha\beta}$	ε_i
1	$\gamma_5\, g_{\alpha\beta}$	-	14	$\gamma_5\, K_\alpha K_\beta \not{q}$	-
2	$\gamma_5\, K_\alpha q_\beta$	+	15	$\gamma_5\, [\gamma_\alpha, \not{q}]\, q_\beta$	+
3	$\gamma_5\, Q_\alpha q_\beta$	-	16	$\gamma_5\, [\gamma_\alpha, \not{q}]\, K_\beta$	-
4	$\gamma_5\, K_\alpha K_\beta$	-	17	$\gamma_5\, [\gamma_\beta, \not{q}]\, K_\alpha$	-
5	$\gamma_5\, Q_\alpha K_\beta$	+	18	$\gamma_5\, [\gamma_\beta, \not{q}]\, Q_\alpha$	+
6	$\gamma_5\, K_\alpha \gamma_\beta$	+	19	$\gamma_5\, [\gamma_\alpha, \gamma_\beta]$	+
7	$\gamma_5\, Q_\alpha \gamma_\beta$	-	20	$i\, \epsilon^{\mu\nu\rho\sigma} \gamma_\rho\, g_{\mu\alpha}\, g_{\nu\beta}\, q_\sigma$	+
8	$\gamma_5\, g_{\alpha\beta} \not{q}$	-	21	$\gamma_5\, q_\alpha q_\beta$	-
9	$\gamma_5\, \gamma_\alpha q_\beta$	-	22	$\gamma_5\, q_\alpha K_\beta$	+
10	$\gamma_5\, Q_\alpha q_\beta \not{q}$	-	23	$\gamma_5\, q_\alpha \gamma_\beta$	-
11	$\gamma_5\, K_\alpha q_\beta \not{q}$	+	24	$\gamma_5\, q_\alpha q_\beta \not{q}$	-
12	$\gamma_5\, \gamma_\alpha K_\beta$	+	25	$\gamma_5\, q_\alpha K_\beta \not{q}$	+
13	$\gamma_5\, Q_\alpha K_\beta \not{q}$	+	26	$\gamma_5\, [\gamma_\beta, \not{q}]\, q_\alpha$	+

can be formed from the associated momenta. There are three such scalars and we will use the Mandelstam variables

$$s = (p_1 + p_2)^2 , \tag{I-10}$$

$$t = (p_1 - q)^2 = (d - p_2)^2 ,$$

and $$u = (p_2 - q)^2 = (d - p_1)^2 .$$

These variables satisfy the relation

$$s + t + u = 2m^2 + M_d^2 + q^2 . \tag{I-11}$$

This means that they are independent only for the case of neutrino disintegration where q^2 is not fixed. In photodisintegration $q^2 = 0$ and in pion disintegration $q^2 = m_\pi^2$.

We will work principally in the center-of-mass frame of the outgoing nucleons. In this frame we introduce the variables E and $\vec{p}$ via

$$p_1 = (E, \vec{p}) \quad , \quad p_2 = (E, -\vec{p}) , \tag{I-12}$$

and hence $$Q = (E, \vec{0}) \qquad \text{and} \qquad K = (0, \vec{p}) .$$

In this reference frame we have $\vec{q} + \vec{d} = \vec{p}_1 + \vec{p}_2 = 0$ and, the Mandelstam variables are

$$s = 4E^2 ,$$

$$t = M_d^2 + m^2 - 2(d^0 E - \vec{q} \cdot \vec{p}) , \tag{I-13}$$

$$u = M_d^2 + m^2 - 2\,(d^0 E + \vec{q}\cdot\vec{P}),$$

Returning to the transition amplitudes, we have

$$T^{\pi} = g_{N\pi}\, U^{\beta} \sum_{\lambda=1}^{6} \bar{u}(P_2) C_{\lambda}^{\pi}(s,t,u)\, I_{\lambda\beta}^{\pi}\, C\, \bar{u}^{T}(P_1)\,, \tag{I-14}$$

$$T^{\gamma} = e\, \epsilon^{\alpha} U^{\beta} \sum_{\lambda=1}^{12} \bar{u}(P_2) C_{\lambda}^{\gamma}(s,t,u)\, I_{\lambda\alpha\beta}^{\gamma}\, C\, \bar{u}^{T}(P_1)\,, \tag{I-15}$$

$$T^{V} = \frac{G}{\sqrt{2}}\, \ell^{\alpha} U^{\beta} \sum_{\lambda=1}^{12} \bar{u}(P_1) C^{V}(s,t,u)\, I_{\lambda\alpha\beta}^{\gamma}\, C\, \bar{u}^{T}(P_2)\,, \tag{I-16}$$

$$T^{A} = \frac{G}{\sqrt{2}}\, \ell^{\alpha} U^{\beta} \sum_{\lambda=1}^{26} \bar{u}(P_1) C^{A}(s,t,u)\, I_{\lambda\alpha\beta}^{A}\, C\, \bar{u}^{T}(P_2)\,. \tag{I-17}$$

These are not the final forms for the transition amplitudes as we have yet to consider exchange of the final-state nucleons.

The Generalized Pauli Principle

A well-known property of systems of identical Fermions is the Pauli principle, which requires that the state vector of the system be antisymmetric under the interchange of space and spin coordinates of any two particles in the system. This same antisymmetric behavior applies to the transition amplitude for a process in which identical fermions appear in the final state.

Evidence from nucleon scattering indicates that the strong interaction does not distinguish between neutrons and protons, and it is believed that the small neutron-proton mass difference arises from the electromagnetic interaction. From quantum electrodynamics, it is known that perturbation theory corrections to particle masses occur in second and higher order only, and this implies that the strong interaction symmetry between neutron and proton is not disturbed by first order electromagnetic interaction. Since the deuteron disintegration process involves the strong interaction, a theory which involves the electromagnetic interaction to no higher than first order, and consequently neglects the small neutron-proton mass difference, should reflect the neutron-proton symmetry characteristic of the strong interaction. Following Heisenberg[16], we associate with the neutron and proton internal variables I, I_3, the total and third component of isospin. The formalism for these variables is identical to that for spin angular momentum, and the specific assignments for proton and neutron, with space and spin variables suppressed, is

$$|p\rangle = |\tfrac{1}{2}\,\tfrac{1}{2}\rangle \qquad \text{and} \qquad |n\rangle = |\tfrac{1}{2}\,-\tfrac{1}{2}\rangle \tag{I-18}$$

Nucleon Pair States. We introduce the neutron-proton symmetry into deuteron disintegration by requiring that the nucleon final states, and consequently the transition amplitudes, satisfy the generalized Pauli principle, i.e., they are antisymmetric under interchange of space, spin, and isospin variables of the final state nucleons. Pair states which satisfy this requirement for the three possible final states are

$$|pp\rangle = \left(\frac{|\alpha(1)\alpha'(2)\rangle - |\alpha'(1)\alpha(2)\rangle}{\sqrt{2}}\right)|\tfrac{1}{2}\,\tfrac{1}{2}\rangle|\tfrac{1}{2}\,\tfrac{1}{2}\rangle\,, \tag{I-19}$$

$$|nn\rangle = \left(\frac{|\beta(1)\beta'(2)\rangle - |\beta'(1)\beta(2)\rangle}{\sqrt{2}}\right)|\tfrac{1}{2}\,-\tfrac{1}{2}\rangle|\tfrac{1}{2}\,-\tfrac{1}{2}\rangle\,, \tag{I-20}$$

$$|np\rangle = \frac{|\alpha(1)\beta(2)\rangle|\tfrac{1}{2}\,\tfrac{1}{2}\rangle|\tfrac{1}{2}\,-\tfrac{1}{2}\rangle - |\beta(1)\alpha(2)\rangle|\tfrac{1}{2}\,-\tfrac{1}{2}\rangle|\tfrac{1}{2}\,\tfrac{1}{2}\rangle}{\sqrt{2}}\,, \tag{I-21}$$

where α and β refer to the space and spin variables of proton and neutron, respectively. The last equation can be written more usefully as

$$|np\rangle = \frac{1}{\sqrt{2}}\left(\frac{|\alpha(1)\beta(2)\rangle - |\beta(1)\alpha(2)\rangle}{\sqrt{2}}\right)\left(\frac{|\tfrac{1}{2}\tfrac{1}{2}\rangle|\tfrac{1}{2}\,\text{-}\tfrac{1}{2}\rangle + |\tfrac{1}{2}\,\text{-}\tfrac{1}{2}\rangle|\tfrac{1}{2}\tfrac{1}{2}\rangle}{\sqrt{2}}\right) \quad \text{(I-22)}$$

$$+ \frac{1}{\sqrt{2}}\left(\frac{|\alpha(1)\beta(2)\rangle + |\beta(1)\alpha(2)\rangle}{\sqrt{2}}\right)\left(\frac{|\tfrac{1}{2}\tfrac{1}{2}\rangle|\tfrac{1}{2}\,\text{-}\tfrac{1}{2}\rangle - |\tfrac{1}{2}\,\text{-}\tfrac{1}{2}\rangle|\tfrac{1}{2}\tfrac{1}{2}\rangle}{\sqrt{2}}\right).$$

Introducing A and S for antisymmetric and symmetric space and spin dependence, and using the standard rules of angular momentum addition, we can express the pair states in terms of I = 0 and I = 1 states as

$$|pp\rangle = |A_{pp}\,1\,1\rangle\,, \quad \text{(I-23)}$$

$$|nn\rangle = |A_{nn}\,1\,\text{-}1\rangle\,, \quad \text{(I-24)}$$

and

$$|np\rangle = \frac{1}{\sqrt{2}}|A_{np}\,1\,0\rangle + \frac{1}{\sqrt{2}}|S_{np}\,0\,0\rangle\,. \quad \text{(I-25)}$$

Finally, we determine the isospin structure of the deuteron state by noting that it is a mixture of s and d states, hence symmetric in space, it has spin 1, and is thus symmetric in spin, and consequently the generalized Pauli principle requires that it be antisymmetric in isospin. Thus,

$$|d\rangle = |S_d\,0\,0\rangle \quad \text{(I-26)}$$

<u>Transition Amplitudes</u>. We have not explicitly considered the iso-

spin structure of the transition amplitudes, but this is easily accomplished, given the pair state structure in equations (I-23) and (I-25). The amplitudes for pion and neutrino disintegration are antisymmetric in space and spin variables of the outgoing nucleon and hence pure isovector amplitudes. The proper forms for these amplitudes are given by

$$T^{\pi} = g_{N\pi} U^{\beta} \sum_{i=1}^{6} \left[C_i^{\pi}(s,t,u) - \epsilon_i C_i^{\pi}(s,u,t) \right] \bar{u}(P_1) I_{i\beta}^{\pi} C \bar{u}^{T}(P_2), \quad \text{(I-27)}$$

$$T^{V} = \frac{G}{\sqrt{2}} \mathcal{I}^{\alpha} U^{\beta} \sum_{i=1}^{12} \left[C_i^{V}(s,t,u) - \epsilon_i C_i^{V}(s,u,t) \right] \bar{u}(P_1) I_{i\alpha\beta}^{r} C \bar{u}^{T}(P_2), \quad \text{(I-28)}$$

and

$$T^{A} = \frac{G}{\sqrt{2}} \mathcal{I}^{\alpha} U^{\beta} \sum_{i=1}^{26} \left[C_i^{A}(s,t,u) - \epsilon_i C_i^{A}(s,u,t) \right] \bar{u}(P_1) I_{i\alpha\beta}^{A} C \bar{u}^{T}(P_2). \quad \text{(I-29)}$$

The photodisintegration amplitude given in equation (I-15) satisfies the generalized Pauli principle if it is constructed consistent with the neglect of higher order electromagnetic corrections, but this is not obvious from its form. To display the symmetry properties of this amplitude we write it by analogy with the np state in equation (I-25) in the form

$$T^{\gamma} = \frac{1}{2}\left(T^{\gamma} + T^{\gamma'}\right) + \frac{1}{2}\left(T^{\gamma} - T^{\gamma'}\right) = T_S^{\gamma} + T_V^{\gamma} , \quad \text{(I-30)}$$

where $T^{\gamma'}$ differs from T^{γ} in the interchange of the space and spin variables of the final state nucleons, and the subscripts S and V refer to isoscalar and isovector parts of the amplitude, respectively. Explicitly, we have

$$T_s^{\gamma} = e\epsilon^{\alpha} U^{\beta} \sum_{i=1}^{12} \left[\frac{\mathcal{C}_i^{\gamma}(s,t,u) + \varepsilon_i \mathcal{C}_i^{\gamma}(s,u,t)}{2} \right] \bar{u}(P_1)\, I^{\gamma}_{i\,\alpha\beta} C \bar{u}^T(P_2), \quad \text{(I-31)}$$

and

$$T_V^{\gamma} = e\epsilon^{\alpha} U^{\beta} \sum_{i=1} \left[\frac{\mathcal{C}_i^{\gamma}(s,t,u) - \varepsilon_i \mathcal{C}_i^{\gamma}(s,u,t)}{2} \right] \bar{u}(P_1)\, I^{\gamma}_{i\,\alpha\beta} C \bar{u}^T(P_2). \quad \text{(I-32)}$$

The remainder of this work is concerned with the explicit construction of the invariant coefficients $\mathcal{C}_i$ for the three deuteron disintegration processes, by means of the techniques outlined in the next chapter.

CHAPTER II

METHOD

A well known feature of deuteron disintegration in the energy range 0-450 MeV is the appearance of a large peak in the total cross section, indicative of the formation of a resonant structure. In 1955, Austern[1] suggested a simple model for the description of this resonance, assuming it to arise from the formation of the $\Delta^{\frac{3}{2},\frac{3}{2}}$ nucleon resonance. A diagrammatic representation of the Austern model is given in Figure 2. In 1966, Barshay[2] gave a relativistic formulation of the Austern model, but both he and Austern confined their attention to the immediate neighborhood of the peak in the total cross section, where the background and resonant amplitudes decouple to allow a direct subtraction of the background cross section, and consequently to allow the determination of a cutoff parameter occuring in the resonant amplitude. In 1967, George[3,14] made a systematic attempt explicitly to account for the background in pion disintegration and photodisintegration of the deuteron and to account for the resonant structure using a modified version of the Austern model. His assumption was that, in the region about the resonant peak, the only important contributions to the transition amplitude are the dominant Austern model resonance, and the lowest order perturbation theory background diagrams. The latter are variously called Born terms or pole terms. Strictly, the phrase "Born term" implies structureless particles, and since deuteron structure is important in the analysis to follow, we will use the pole

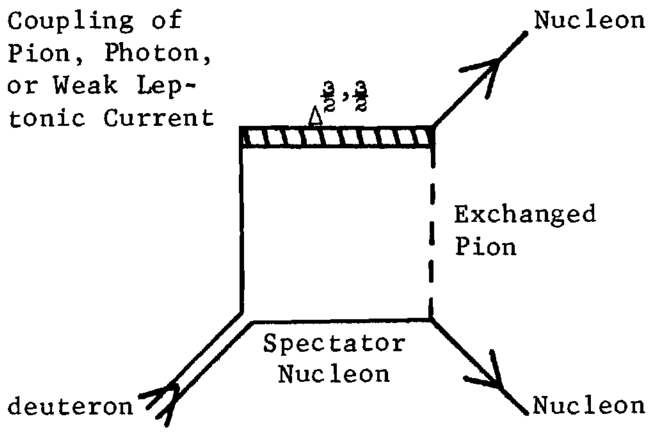

Figure 2. Diagrammatic Representation of Austern Model for Resonant Deuteron Disintegration

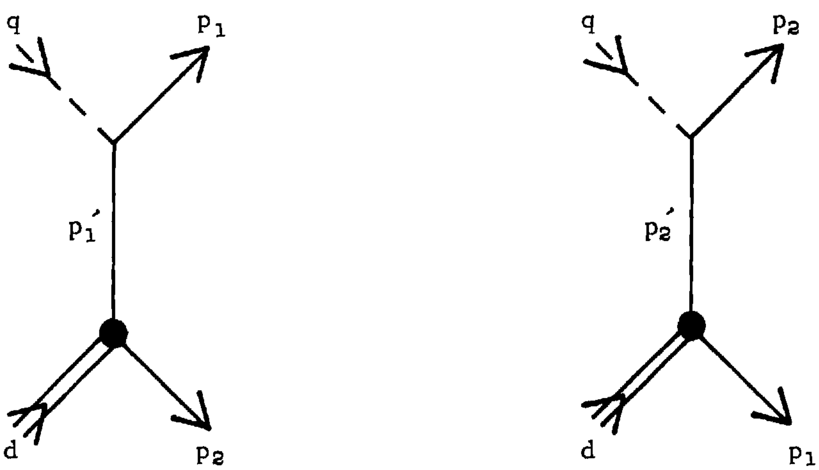

Figure 3. George Background for Pion Disintegration of the Deuteron

designation, refering to the singular nature of the propagator denominator associated with these terms. The George background diagrams for pion disintegration are shown in Figure 3, and for photodisintegration, in Figure 4.

Deuteron Structure

Of particular significance in the background amplitudes are the effects of deuteron structure, indicated symbolically by the darkened circles in Figures 3 and 4. At this point we examine deuteron structure in perturbation theory diagrams in general terms. We will use invariance arguments similar to those in Chapter I. The deuteron enters perturbation theory diagrams thru the deuteron-two-nucleon (dNN) vertex shown in Figure 5. Associated with the vertex is the scalar vertex function, Γ_{dNN}, which is a function of the deuteron polarization U, the momenta entering and leaving the vertex, and the Dirac gamma matrices. In general, the momenta associated with the deuteron and nucleon lines in Figure 5 do not necessarily satisfy the Einstein energy-momentum relation, e.g., $p^2 \neq m^2$, and in such cases the associated "particles" are said to be "off the mass shell." If the deuteron is off the mass shell, we have $U \cdot d \neq 0$. In Table 6 we list the most general set of elementary vertex scalars which are linear in U, after utilizing momentum conservation at the vertex to eliminate terms involving $\not{d}$ or $U \cdot p'$.

The dNN vertex function is constructed as a linear combination of the S_i in Table 6 with coefficients which are functions of the independent scalars which can be formed from d, p, and p'. In general there are three such scalars and we choose them to be d^2, p^2, and p'^2. The explicit form we choose for Γ_{dNN} is

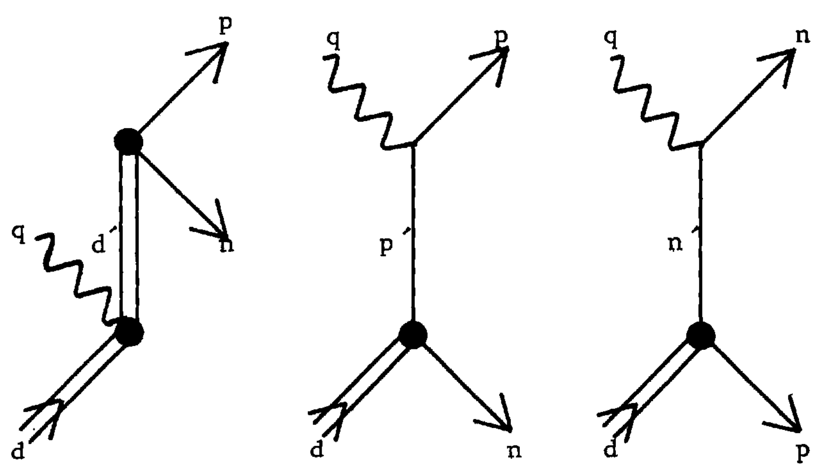

Figure 4. George Background for Photodisintegration of the Deuteron

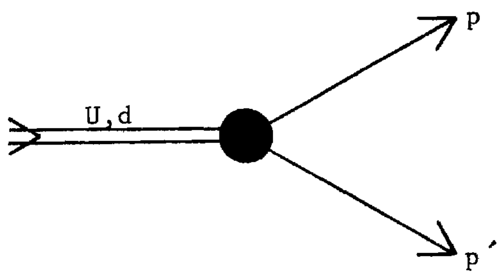

Figure 5. Deuteron-Two-Nucleon Vertex Appearing in Perturbation-Theory Diagrams

Table 6. Elementary dNN Vertex Scalars

i	S_i
1	$U \cdot d$
2	$U \cdot d \not{p}$
3	$U \cdot d \not{p}'$
4	$U \cdot p$
5	$U \cdot p \not{p}$
6	$U \cdot p \not{p}'$
7	$\not{U}$
8	$\not{U} \not{p}$
9	$\not{U} \not{p}'$

$$A\, U\cdot d + B\, U\cdot d\not{p} + C\, U\cdot d\not{p}' \tag{II-1}$$

$$+ F\not{U} - \frac{G}{m} U\cdot p + \left(\frac{m-\not{p}}{m}\right)\left[H\not{U} - \frac{I}{m} U\cdot p\right]$$

$$+ \left[H'\not{U} - \frac{I'}{m} U\cdot p\right]\left(\frac{m+\not{p}'}{m}\right).$$

We have three special cases to consider for purposes of constructing the background amplitudes in deuteron disintegration.

A: The deuteron and one of the nucleons are on the mass shell. Then $U\cdot d = 0$, $d^2 = M_d^2$, $p'^2 = m^2$, and the projection operator associated with the on-shell nucleon operates on a nucleon spinor to give zero. In this case the dNN vertex function reduces to

$$\Gamma_{dNN} = F(p^2)\not{U} - \frac{G}{m}(p^2)\, U\cdot p - \left(\frac{m-\not{p}}{m}\right)\left[H(p^2)\not{U} - \frac{I}{m}(p^2)\, U\cdot p\right]. \tag{II-2}$$

B: Both nucleons are on the mass shell. Then $p^2 = p'^2 = m^2$, both projection operators give zero, and $\not{p}$ and $\not{p}'$ operate to give m. Then

$$\Gamma_{dNN} = A'(d^2)\, U\cdot d + F(d^2)\not{U} - \frac{G}{m}(d^2)\, U\cdot p. \tag{II-3}$$

C: All three particles are on the mass shell. Then

$$\Gamma_{dNN} = F_0 \not{U} - \frac{G_0}{m} U\cdot p \quad , \tag{II-4}$$

where $\quad F_0 = F\left(M_d^2, m^2, m^2\right), \quad$ etc.

The form given in equation (II-2) has been given previously by Blankenbecler and Cook.[15] The constants F_0 and G_0 have been given in terms of static deuteron properties by McGee.[47] They are

$$F_0 = \left[\frac{16\pi\alpha}{m(1-\alpha r_e)(1+\rho^2)}\right]^{\frac{1}{2}} \left(1 + \frac{\rho}{\sqrt{2}}\right) \tag{II-5}$$

and
$$G_0 = \left[\frac{16\pi\alpha}{m(1-\alpha r_e)(1+\rho^2)}\right]^{\frac{1}{2}} \frac{3m^2\rho}{\sqrt{2}\,\alpha^2} + \frac{F_0}{2} \tag{II-6}$$

where $\alpha = (mB)^{\frac{1}{2}}$, B is the deuteron binding energy, ρ is the asymptotic deuteron d-to-s admixture ratio, whose value is approximately three percent as determined from the deuteron magnetic moment, and r_e is the triplet effective range.[45]

In the present work we derive a relation between F_0 and H_0 which is

$$F_0 = 2H_0 \tag{II-7}$$

This relation, which is derived in Chapter 6, is based on the PCAC hypothesis, and the assumption that the Austern model gives the correct behavior of the non-pole part of the pion disintegration amplitude, extrapolated off the mass shell, in the limit of zero momentum transfer.

The form given in equation (II-2) is examined in detail in Chapter IV where it is developed in terms of phenomenological deuteron wave functions following a technique originated by Gross,[4] accompanied by an alternative interpretation of his results based on equation (II-7) which suggests the symmetric relation

$$G_0 = 2I_0 \tag{II-8}$$

The form given in equation (II-3) is discussed in Chapter V, which contains a reexamination of George's photodisintegration results.

George's Calculational Scheme

In George's analysis of pion and photon disintegration of the deuteron, the dNN vertex occurs in the nucleon-pole diagrams with one nucleon off the mass shell. Consequently, a rigorous treatment of these terms requires the vertex function (II-2). Lacking a way to specify the functions H and I, George ignored them and sought to use a modified vertex function of the form

$$\Gamma_{dNN} = \left[F_0 \not{U} - \frac{G_0}{m} U \cdot p \right] W(p^2) , \tag{II-9}$$

where $W(p^2)$ is a form factor derived by Lebellac, et al.[12] for deuteron photodisintegration below 150 MeV, and corresponds to the assumption of the same form of Hulthén wave function for both the deuteron s and d states. Its explicit form is

$$W(p^2) = \frac{-2(\beta^2 - \alpha^2)}{p^2 - m^2 - 2(\beta^2 - \alpha^2)} , \tag{II-10}$$

where $\beta = 5.18\alpha$, and α is as defined previously. George discovered that when this vertex function is inserted in the background amplitudes for pion and photodisintegration, the resulting contribution to the cross section completely obscures the resonant peak.

Lacking an adequate description of deuteron structure, George chose to use a parametric treatment. As parameters, he chose the cutoff momentum appearing in the analysis of the Austern model and described in Chapter III, and the d-to-s ratio ρ appearing in the expressions for F_o and G_o given in equations (II-5) and (II-6). His program was to select values for these parameters using the excellent data available on pion disintegration. The parameter values chosen in this way would then be used to construct a parameter-free theory of photodisintegration, where the available data are poorer. He reports success in this program except for a severe lack of agreement with the photodisintegration differential cross section.

Our Calculational Scheme

We adopt George's simple perturbation model for deuteron disintegration, but we make a number of theoretical and calculational modifications. In Chapter III, we present George's analysis of the Austern model resonant amplitudes without formal modification. There we show that George made two mutually compensating errors in the isospin weight and cut-off momentum for pion disintegration, and the error in cut-off momentum appears, uncompensated, in photodisintegration. With the resonant scale factors properly adjusted, we examine the resonant contributions to the invariant coefficients for pion and photodisintegration. We find that George made some algebraic errors in the coefficients for pion disintegration, and when we use our corrected coefficients, and George's background amplitudes, we obtain a result for the total cross section which differs from George's published curve in two ways. First, we find it necessary to use a Δ mass of 1210 MeV to correctly locate the peak, compared to George's value of 1190 MeV, and, second, our curve fits the experimental data at high energies better than George's.

Upon recalculating the resonant photodisintegration coefficients, we find results which differ considerably from George's published coefficients. Comparing total cross sections calculated with George's background amplitudes and the two sets of resonant coefficients, we find that George's coefficients produce meaningless results, whereas our coefficients essentially reproduce George's published curve. We also find that our coefficients produce a differential cross section which peaks at 90 degrees center-of-mass scattering angle, as originally predicted by Austern,[1] and does not show the forward-backward peaking reported by George. Finally, we note that we find it necessary to use George's 1190 MeV Δ mass to correctly locate the peak in the photodisintegration total cross section, whereas, as mentioned above, we find a value of 1210 MeV necessary in pion disintegration. In Chapter V, we examine inadequacies in the George perturbation model for photodisintegration which may explain the two different Δ masses.

The modifications discussed above pertain to the correction of calculational errors in George's work, and contain no new physics. We introduce a new physical approach by reexamining the treatment of the dNN vertex function. There are two flaws in George's vertex function. The first is in the form chosen for F and G. As mentioned previously, the form given in equation (II-9) and (II-10) corresponds to s and d wave functions which have the same functional form, and this is not sufficiently general for an adequate treatment of the deuteron.[45] Second, there is no reason to believe that H and I produce insignificant contributions to the dNN vertex in the energy range of interest, and neglecting them is not justified. Indeed, in Chapter V (see Figure 13) we show that I contributes significantly to cross sections.

As mentioned previously, we introduce phenomenological vertex invariants in Chapter IV, using a prescription given by Gross,[4] with an interesting theoretical reinterpretation which appears to have fundamental significance. In Chapter V, we apply these invariants to pion and photodisintegration of the deuteron with excellent results, equal or superior to those obtained using George's essentially mathematical technique.

In Chapter VI, we consider the problem of neutrino disintegration of the deuteron. The method used here is based on the conservation hypotheses of CVC and PCAC for the weak vector and axial-vector currents, respectively. We use the PCAC hypothesis to construct the weak axial-vector amplitude from the pion disintegration amplitude, and CVC to construct the weak vector amplitude from the isovector part of the photodisintegration amplitude. It is in the application of PCAC that the relation (II-7) is derived.

Finally, in Chapter VII, we construct the cross section for forward scattering of the massive lepton in the laboratory. Here, we examine the kinematical constraints on the cross section due to the limitation of our model to energy transfers less than 450 MeV, and due to the assumption of constant nucleon vertex functions. We give the separate vector, interference, and axial-vector contributions to the cross section. In this connection, we examine a theorem due to Adler[51] which states that, in a CVC theory of high-energy neutrino processes with a forward-scattered massive lepton, the cross section will be pure axial-vector, in the limit of vanishing lepton mass. This theorem provides a valuable check on the complicated spin sums and computer programs for photodisintegration and the vector and interference contributions to neutrino disintegration.

CHAPTER III

THE RESONANT AMPLITUDES

In this Chapter we examine the resonant contributions to pion disintegration and photodisintegration of the deuteron. The analysis is essentially that given by George, with some additional comments about deuteron structure contributions. The momentum labels used in the analysis are defined in Figure 6, and Figures 7 and 8 give the charge states for resonant pion disintegration and photodisintegration, respectively.

Vertex Functions

Before considering the Austern model explicitly, we consider the vertex functions required in the analysis. For the dNN vertex we initially follow Barshay[2] and George[3] and use the form appropriate to an on-shell deuteron and two on-shell nucleons. Thus we use equation (II-4). For the other vertex functions, we use the forms appropriate to having all particles entering and leaving the vertex on the mass shell. This is certainly incorrect in principle, but is consistent with the assumptions of the Austern model.

We list the vertex functions in Table 7. The quantities listed are, from left to right, the particle labels for the vertex, the field operator form of the interaction, with the fields denoted by the corresponding particle labels, and the momentum space vertex functions needed in the analysis. The coupling constants multiply everything to the right

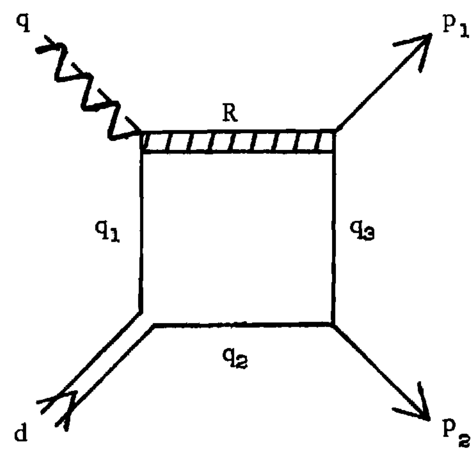

Figure 6. Momentum Labels for Resonance Diagram

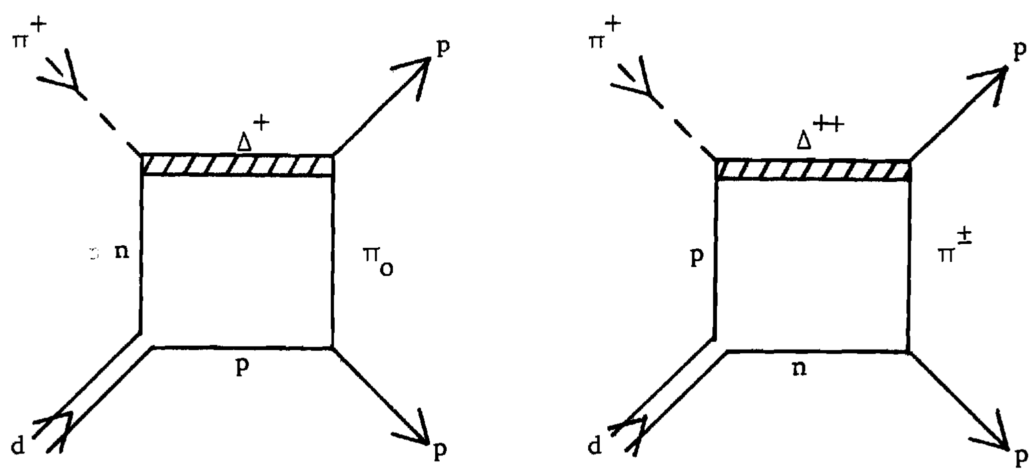

Figure 7. Charge States in Resonant Pion Disintegration

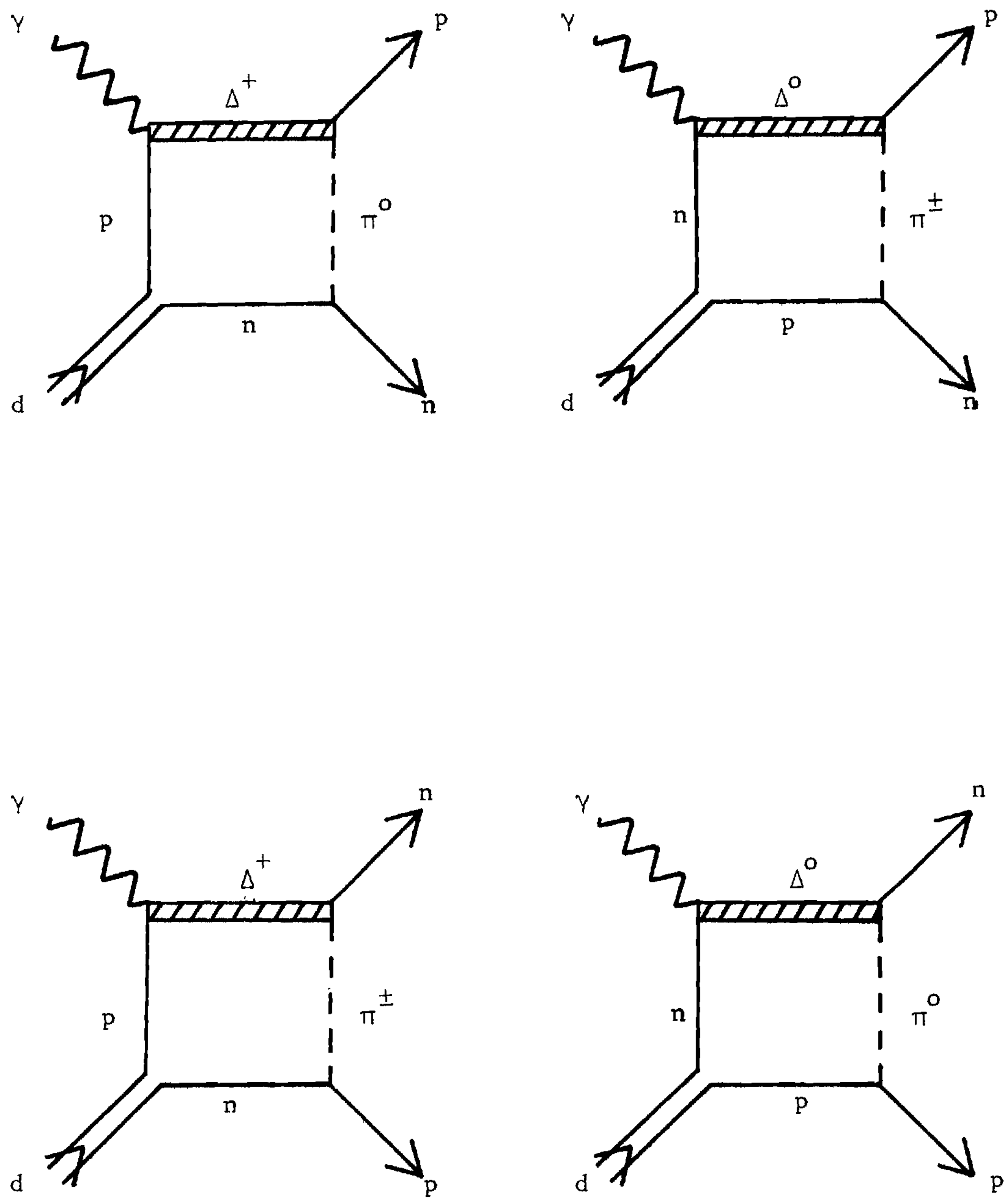

Figure 8. Charge States in Resonant Photodisintegration

Table 7. Vertex Functions for Construction of Austern Model Amplitudes

Vertex	Interaction		Momentum Space Vertex
$pp\pi^0$	$g_{N\pi}$	$(\bar{N}\gamma_5 N + h.c.)$	γ_5
$nn\pi^0$	$-g_{N\pi}$		
$pn\pi^+$	$\sqrt{2}\,g_{N\pi}$		
$np\pi^-$	$\sqrt{2}\,g_{N\pi}$		
$\Delta^{++}p\pi^+$	λ/m_π	$(\bar{N}\Delta_\mu \partial^\mu \pi + h.c.)$	q^μ
$\Delta^+ n\pi^+$	$\sqrt{1/3}\,\lambda/m_\pi$		
$\Delta^+ p\pi^0$	$-\sqrt{2/3}\,\lambda/m_\pi$		
$\Delta^0 p\pi^-$	$-\sqrt{1/3}\,\lambda/m_\pi$		
$\Delta^0 n\pi^0$	$-\sqrt{2/3}\,\lambda/m_\pi$		
$\Delta^+ p\gamma$	$-eC_3/m_\pi$	$(\bar{N}\gamma_\mu\gamma_5\Delta_\nu + h.c.)f^{\mu\nu}$ (†)	$-i\gamma_\mu\gamma_5 f^{\mu\nu}$
$\Delta^0 n\gamma$	eC_3/m_π		

† $f^{\mu\nu}$ is the electromagnetic field tensor $\partial^\mu A^\nu - \partial^\nu A^\mu$ where A^ν is the photon field. The momentum space form of $f^{\mu\nu}$ is $q^\mu\epsilon^\nu - q^\nu\epsilon^\mu$ with q and ϵ the momentum and polarization of the photon.

of the curly brackets. The value for λ is 2.07, as given by Dalitz and Sutherland,[17] who also determine C_3 as 0.29.

Propagators

To complete the prescription for constructing the resonant amplitudes, we need to give the propagators for the nucleon, pion and Δ. These are

$$P(N) = \frac{i\,(\not{N} + m)}{N^2 - m^2} \tag{III-1}$$

$$P(\pi) = \frac{i}{\pi^2 - m_\pi^2} \tag{III-2}$$

and

$$P(\Delta) = \frac{i\,P_{\mu\nu}(\not{R} + m^*)}{R^2 - \overline{m}^2} \;. \tag{III-3}$$

Here, $P_{\mu\nu}$ is the Mohan-Agarwahl[18] form given by

$$P_{\mu\nu} = -\frac{2}{3}\left(g_{\mu\nu} - \frac{R_\mu R_\nu}{m^{*2}}\right) + \frac{i}{3m^*}\,\epsilon_{\mu\nu\lambda\sigma}\gamma_5\gamma^\lambda R^\sigma \;, \tag{III-4}$$

where the last term may be reduced by equation (I-7), and $\overline{m}$ is a complex mass corresponding to a Breit-Wigner[19] form for the resonance, and whose value is $m^* + i\Gamma/2$. For the resonance observed in π-N scattering, m^* = 1236 MeV and the width Γ is approximately 120 MeV. In deuteron disintegration, the best fit, using the Austern model, is found for m^* = 1210 MeV in pion disintegration, and m^* = 1190 MeV in photodisintegration. The difference between the pion and photodisintegration values is discussed in Chapter V.

Ferrari-Selleri Form Factor

Ferrari and Selleri[20] analyzed $\Delta N \rightarrow NN$ by one-pion exchange and found it necessary to incorporate a form factor. The form chosen was

$$h(q^2) = A - \frac{B m_\pi^2}{q^2 - C m_\pi^2} \tag{III-5}$$

where q is the pion four-momentum. The values chosen for the constants are A = 0.28, B = 3.42, and C = 5.75.

The Closed-Loop Integral

Having defined the factors pertinent to the analysis, we consider the construction of the resonant amplitude. The form for the amplitude for both pion and photodisintegration is

$$A = \frac{i}{(2\pi)^4} \int \frac{d^4V\; N}{(R^2 - \bar{m}^2)(q_1^2 - m^2)(q_2^2 - m^2)(q_3^2 - m_\pi^2)} \; . \tag{III-6}$$

Here, the momentum labels are taken from Figure 6, and V is a momentum internal to the closed loop, and defined by

$$V = \frac{q_1 - q_2}{2} \tag{III-7}$$

The numerator N differs for pion and photodisintegration. It consists of factors of momentum space vertex functions and propagator numerators sandwiched between spinors for the outgoing nucleons. We first consider the over-all coupling constants for the two processes. For pion disintegration we sum the two contributions corresponding to the two diagrams of Figure 7, and use Table 7 to obtain*

$$G_\pi = -\frac{\sqrt{2}}{3}\frac{\lambda^2}{m_\pi^2}g_{N\pi} + \sqrt{2}\frac{\lambda^2}{m_\pi^2}g_{N\pi} = \frac{2\sqrt{2}}{3}\left(\frac{\lambda}{m_\pi}\right)^2 . \qquad \text{(III-8)}$$

For photodisintegration we sum the first two diagrams of Figure 8 to obtain**

$$G_\gamma = -\sqrt{\frac{2}{3}}\,\frac{eC_3\lambda\, g_{N\pi}}{m_\pi^2} - \sqrt{\frac{2}{3}}\,\frac{eC_3\lambda\, g_{N\pi}}{m_\pi^2} = -2\sqrt{\frac{2}{3}}\,\frac{eC_3\lambda\, g_{N\pi}}{m_\pi^2} \qquad \text{(III-9)}$$

Next, we write down the numerators for the two processes, ignoring the requirements of the generalized Pauli principle for the time being, as this requirement is easily satisfied once the numerators have been decomposed into invariant amplitudes. For pion disintegration, the

---

*We note that this coupling constant is one-half that used by George. George uses the same coupling constant as Vasvada,[52] but careful examination of Vasvadas' work shows that Vasvada defines the $\Delta^{++}p\pi^+$ coupling as $\lambda/2m_\pi$. Thus, using an isospin weight too large by a factor of two, George claims to obtain the same value of cut-off momentum as that given by Barshay.[2] The difficulty is resolved when we note that the Ferrari-Selleri form factor has a value of approximately one-half at the resonant peak in pion disintegration, and Barshay does not use the Ferrari-Selleri form factor. In our work, we use the correct isospin factor, and the Ferrari-Selleri form factor, and thus our cut-off momentum is larger than Barshay's.

**This isospin coefficient is in agreement with George's, and this means his cut-off momentum is inconsistent with the use of the Ferrari-Selleri form factor, and will lead to photodisintegration amplitudes too small by a factor of two. However, George's published amplitudes suffer from other more serious defects, and we make no attempt to explain how he could have gotten consistent photodisintegration results. Instead we provide a consistent reevaluation of the photodisintegration resonant amplitudes, as discussed in the sequel.

numerator is

$$N_\pi = -i\, G_\pi\, \bar{u}(p_1)\, q_3^\mu\, P_{\mu\nu}\, (\not{K}+m^*)\, q^\nu (\not{q}_1+m)\, h(q_3^2)\, \times$$
$$\left[F_0 \not{U} - \frac{G_0}{m}\, U\cdot q_1\right] C\, [\bar{u}(p_2)\, \gamma_5 (\not{q}_2+m)]^T \,, \qquad \text{(III-10)}$$

and for photodisintegration

$$N_\gamma = -\, G_\gamma\, \bar{u}(p_1)\, q_3^\mu\, P_{\mu\nu}\, (\not{K}+m^*)\, f^{\nu\rho} \gamma_\rho \gamma_5 (\not{q}_1+m)\, h(q_3^2)\, \times$$
$$\left[F_0 \not{U} - \frac{G_0}{m}\, U\cdot q_1\right] C\, [\bar{u}(p_2)\, \gamma_5 (\not{q}_2+m)]^T \,. \qquad \text{(III-11)}$$

The Austern Model

Austern's assumption was that the principal contribution to the deuteron disintegration amplitude in the vicinity of the experimental peak is due to the process depicted in Figure 6, in which the incoming particle couples to one of the nucleons in the deuteron to form an excited state of the nucleon, with the second nucleon acting as a spectator. The process is then completed via deexcitation of the excited state by pion exchange with the spectator nucleon. By analyzing the experimental data on the outgoing nucleons, Austern concluded that the principal contribution from the excited state, now called the Δ, was from the $I = 3/2$ state. This assumption is intrinsic to the charge state decompositions depicted in Figures 7 and 8. The weights assigned to the various charge states in Table 7 can be understood by examining the addition of $I = 1$ states to $I = 1/2$ states to form $I = 3/2$ states. We have the conventional assignments

$$|p\rangle = |\tfrac{1}{2}\,\tfrac{1}{2}\rangle\,, \quad |n\rangle = |\tfrac{1}{2}\,-\tfrac{1}{2}\rangle\,, \tag{III-12}$$

$$|\pi^+\rangle = -|1\,1\rangle\,, \quad |\pi^\circ\rangle = |1\,0\rangle\,, \quad |\pi^-\rangle = |1\,-1\rangle\,,$$

$$|\Delta^{++}\rangle = |\tfrac{3}{2}\,\tfrac{3}{2}\rangle, \quad |\Delta^{+}\rangle = |\tfrac{3}{2}\,\tfrac{1}{2}\rangle, \quad |\Delta^{\circ}\rangle = |\tfrac{3}{2}\,-\tfrac{1}{2}\rangle, \quad |\Delta^{-}\rangle = |\tfrac{3}{2}\,-\tfrac{3}{2}\rangle.$$

Then we can use the angular momentum addition rule

$$|\tfrac{3}{2}\,I_3\rangle = \sum_{I_3' I_3''} \left(1\,I_3'\,\tfrac{1}{2}\,I_3''\,\middle|\,\tfrac{3}{2}\,I_3\right) |1\,I_3'\rangle |\tfrac{1}{2}\,I_3''\rangle\,, \tag{III-13}$$

where the coefficients are the standard Clebsch-Gordon[21] coefficients, to deduce

$$|\Delta^{++}\rangle = -|p\rangle|\pi^+\rangle\,, \tag{III-14}$$

$$|\Delta^{+}\rangle = \sqrt{\tfrac{2}{3}}\,|p\rangle|\pi^\circ\rangle - \sqrt{\tfrac{1}{3}}\,|n\rangle|\pi^+\rangle\,,$$

$$|\Delta^{\circ}\rangle = \sqrt{\tfrac{1}{3}}\,|p\rangle|\pi^-\rangle + \sqrt{\tfrac{2}{3}}\,|n\rangle|\pi^\circ\rangle\,,$$

and

$$|\Delta^{-}\rangle = |n\rangle|\pi^-\rangle\,.$$

The magnitudes of the coefficients for the different decay modes yield the coupling constants shown in Table 7.

Austern further assumed that the excited and spectator nucleons are almost relatively at rest. In terms of the momenta in Figure 6, this implies that $|\vec{v}+\vec{q}/2|^2/m^2 << 1$. This assumption is made only in the denominator of (III-6). In the numerator it is assumed that $q_1 = q_2 = d/2$. This assumption due to Barshay, permits most of the numerator to be factored from the integrand. Both of these assumptions, together with the assumption of static vertex functions in the numerator, are made consistent by the smallness of the cut-off for the momentum $|\vec{V}|$ as determined by experimental fitting of the peak.

With the Barshay assumption, $R = q_1 + q_2 = q + d/2$, and $U \cdot q = U \cdot d/2 = 0$, since d is on the mass shell. This removes the G_0 term from the dNN vertex function and the resonant amplitude assumes the form

$$A = \frac{N'}{D'} \quad . \tag{III-15}$$

The denominator D' is common to both pion disintegration and photodisintegration and has the form

$$\frac{1}{D'} = \frac{i}{(2\pi)^4} \int \frac{d^4V \; h(q_3^2)}{(R^2 - \bar{m}^2)(q_1^2 - m^2)(q_2^2 - m^2)(q_3^2 - m_\pi^2)} \quad . \tag{III-16}$$

For pion disintegration, N'_π is given by

$$N'_\pi = -i F_0 G_\pi \bar{u}(P_1) \left(\frac{d^\mu}{2} + q^\mu - P_1^\mu \right) P_{\mu\nu} \left(\frac{\not{d}}{2} + \not{q} + m^* \right) q^\nu \times \left(\frac{\not{d}}{2} + m \right) \not{U} C \left[\bar{u}(P_2) \gamma^5 \left(\frac{\not{d}}{2} + m \right) \right]^T , \tag{III-17}$$

and for photodisintegration

$$N'_\gamma = -F_0 G_\gamma \bar{u}(P_1) \left(\frac{d^\mu}{2} + q^\mu - P_1^\mu \right) P_{\mu\nu} \left(\frac{\not{d}}{2} + \not{q} + m^* \right) f^{\nu\rho} \times \gamma_\rho \gamma_5 \left(\frac{\not{d}}{2} + m \right) \not{U} C \left[\bar{u}(P_2) \gamma_5 \left(\frac{\not{d}}{2} + m \right) \right]^T . \tag{III-18}$$

We remark that q_3^μ has been evaluated using Barshay's assumption and factored from the integral, while the Ferrari-Selleri form factor $h(q_3^2)$ has been left in the integrand with q_3^2 evaluated according to Austern's assumption. This has been done to preserve the relativistic form of the numerator and facilitate reduction into invariant amplitudes.

It remains to evaluate the integral in (III-16). The momenta are related to the internal momentum V and the external momenta by

$$A = \frac{d}{2} + q + V = \left(\frac{d_0}{2} + q_0 + V_0 \, , \, \vec{V} + \frac{\vec{q}}{2} \right) , \qquad \text{(III-19)}$$

$$q_1 = \frac{d}{2} + V = \left(\frac{d_0}{2} + V_0 \, , \, \vec{V} - \frac{\vec{q}}{2} \right) ,$$

$$q_2 = \frac{d}{2} - V = \left(\frac{d_0}{2} - V_0 \, , \, -\vec{V} - \frac{\vec{q}}{2} \right) ,$$

and

$$q_3 = \frac{q}{2} - K + V = \left(\frac{q_0}{2} + V_0 \, , \, \frac{\vec{q}}{2} - \vec{p} + \vec{V} \right) ,$$

where K is defined in (I-5), and the right hand forms give the momenta in the center of mass frame of the outgoing nucleons, also discussed in Chapter I.

We will evaluate the integral by performing the V_0 integration first. The denominator of the integrand has a number of poles on the axis, so what we really seek is the Cauchy principle value of the V_0 integral. We accomplish this by assigning each of the particles a small imaginary component of mass (unnecessary for the Δ) and thus shift the poles above and below the V_0 axis. Then we convert the V_0 integral into a contour integral, closing the contour either in the upper or lower half plane, and obtaining the desired result from the residues of the integrand in the limit of vanishing imaginary mass (except for the Δ). Thus we need the zeros of each of the factors in the denominator. Evaluating these, we find

$$R^2-\overline{m}^2: \quad V_{01}^{\pm} = -\frac{(d_0+2q_0)}{2} \pm \overline{m}\left(1+\frac{1}{\overline{m}^2}\left[\vec{V}+\frac{\vec{q}}{2}\right]^2\right)^{\frac{1}{2}}, \qquad \text{(III-20)}$$

$$q_1^2-m^2: \quad V_{02}^{\pm} = -\frac{d_0}{2} \pm m\left(1+\frac{1}{m^2}\left[\vec{V}-\frac{\vec{q}}{2}\right]^2\right)^{\frac{1}{2}},$$

$$q_2^2-m^2: \quad V_{03}^{\pm} = \frac{d_0}{2} \pm m\left(1+\frac{1}{m^2}\left[\vec{V}+\frac{\vec{q}}{2}\right]^2\right)^{\frac{1}{2}},$$

$$q_3^2-m_\pi^2: \quad V_{04}^{\pm} = -\frac{q_0}{2} \pm \left(\left[\vec{V}+\frac{\vec{q}}{2}\right]^2+2\,\vec{P}\cdot\left[\vec{V}-\frac{\vec{q}}{2}\right]+\vec{P}^2+m_\pi^2\right)^{\frac{1}{2}}.$$

Now, the integral in (III-16) assumes the form

$$\frac{1}{D'} = \frac{1}{(2\pi)^4}\int d^3V\left[i\int_{-\infty}^{\infty}\frac{dV_0\, h(q_3^2)}{\prod_j (V_0-V_{0j}^-)(V_0-V_{0j}^+)}\right]. \qquad \text{(III-21)}$$

We choose to place the V_{0j}^- poles above the V_0 axis and close the contour in the upper half plane. Then (III-21) is replaced by the sum of residues at each V_{0j}^- or,

$$\frac{1}{D'} = \frac{1}{(2\pi)^4}\int d^3V\left(-2\pi\sum_j R_j\right) \qquad \text{(III-22)}$$

$$= -\frac{1}{(2\pi)^3}\int d^3V\left[\sum_{j=1}^{4}\frac{h(q_3^2|_{V_{0j}^-})}{(V_{0j}^- - V_{0j}^+)\prod_{j\neq i}(V_{0j}^- - V_{0i}^-)(V_{0j}^- - V_{0i}^+)}\right].$$

Defining

$$\delta_{\pm} = 1 + \frac{1}{m^2}\left(\vec{V} \pm \frac{\vec{q}}{2}\right)^2 ,$$

$$\rho = m_\pi^2 + \vec{p}^{\,2} - 2\,\vec{p}\cdot\left(\vec{V} - \frac{\vec{q}}{2}\right) + \left(\vec{V} + \frac{\vec{q}}{2}\right)^2 ,$$

and
$$\sigma = 1 + \frac{1}{\bar{m}^2}\left(\vec{V} + \frac{\vec{q}}{2}\right)^2 .$$

We give the values of the residues by listing, for each residue, the factors in the order that the denominator factors are given in equation (III-16). We have

$$R_1: \quad -1/2\bar{m}\sqrt{\sigma} , \qquad \left(h\left[-\frac{d_0}{2} - q_0 - \bar{m}\sqrt{\sigma}\right]\right) \tag{III-23}$$

$$1/\left(q_0^2 + 2\bar{m}\,q_0\sqrt{\sigma} + 2\vec{V}\cdot\vec{q} + \bar{m}^2 - m^2\right),$$

$$1/\left(\left[d_0 + q_0\right]^2 + 2\left[d_0 + q_0\right]\bar{m}\sqrt{\sigma} + \bar{m}^2 - m^2\right),$$

$$1/\left(m^2 + 2\bar{m}\left[d_0 + q_0\right]\sqrt{\sigma} + \vec{V}\cdot\left[\vec{q} + 2\vec{p}\right] + \frac{\vec{q}^{\,2}}{4} + \bar{m}^2 - m_\pi^2\right),$$

$$R_2: \quad 1/\left(q_0^2 - 2m\,q_0\sqrt{\delta_-} - 2\vec{V}\cdot\vec{q} + m^2 - \bar{m}^2\right),\ \left(h\left[-\frac{d_0}{2} - m\sqrt{\delta_-}\right]\right) \tag{III-24}$$

$$-1/2m\sqrt{\delta_-} ,$$

$$1/\left(d_0^2 + 2m\,d_0\sqrt{\delta_-} - 2\vec{V}\cdot\vec{q}\right),$$

$$1/\left(\left[q_0 - d_0\right]^2/4 - m\left[q_0 - d_0\right]\sqrt{\delta_-} - \vec{V}\cdot\left[\vec{q} - 2\vec{p}\right] - \vec{q}^{\,2}/4 - \vec{p}^{\,2} + m^2 - m_\pi^2\right),$$

$$R_3:\ 1/([d_0+q_0]^2-2[d_0+q_0]m\sqrt{s_+}+m^2-\bar{m}^2),\quad (h\,[\tfrac{d_0}{2}-m\sqrt{s_+}]) \tag{III-25}$$

$$1/(d_0^2-2m\,d_0\sqrt{s_+}+2\vec{V}\cdot\vec{q}),$$

$$-1/2m\sqrt{s_+},$$

$$1/([d_0+q_0]^2/4-m[d_0+q_0]\sqrt{s_+}+m^2-2\vec{p}\cdot[\vec{V}-\tfrac{\vec{q}}{2}]-\vec{p}^{\,2}-m_\pi^2),$$

$$R_4:\qquad (h\,[-\tfrac{q_0}{2}-\sqrt{\rho}]) \tag{III-26}$$

$$1/([d_0+q_0]^2/4-[d_0+q_0]\sqrt{\rho}+\rho-[\vec{V}+\tfrac{\vec{q}}{2}]^2-\bar{m}^2),$$

$$1/([d_0-q_0]^2/4-[d_0-q_0]\sqrt{\rho}+\rho-[\vec{V}+\tfrac{\vec{q}}{2}]^2+2\vec{V}\cdot\vec{q}-m^2),$$

$$1/([d_0+q_0]^2/4+[d_0+q_0]\sqrt{\rho}+\rho-[\vec{V}+\tfrac{\vec{q}}{2}]^2-m^2),$$

$$1/2\sqrt{\rho}\,.$$

We estimate the relative importance of the residues in the limit $(\vec{V}\pm\vec{q}/2)\to 0$. We find

$$R_1\sim 10^{-2}/m^7,\quad R_2\sim 10^{-2}/m^7, \tag{III-27}$$

$$R_3\sim 10^{4}/m^7,\quad R_4\sim 10^{1}/m^7.$$

Neglecting all the residues but R_3, we examine its behavior in the limit that $|\vec{V}\pm\vec{q}/2|^2/m^2$ is small but non-vanishing, and neglect such terms relative to unity. With this, the first, third and fourth factors in R_3 become

$$1/([d_0+q_0-m]^2-\overline{m}^2), \tag{III-28}$$

$$-1/2m,$$

and

$$1/(2m[m-E]-m_\pi^2),$$

where, in the last factor, we have used the center-of-mass relation $d_0+q_0=2E$, and the energy momentum relation E^2 .

The second factor in R_3 requires special treatment. We expand $\sqrt{S_+}$ to first order in $|\vec{V}+\vec{q}/2|^2/m^2$, use $d_0=(\vec{q}^2+M_d^2)^{\frac{1}{2}}$ expanded to first order, and write $M_d=2m-B=2m-\alpha^2/m$, where B is the deuteron binding energy. Retaining only first order terms, we obtain $-1/2(\vec{V}^2+\alpha^2)$ for the second factor in R_3. Thus,

$$R_3 \cong \frac{h(2m[m-E])}{[(d_0+q_0-m)^2-\overline{m}^2][-2(\vec{V}^2+\alpha^2)](-2m)[2m(m-E)-m_\pi^2]}. \tag{III-29}$$

The remaining integral has the form

$$\frac{1}{(2\pi)^3}\int\frac{d^3V}{\vec{V}^2+\alpha^2} = \frac{1}{2\pi^2}\int_0^\infty\frac{d|\vec{V}|\,\vec{V}^2}{\vec{V}^2+\alpha^2} \tag{III-30}$$

which is obviously divergent. Consequently, we introduce a cut-off, Λ, and obtain

$$\frac{1}{2\pi^2}\int_0^{\Lambda}\frac{d|\vec{V}|\,\vec{V}^2}{\vec{V}^2+\alpha^2} = \frac{1}{2\pi^2}\left[\Lambda - \mathrm{Tan}^{-1}\left(\frac{\Lambda}{\alpha}\right)\right]. \qquad \text{(III-31)}$$

By fitting to the experimental peak in pion disintegration, it is found that* $\Lambda = 4.13\alpha \cong 185$ MeV. Then, for an incoming pion or photon with an energy of 300 MeV, $|\vec{V} \pm q/2|^2/m^2 < .12$, justifying the form obtained for R_3 and the Austern assumption. Then it is easy to show that

$$\frac{1}{m^2}\left(\frac{q_1 - q_2}{2}\right)^2 = \frac{V^2}{m^2} \cong -\frac{\vec{V}^2}{m^2} \cong -0.039 \ ,$$

and this, together with

$$\frac{1}{m^2}\left(\frac{q_1 + q_2}{2}\right)^2 = \frac{d^2}{4m^2} \cong 1 \ ,$$

establishes that the nucleons associated with the dNN vertex are very close to the mass shell, and justifies the use of the static dNN vertex functions F_0 and G_0, and the Barshay assumption. We remark that the word "justifies" means that we have established the self-consistency of the model.

Other Contributions to the Resonant Amplitude

We have indicated in equation (II-7) that, near the mass shell, H and H' are comparable in size to F. At this point we would like to indicate why these terms in the vertex function do not contribute significantly

*See the footnote on page 37.

within the context of the Austern model.

Examination of equation (II-1) shows that H and H' occur in the dNN vertex function in the form

$$\frac{(m - \not{q}_1)}{m} H \not{\xi} + H' \not{\xi} \frac{(m + \not{q}_2)}{m} \tag{III-32}$$

When this is inserted in the numerators in equations (III-10) and (III-11), we note that the nucleon propagators there will combine with (III-32) to give the additional term

$$N = \bar{u}(P_1)\,(\text{Factor}) \Big[\frac{(q_1^2 - m^2)}{m} H \not{\xi} (\not{q}_2 - m) \tag{III-33}$$

$$- (\not{q}_1 + m) H' \not{\xi} \frac{(q_2^2 - m^2)}{m} \Big] \gamma_5 C \bar{u}^T(P_2),$$

where we have used

$$C \left[\bar{u}(P_2) \gamma_5 (\not{q}_2 + m) \right]^T = - (\not{q}_2 - m) \gamma_5 C \bar{u}^T(P_2). \tag{III-34}$$

Inserting (III-33) in the integral (III-6), we see that we obtain cancellation of a factor in the denominator and change the character of the V_0 integral. Specifically, we have two additional integrals to consider,

$$I_1 = \frac{i}{m^2} \int \frac{dV_0 \; h(q_3^2)}{(R^2 - \bar{m}^2)(q_2^2 - m^2)(q_3^2 - m_\pi^2)} \tag{III-35}$$

and

$$I_2 = \frac{i}{m^2} \int \frac{dV_0 \; h(q_3^2)}{(R^2 - \bar{m}^2)(q_1^2 - m^2)(q_3^2 - m_\pi^2)} , \qquad \text{(III-36)}$$

where we have replaced the missing propagator numerators in N with m to maintain dimensional consistency for purposes of comparison.

Now the dominance of the residue R_3 in the integral (III-16) arises from the factor $1/(q_1^2 - m^2) \cong -1/2\,(\vec{V}^2 + \alpha^2)$ at the pole in $q_2^2 - m^2$. Thus, the integrals (III-35) and (III-36) will not be significant because the factors $1/(q_1^2 - m^2)$ and $1/(q_2^2 - m^2)$ do not occur simultaneously. Writing I_1 and I_2 as

$$I_1 = -2\pi\,(R_1' + R_2' + R_3') ,$$

$$I_2 = -2\pi\,(R_1'' + R_2'' + R_4'') ,$$

and using the pertinent entries in (III-23--III-26), we find for $(\vec{V} \pm \vec{q}/2) \rightarrow 0$,

$$R_1' \sim 10^1/m^7 \qquad R_1'' \sim 10^1/m^7$$

$$R_3' \sim 10^1/m^7 \qquad R_2'' \sim 10^{-1}/m^7$$

$$R_4' \sim 10^{-2}/m^7 \qquad R_4'' \sim 10^{-1}/m^7 ,$$

and these terms are no more important than those neglected in evaluating (III-16).

Finally, we remark that the smallness of the cut-off parameter found by retaining only R_3 in (III-22) greatly enhances the dominance of this term. This is because the remaining three-dimensional integral for all other residues has the form

$$\frac{1}{(2\pi)^3}\int_0^{\Lambda}\frac{d^3V}{m^2} = \frac{\Lambda}{2\pi^2}\left(\frac{\Lambda^2}{3m^2}\right) \cong \frac{5\alpha^2}{m^2}\left(\frac{\Lambda}{2\pi^2}\right) \qquad \text{(III-37)}$$

Consequently, these integrals are depressed by an additional factor of $5\alpha^2/m^2 \cong 10^{-2}$.

Evaluation of the Resonant Amplitudes

We turn now to the problem of reducing the resonant amplitudes to the forms given in equations (I-27) and (I-31). These amplitudes have the form given in equation (III-15) and we have obtained D' as

$$\frac{1}{D'} = \frac{[\Lambda - \mathrm{Tan}^{-1}(\Lambda/\alpha)][A + Bm_\pi^2/(2m[E-m]+Cm_\pi^2)]}{8m\pi^2[(d_0+q_0-m)^2-\overline{m}^2][2m(E-m)+m_\pi^2]} \qquad \text{(III-38)}$$

where we have used equations (III-5), (III-22), (III-29), and (III-31). We remark that this differs from George's result[3] by the occurrence of an additional factor of 1/2, and C instead of C + 1 in the Ferrari-Selleri form factor. It remains now to reduce N'_π and N'_γ given in equations (III-17) and (III-18), with $P_{\mu\nu}$ given by (III-4) and expanded via equation (I-7), and $f^{\nu\rho}$ given in the footnote on page 34.

Reduction of N'_π

The reduction of N'_π proceeds by making the substitution $\not{d} = \not{P}_1 + \not{P}_2 - \not{q}$, and using the anticommutation relations to move $\not{P}_1$ and $\not{P}_2$ next to the appropriate spinor to utilize the Dirac equation, and eliminate these matrices (we note that $\not{P}_2 C\bar{u}^T(P_2) = -mC\bar{u}^T(P_2)$). The algebra is tedious but straight-forward, and once accomplished leads to terms which may then be written in terms of the invariant amplitudes given in Table 1. As an example, we consider the reduction of $\bar{u}(P_1)\gamma_5\not{K}\not{q}\not{U}C\bar{u}^T(P_2)$, which is the most complicated term occurring in N'_π, once it is expanded and similar terms are collected together. We have

$$\bar{u}(P_1)\gamma_5\not{K}\not{q}\not{U}C\bar{u}^T(P_2) = \bar{u}(P_1)\gamma_5\left(\frac{\not{P}_1+\not{P}_2+\not{q}}{2}\right)\not{q}\not{U}C\bar{u}^T(P_2)$$

$$= \bar{u}(P_1)\frac{\gamma_5}{2}\left(\not{P}_1\not{q}\not{U}+\not{P}_2\not{q}\not{U}+m_\pi^2\not{U}\right)C\bar{u}^T(P_2).$$

We use

$$\gamma_5\not{P}_1 = -\not{P}_1\gamma_5$$

and

$$\not{P}_2\not{q}\not{U} = -\not{U}\not{q}\not{P}_2 + 2U\cdot q\not{P}_2 - 2U\cdot P_2\not{q} + 2q\cdot P_2\not{U},$$

together with

$$U\cdot P_2 = U\cdot Q - U\cdot K = \frac{U\cdot q}{2} - U\cdot K$$

and

$$q\cdot P_2 = q\cdot Q - q\cdot K$$

to obtain

$$\bar{u}(P_1)\frac{\gamma_5}{2}\Big(-m\not{q}\not{U}+m\not{U}\not{q}-2mU\cdot q-U\cdot q\not{q}$$

$$+2U\cdot K\not{q}+\left[2q\cdot Q-2q\cdot k+m_\pi^2\right]\not{U}\Big)C\bar{u}^T(P_2).$$

Comparing this with Table 1, we obtain

$$\bar{u}(P_1)\Big[-m^2 I_4^\pi-2m^2 I_1^\pi-m^2 I_5^\pi+m^2 I_6^\pi$$

$$+\left(q\cdot Q-q\cdot k+\frac{m_\pi^2}{2}\right)I_3^\pi\Big]C\,\bar{u}^T(P_2),$$

where we have defined $I_i^\pi=U^\beta I_{i\beta}^\pi$. The only operation remaining is to antisymmetrize this term and this is accomplished by the rule

$$\alpha_i(P_1,P_2)I_i^\pi\longrightarrow\left[\alpha_i(P_1,P_2)-\varepsilon_i\alpha_i(P_2,P_1)\right]I_i^\pi$$

When this is done for our present example, there results

$$\bar{u}(P_1)\left[4m^2 I_1^\pi+2m^2 I_5^\pi+\left(2q\cdot Q+m_\pi^2\right)I_6^\pi\right]C\,\bar{u}^T(P_2).$$

When the decomposition scheme outlined above is applied to N_π', and the resulting terms appropriately antisymmetrized, there result the invariant coefficients shown in Table 8. Here, we have specialized to the center of mass frame, and introduced the variables

$$\sigma=\frac{q^2}{m^2}\;,\quad w=-\frac{q\cdot k}{m^2}=\frac{\vec{q}\cdot\vec{p}}{m^2}\;, \tag{III-39}$$

$$y=-\frac{k^2}{m^2}=\frac{\vec{p}^{\,2}}{m^2}\;,\qquad \eta=\frac{m^*}{m}\;.$$

Table 8. Invariant Coefficients for Resonant Pion Disintegration of the Deuteron, Specialized to the Center-of-Mass Frame

i	$R_i^{\pi} = g_{N\pi}\left[C_i^{\pi}(P_1, P_2) - \varepsilon_i C_i^{\pi}(P_2, P_1)\right]$
1	0
2	$-\dfrac{4 i m^5 F_0 G_\pi W}{3\eta^2 D'}\left[2\eta^3 + 3\eta^2 + \eta\left(1 + y - \dfrac{3\sigma}{4}\right) - \dfrac{3\sigma}{4} - y\right]$
3	$\dfrac{i m^5 F_0 G_\pi}{3\eta^2 D'}\Big[-2\sigma\eta(2\eta^2 + \eta - 1) - \sigma y(3\eta^2 - 7\eta - 6 - 5y)$ $+ W^2(10\eta^2 - 2\eta - 3\sigma - 4y) - 2y^2(\eta^2 - \eta - 2[1 + y])\Big]$
4	$-\dfrac{2 i m^5 F_0 G_\pi W}{3\eta^2 D'}\left[2\eta^3 + 3\eta^2 + \eta\left(1 + y - \dfrac{3\sigma}{4}\right) - \dfrac{3\sigma}{4} - y\right]$
5	$-\dfrac{i m^5 F_0 G_\pi}{6\eta^2 D'}\left[16\eta(\eta + 1) + \sigma(7\eta^2 - \eta - 12y) + 4y(\eta^2 + 5\eta - 2y)\right]$
6	$\dfrac{2 i m^5 F_0 G_\pi W}{3\eta^2 D'}\left[5\eta^2 - \eta - 2y - \dfrac{3\sigma}{2}\right]$

We note that our coefficients are somewhat different from George's, although the actual numerical differences in the cross section are relatively small, with our coefficients giving a better fit to the total cross section at high energies than George's reported result, and requiring a value of $m^* = 1210$ MeV, rather than 1190 MeV as reported by George, to locate the resonant peak.

<u>Reduction of N'_γ</u>

The reduction of N'_γ is considerably more complicated than that for N'_π, for two reasons. First, it is a considerably more complicated expression, and second, once $\not{p}_1$ and $\not{p}_2$ are removed, the reduction of the remaining terms to the invariant amplitudes listed in Table 4 is complicated. For this reason, George chose to use a symbol-manipulation computer program[22] to perform the reduction. Lacking access to facilities to implement this program, we had hoped to use George's published amplitudes. However, upon performing numerical calculations of the photodisintegration total cross section using George's amplitudes, we obtained results which were totally unreasonable. Consequently, we found it necessary to perform the reduction of N'_γ by means of a hand calculation.

The elimination of $\not{p}_1$ and $\not{p}_2$ is straightforward. Once this has been accomplished, there remains the reduction to invariant amplitudes. To accomplish this, two relations developed by Sakita,[13] and reported Lebellac,[12] are indispensible. These relations may be written in terms of the I_λ^γ listed in Table 4 and the N_λ in Table 3, where $N_\lambda = \epsilon^\alpha U^\beta N_{\lambda\alpha\beta}$, and $I_\lambda^\gamma = \epsilon^\alpha U^\beta I_{\lambda\alpha\beta}^\gamma$. We have

$$- q\cdot K\, N_9 + N_{11} + 2\left(q\cdot Q\, N_{12} - N_{13}\right) \tag{III-39}$$

$$= -2m^3\left[\frac{2K^2}{m^2} I_{12}^r - I_4^r + I_9^r + I_{10}^r + 2 I_2^r\right],$$

and

$$-q\cdot Q N_9 + N_{10} = m\left(2Q^2 - q\cdot Q\right) I_8^r - m\, q\cdot Q I_{11}^r + m\, q\cdot K\left(I_9^r + I_{10}^r + 2 I_{12}^r\right). \tag{III-40}$$

We remark that the I_{12}^r we use is opposite in sign to that used by Lebellac.

In addition to using the relations (III-39) and (III-40), we can facilitate the reduction of the elementary terms in N_r' by choosing the time component of ϵ to vanish in the center-of-mass frame. With this,

$$\epsilon\cdot Q = (0, \vec{\epsilon})\cdot(E, \vec{0}) = 0 \quad ,$$

and the I_i^r are considerably simplified. We summarize the results by giving a table of relations between elementary terms in N_r' and the I_i^r. These are listed in Table 9, where we have defined $R = q\cdot K/q\cdot Q$.

To complete the specification of the resonant amplitude, we note that the Austern model implies that it is pure isovector. To see this, note that the incoming deuteron in Figure 5 has I = 0, and the photon may be regarded as a mixture of I = 0 and I = 1. Consequently the in state is composed of I = 0 or I = 1. The assumption of the dominance of the $\Delta^{\frac{3}{2},\frac{3}{2}}$ in the intermediate state requires the resonance-spectator pair to have I = 1 or I = 2. Consequently, the resonance-spectator pair are in an I = 1 state, and the pion exchange conserves isospin to leave the outgoing nucleons in an I = 1 state.

Table 9. Relation Between Elementary Terms in N_γ' and the I_i^γ of Table 4

$$\not{q}\not{\epsilon}\not{U} = 2m\left(I_5^\gamma + I_{12}^\gamma\right)$$

$$\epsilon\cdot k\not{U} = m^3 I_4^\gamma / q\cdot Q$$

$$U\cdot q\not{q}\not{\epsilon} = -2m^2 I_8^\gamma$$

$$U\cdot k\not{q}\not{\epsilon} = -m^2 I_9^\gamma$$

$$\epsilon\cdot k\, U\cdot k = m^4 I_3^\gamma / q\cdot Q$$

$$\epsilon\cdot k\, U\cdot q = m^2\left(I_1^\gamma + R I_2^\gamma\right)$$

$$\not{\epsilon}\not{U} = m^2\left(2I_1^\gamma + 2I_2^\gamma - I_{11}^\gamma\right)/q\cdot Q$$

$$\epsilon\cdot k\not{q}\not{U} = 2m^2(1+R)\left(I_1^\gamma + I_2^\gamma\right) + m^2\left(I_{10}^\gamma - R I_{11}^\gamma\right)$$

$$U\cdot q\not{\epsilon} = m\left[1 - 2Q^2/q\cdot Q\right] I_8^\gamma + m I_{11}^\gamma - mR\left(I_9^\gamma + I_{10}^\gamma + 2I_{12}^\gamma\right)$$

$$U\cdot k\not{\epsilon} = -m^3\left(I_7^\gamma + 2k^2 I_{12}^\gamma/m^2 + 2I_2^\gamma - I_4^\gamma + I_9^\gamma + I_{10}^\gamma\right)/2q\cdot Q$$

$$\epsilon\cdot k\, U\cdot q\not{q} = m^3\left(-2I_2^\gamma + I_4^\gamma + I_7^\gamma\right) - mR\left(2Q^2 - q\cdot Q\right) I_8^\gamma$$
$$- \left(m^3 + m q\cdot k R\right)\left(I_9^\gamma + I_{10}^\gamma\right) + m q\cdot k I_{11}^\gamma - 2m\left(k^2 + q\cdot k R\right) I_{12}^\gamma$$

$$\epsilon\cdot k\, U\cdot k\not{q} = -m^3 R\left(2I_2^\gamma - I_4^\gamma + I_7^\gamma\right)/2 - m^3 I_6^\gamma + m\left(Q^2 - q\cdot Q/2\right) I_8^\gamma$$
$$+ m\left(q\cdot k - m^2 R\right)\left(I_9^\gamma + I_{10}^\gamma\right)/2 - m\, q\cdot Q I_{11}^\gamma/2 + m\left(q\cdot k - R k^2\right) I_{12}^\gamma$$

Since the resonance amplitude is pure isovector, the decomposition given in equation (I-30) is unnecessary. The amplitude is given directly by the four diagrams in Figure 8. Since the second two diagrams are the exchange counterparts of the first two, the amplitude may be constructed from N_γ' using the same rule as that for pion disintegration (see top of page 51).

We have performed the reduction of N_γ' and have carefully double-checked the algebra. We then used the substitution rules given in Table 9 to extract the invariant coefficients. We remark at this point that the reduction scheme given by Table 9 is also used to obtain the background invariant coefficients in Chapter V, and the results agree with Lebellac, except for a minor discrepancy noted by George. Thus, we have a high level of confidence in our results for the resonant invariant coefficients, given in Table 10.

Table 10. (Isovector) Invariant Coefficients for the Resonant Amplitude in Photodisintegration, Specialized to the Center-of-Mass Frame

i	$R_i^\gamma = e\left[C_i^\gamma(P_1,P_2) - \varepsilon_i C_i^\gamma(P_2,P_1)\right]$
1	$\frac{8m^5 F_0 G_\gamma W}{3\eta^2 D'}\left[1+3\eta^2\right]$
2	$-\frac{4m^5 F_0 G_\gamma}{3\eta^2 D'}\left[6\eta^3+5\eta^2-\eta+y(6\eta^2-1)\right]$
3	$-\frac{8m^5 F_0 G_\gamma}{D'}$
4	$\frac{2m^5 F_0 G_\gamma}{3\eta^2 D'}\left[6\eta^3+5\eta^2-\eta-y\right]$
5	$\frac{4m^5 F_0 G_\gamma W}{3\eta^2 D'}\left[2\eta^3+3\eta^2+\eta+y(2\eta-1)\right]$
6	0
7	$\frac{2m^5 F_0 G_\gamma}{3\eta^2 D'}\left[2\eta^3-\eta^2-3\eta-y(4\eta+1)\right]$
8	$-\frac{2m^5 F_0 G_\gamma}{3\eta^2 D'}\left[4\eta^2-2\eta-2-3y\right]$
9	$-\frac{2m^5 F_0 G_\gamma}{3\eta^2 D'}\left[2\eta^3-\eta^2-3\eta-y(4\eta^2+4\eta-1)+2y^2+W^2\right]$
10	$-\frac{2m^5 F_0 G_\gamma}{3\eta^2 D'}\left[6\eta^3+5\eta^2-\eta+y(2\eta^2+1)+2y^2+W^2\right]$
11	$-\frac{2m^5 F_0 G_\gamma W}{3\eta^2 D'}\left[2\eta^2+2\eta+2+3y\right]$
12	$\frac{4m^5 F_0 G_\gamma}{3\eta^2 D'}\left[(2\eta^3+3\eta^2+\eta)y+2\eta y^2-W^2\right]$

CHAPTER IV

dNN VERTEX FUNCTION WITH ONE NUCLEON OFF THE MASS SHELL

In this Chapter we develop a prescription for relating the vertex invariants appearing in the dNN vertex function with one off-shell nucleon to phenomenological deuteron s and d state wave functions determined from nucleon scattering experiments. The initial discussion follows that given by Gross,[4] but we add some speculative remarks concerning the PCAC result given in equation (II-7).

In a general scattering process involving the deuteron, the relativistic counterpart of the deuteron wave function is the Bethe-Salpeter[23] amplitude, defined in momentum space by

$$\Psi(p_1, p_2) = S_F(p_1)\, \Gamma^{\alpha}(p_1, p_2)\, C\, S_F^T\, U_\alpha \, . \qquad \text{(IV-1)}$$

Here, p_1 , p_2 are the momenta of the nucleons in the deuteron, $S_F(p)$ is the full Feynman Propagator[50] for a nucleon of momentum p, $\Gamma^{\alpha}(p_1, p_2)$ is the dNN vertex function with both nucleons off the mass shell (cf. equation (II-1)), and U_α is the deuteron polarization vector. We indicate this amplitude symbolically in Figure 9. Here, the triple lines signify that the deuteron contains, in addition to simple nucleon bound states, contributions from bound $N\Delta$ and higher mass states, examples of which are shown in Figure 10. If the relative momentum $\vec{r} = (p_1 - p_2)/2$ is restricted to values $\vec{r}^{\,2} < m m_\pi \cong$ (370 MeV)^2, the contributions from the higher mass

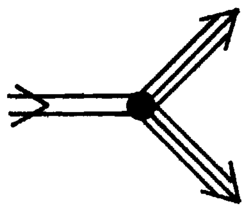

Figure 9. Diagrammatic Representation of the Bethe-Salpeter Amplitude for the Deuteron

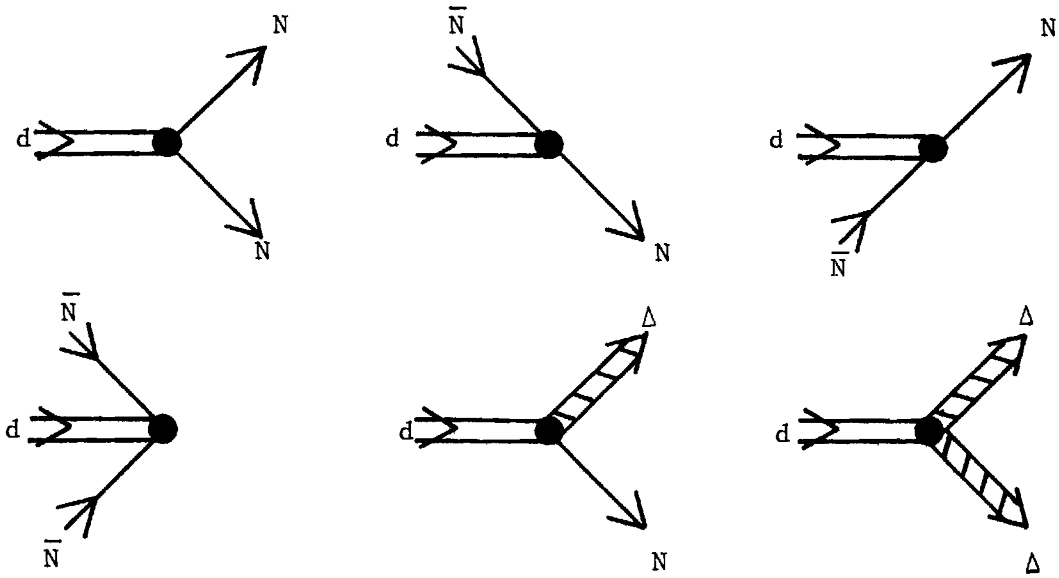

Figure 10. Lower Energy Contributions to the Bethe-Salpeter Amplitude (The First Four Diagrams Constitute the One-Channel Coupling Approximation, and Only the First Two Are Important.)

states may be neglected, and the only significant diagrams are the nucleon diagrams in Figure 10. This is called the one-channel coupling approximation. In analytical terms, the one-channel coupling approximation implies neglecting all singularities in (IV-1) except the simple nucleon poles occurring at $p_1^2 = m^2$ and $p_2^2 = m^2$.

In an analysis of the singularity structure of (IV-1), Gross has shown that its contribution to scattering amplitudes is accurately described in the one-channel coupling approximation by taking one of the nucleons to be on the mass shell. This gives an approximate relativistic deuteron wave function of the form

$$\Phi_d(\vec{r},\vec{d}) = \frac{(\not{p}_1+m)\,\Gamma^{\alpha}(p_1)\,C\,(\not{p}_2+m)^T U_\alpha}{4m^2(p_1^2-m^2)} \tag{IV-2}$$

where $\Gamma^{\alpha}(p_1)$ is given in equation (II-2). Here,

$$\vec{r} = \frac{\vec{p}_1-\vec{p}_2}{2}\ , \quad \vec{d} = \vec{p}_1+\vec{p}_2\ , \tag{IV-3}$$

$$d_0 = (M_d^2+\vec{d}^{\,2})^{\frac{1}{2}}\ , \quad r_0 = \frac{d_0}{2} - \left(m^2+\left[\frac{\vec{d}}{2}-\vec{r}\right]^2\right)^{\frac{1}{2}},$$

and p_1 is the off-shell momentum.

Now, any attempt to relate the vertex invariants in equation (II-2) to deuteron s and d wave functions must be accomplished by relating (IV-2) to the non-relativistic deuteron wave function, the 3-space form of which is given by

$$\Psi^{NR}_{(\lambda)}(\vec{x}) = \frac{1}{\sqrt{4\pi}}\chi^{T}_{1(\lambda)}\Big[\frac{u(x)}{x}\,\vec{\sigma}\cdot\vec{U}^{(\lambda)} - \frac{1}{\sqrt{2}}\,\frac{W(x)}{x}\times \tag{IV-4}$$

$$\Big(\frac{3[\vec{\sigma}\cdot\vec{x}][\vec{x}\cdot\vec{U}^{(\lambda)}]}{x^2} - \vec{\sigma}\cdot\vec{U}^{(\lambda)}\Big)\Big]\frac{i\,\sigma_2}{\sqrt{2}}\chi_{2(\lambda)}\ .$$

Here, u and W are the deuteron s and d state wave functions, $\vec{\sigma}$ is the 3-vector Pauli spin matrix,[10] χ is a nucleon spinor, and λ is a polarization index with values -1, 0, 1 where

$$\vec{U}^{(0)} = (0, 0, 1)\ ,$$

$$\vec{U}^{(\pm 1)} = (\mp 1/\sqrt{2}\,,\ -i/\sqrt{2}\,,\ 0)\ ,$$

and the spinors $\chi_{1(\lambda)}, \chi_{2(\lambda)}$ are determined by λ via angular momentum addition. The normalization is chosen to satisfy

$$\sum_{\lambda}\int d^3\vec{x}\,\left|\Psi^{NR}_{(\lambda)}(\vec{x})\right|^2 = \int_0^\infty\left[u(x)^2 + W(x)^2\right]dx$$

The connection between (IV-4) and more conventional forms for the deuteron wave function, such as that given by Blatt and Weisskopf,[24] may be found in Appendix D of reference (12). For our purposes, the 3-space Fourier-Bessel transform of (IV-4) is more appropriate. This is given by

$$\Phi^{NR}_{(\lambda)}(\vec{r}) = \sqrt{4\pi}\,\chi^{T}_{1(\lambda)}\Big[u_0(r)\,\vec{\sigma}\cdot\vec{U}^{(\lambda)} + \frac{1}{\sqrt{2}}\,W_2(r)\times \tag{IV-5}$$

$$\Big(\frac{3[\vec{\sigma}\cdot\vec{r}][\vec{r}\cdot\vec{U}^{(\lambda)}]}{r^2} - \vec{\sigma}\cdot\vec{U}^{(\lambda)}\Big)\Big]\frac{i\,\sigma_2}{\sqrt{2}}\chi_{2(\lambda)}\ ,$$

where

$$u_0(r) = \int_0^\infty u(x)\, j_0(rx)\, x\, dx \;, \tag{IV-6}$$

$$w_2(r) = \int_0^\infty w(x)\, j_2(rx)\, x\, dx \;, \tag{IV-7}$$

and

$$j_\ell(x) = (-x)^\ell \left(\frac{1}{x}\frac{d}{dx}\right)^\ell \frac{\sin x}{x} \tag{IV-8}$$

are the spherical Bessel functions.

To relate (IV-2) and (IV-5), we write the off-shell projection operator in terms of on-shell nucleon spinors via

$$\frac{\not{P}+m}{2m} = \frac{1}{2}(1+\beta)\, u(\vec{P})\bar{u}(\vec{P}) - \frac{1}{2}(1-\beta)\, v(-\vec{P})\bar{v}(-\vec{P}), \tag{IV-9}$$

where

$$\beta = \frac{P_0}{E} \qquad\qquad E = \left(\vec{P}^2 + m^2\right)^{\frac{1}{2}}$$

This decomposition suggests that the off-mass-shell nucleon be regarded as a superposition of positive and negative energy states (nucleons and antinucleons) with the negative energy contribution vanishing in the limit that the nucleon is on the mass shell ($\beta = 1$).

If we substitute (IV-9) into (IV-2), we obtain

$$\Phi_d(\vec{r}, \vec{d}) = \phi^{++}(\vec{r}, d)\, u(\vec{P}_1)\bar{u}^T(\vec{P}_2) + \phi^{-+}(\vec{r}, \vec{d})\, v(-\vec{P}_1)\bar{u}^T(\vec{P}_2), \tag{IV-10}$$

where

$$\phi^{++}(\vec{r},\vec{d}) = \frac{(1+\beta)}{2(m^2-P_1^2)} \bar{u}(\vec{P}_1)\,\Gamma^{\alpha}(P_1)\,C\,\bar{u}^T(\vec{P}_2)\,U_\alpha \,, \qquad \text{(IV-11)}$$

and

$$\phi^{-+}(\vec{r},\vec{d}) = \frac{-(1-\beta)}{2(m^2-P_1^2)} \bar{v}(-\vec{P}_1)\,\Gamma^{\alpha}(P_1)\,C\,\bar{u}^T(\vec{P}_2)\,U_\alpha \,. \qquad \text{(IV-12)}$$

Here, ϕ^{++} corresponds to the first, and ϕ^{-+} to the second, diagram in Figure 9. The third and fourth diagrams contribute only when the second nucleon is also off the mass-shell. Now, to make a connection between the relativistic wave functions (IV-11) and (IV-12), and the non-relativistic wave function (IV-5), we note that phenomenological analyses of nucleon scattering are generally based on a non-relativistic formalism, and hence contain no explicit provision for contributions from negative energy states. Whatever the effects of these negative energy states are, they are incorporated as well as can be expected by virtue of the fact that the non-relativistic wave functions $u_0(r)$ and $W_2(r)$ are chosen to fit the experimental data. Also, the nonrelativistic analyses are performed in the nucleon center-of-mass frame. In the case of the relativistic wave function $\phi_d(\vec{r},\vec{d})$, the center-of-mass frame of the nucleons is the deuteron rest frame $\vec{d} = 0$. Following Gross then, we make the identifications

$$\phi^{++}(\vec{r},0) = \phi^{NR}(\vec{r}) \,, \qquad \text{(IV-13)}$$

and

$$\Phi^{-+}(\vec{r}, 0) = 0 \; . \tag{IV-14}$$

The two equations (IV-13) and (IV-14) provide a direct means of relating the invariant functions F, G, H, and I to the phenomenological wave functions u_0 and W_2 contained in (IV-5). To make the identification explicit, we use the limiting form of the nucleon spinors given in reference (10). We have

$$\vec{d} = 0 \, , \quad \vec{P}_1 = \vec{r} \, , \quad \vec{P}_2 = -\vec{r} \, ,$$

$$u(\vec{r}) \longrightarrow \begin{pmatrix} \chi \\ \frac{\vec{\sigma}\cdot\vec{r}}{2m}\chi \end{pmatrix} \tag{IV-15}$$

and

$$V(-\vec{r}) \longrightarrow \begin{pmatrix} -\frac{\vec{\sigma}\cdot\vec{r}}{2m}\chi \\ \chi \end{pmatrix} \tag{IV-16}$$

We repeat equation (II-2) here for reference. It is

$$\Gamma(P_1) = F(P_1^2)\not{U} - \frac{G(P_1^2)}{m} U\cdot P_1 - \frac{(m-\not{P}_1)}{m}\left[H(P_1^2)\not{U} - \frac{I(P_1^2)}{m} U\cdot P_1\right]. \tag{II-2}$$

We will find it convenient to extract the projection operator in (II-2) as follows

$$\bar{u}(\vec{P}_1)\frac{(m-\not{P}_1)}{m} = \bar{u}(\vec{P}_1)\left(\frac{m - E_1\gamma_0 + \vec{P}_1\cdot\vec{\gamma} + E_1\gamma_0 - P_1^0\gamma_0}{m}\right) \tag{IV-17}$$

$$= \bar{u}(\vec{P}_1)\left(\frac{m - E_1\gamma_0 + \vec{P}_1\cdot\vec{\gamma} + E_1[1-\beta]\gamma_0}{m}\right)$$

$$= \bar{u}(\vec{P}_1)\,\frac{E_1}{m}\,(1-\beta)\gamma_0 = \bar{u}(\vec{P}_1)\,\delta\,\gamma_0 \;,$$

and similarly

$$\bar{V}(-\vec{P}_1)\frac{(m-\not{P}_1)}{m} = \bar{V}(-\vec{P}_1)\,(2+\delta)\,. \qquad \text{(IV-18)}$$

Using (IV-17) and (IV-18) we have

$$\phi^{++}(\vec{r}) = \frac{(1+\beta)}{2(m^2-P_1^2)}\,\bar{u}(\vec{r})\left[(F-H\delta\gamma_0)\not{U} - \frac{(G-I\delta\gamma_0)}{m}U\cdot P_1\right]C\bar{u}^T(-\vec{r}), \qquad \text{(IV-19)}$$

and

$$\phi^{-+}(\vec{r}) = \frac{-(1-\beta)}{2(m^2-P_1^2)}\,\bar{V}(-\vec{r})\left[(F-2H-H\delta\gamma_0)\not{U} - (G-2I-I\delta\gamma_0)U\cdot P_1\right]C\bar{u}^T(-\vec{r}). \qquad \text{(IV-20)}$$

Next, we use

$$P_1^0 = M_d - (\vec{r}^{\,2}+m^2)^{\frac{1}{2}} \cong 2m - \frac{\alpha^2}{m} - m\left(1+\frac{\vec{r}^{\,2}}{2m^2}\right) \;, \qquad \text{(IV-21)}$$

to write

$$m^2 - P_1^2 \cong 2(\vec{r}^{\,2}+\alpha^2) \;, \qquad \text{(IV-22)}$$

$$\delta = \frac{E_1}{m}(1-\beta) \cong 1-\beta \cong \frac{\vec{r}^{\,2}+\alpha^2}{m^2} \;, \qquad \text{(IV-23)}$$

and

$$1+\beta \cong 2 - \frac{\alpha^2}{m^2} - \frac{r^2}{m^2} \quad . \tag{IV-24}$$

Retaining only terms thru order $\vec{r}^{\,2}/m^2$, we can now use (IV-15) and (IV-16) and the matrix conventions in appendix A to rewrite (IV-19) and (IV-20) as

$$\phi^{++}_{(\lambda)}(\vec{r}) = \frac{i}{2(\vec{r}^{\,2}+\alpha^2)} \chi^T_{1(\lambda)} \left\{ \vec{U}^{(\lambda)}\cdot\vec{\sigma} \left[F\left(1 - \frac{\alpha^2}{2m^2} - \frac{\vec{r}^{\,2}}{4m^2}\right) - H\left(\frac{\vec{r}^{\,2}+\alpha^2}{m^2}\right)\right] \right. \tag{IV-25}$$

$$\left. + \frac{(\vec{U}^{(\lambda)}\cdot\vec{r})(\vec{\sigma}\cdot\vec{r})}{m^2} \left[F\left(-\frac{1}{2} + \frac{\alpha^2}{4m^2} + \frac{\vec{r}^{\,2}}{4m^2}\right) - H\left(\frac{\vec{r}^{\,2}+\alpha^2}{2m^2}\right) + G\left(1 - \frac{\alpha^2+\vec{r}^{\,2}}{2m^2}\right)\right]\right\} \sigma_2 \chi_{2(\lambda)} ,$$

and

$$\phi^{-+}_{(\lambda)}(\vec{r}) = \frac{-i}{4m^2} \chi^T_{1(\lambda)} \left\{ \frac{\vec{U}^{(\lambda)}\cdot\vec{r}}{m} \left[-F + 2H + G\left(1 - \frac{\vec{r}^{\,2}}{4m^2}\right) \right. \right. \tag{IV-26}$$

$$\left. \left. - I\left(2 + \frac{\vec{r}^{\,2}}{2m^2} + \frac{\alpha^2}{m^2}\right)\right] - \frac{\vec{\sigma}\cdot\vec{U}^{(\lambda)}\times\vec{r}}{m} \left[H\,\frac{(\vec{r}^{\,2}+\alpha^2)}{m^2}\right]\right\} \sigma_2 \chi_{2(\lambda)} .$$

Now, using equations (IV-5), (IV-13), and (IV-14), we compare coefficients of the independent spin matrix combinations to obtain

$$H = 0 \quad , \tag{IV-27}$$

$$-F + G\left(1 - \frac{\vec{r}^{\,2}}{4m^2}\right) + I\left(-\frac{\vec{r}^{\,2}}{2m^2} - \frac{\alpha^2}{m^2}\right) = 0 \quad , \tag{IV-28}$$

$$u_0(r) - \frac{1}{\sqrt{2}} W_2(r) = \frac{1}{\sqrt{8\pi}} \left[F\left(1 - \frac{\alpha^2}{2m^2} - \frac{\vec{r}^{\,2}}{4m^2}\right)\right] \frac{1}{\vec{r}^{\,2}+\alpha^2} \quad , \tag{IV-29}$$

and

$$\frac{3m^2 W_2(r)}{\sqrt{2}\,\vec{r}^{\,2}} = \frac{1}{\sqrt{8\pi}}\left[F\left(-\frac{1}{2}+\frac{\alpha^2+\vec{r}^{\,2}}{4m^2}\right)+\left(1-\frac{\alpha^2+\vec{r}^{\,2}}{2m^2}\right)\right]\frac{1}{\vec{r}^{\,2}+\alpha^2}\,. \tag{IV-30}$$

Then, combining (IV-27)-(IV-30) we obtain a prescription for the dNN vertex invariants in terms of phenomenological deuteron s and d state wave functions which is

$$F = \sqrt{8\pi}\,(\vec{r}^{\,2}+\alpha^2)\left(1+\frac{\alpha^2}{2m^2}+\frac{r^2}{4m^2}\right)\left[u_0(r)-\frac{1}{\sqrt{2}}\,W_2(r)\right], \tag{IV-31}$$

$$G = \frac{3m^2\sqrt{8\pi}}{\sqrt{2}}\left(1+\frac{\alpha^2}{\vec{r}^{\,2}}\right)\left(1+\frac{\alpha^2+\vec{r}^{\,2}}{2m^2}\right)W_2(r) + \frac{F}{2}\;, \tag{IV-32}$$

$$H = 0 \tag{IV-33}$$

and

$$I = \frac{1}{2}\,(G-F)\left(1-\frac{\vec{r}^{\,2}+\alpha^2}{2m^2}\right) - \frac{\vec{r}^{\,2}F}{8m^2}\,. \tag{IV-34}$$

A remark is in order concerning equation (IV-33). This is in direct contradiction to our PCAC result (equation (II-7)), and Gross himself points out that it is in disagreement with estimates of H based on single-pion-exchange calculations.[49] His argument is that, by using (IV-31)-(IV-34), we are entitled to take H = 0 because the error is compensated by adjustments in F, G, and I due to the fact that they are determined from experimental non-relativistic wave functions. In the next section, we make some speculative remarks about the behavior of the antiparticle contribution to ϕ_d, ϕ^{-+}, and derive an alternative prescription for the dNN vertex function. In Chapter V, we show that there is very little difference in cross sections calculated using the two procedures.

Rederivation of dNN Vertex Invariants

Examination of the square brackets in the expression for ϕ^{-+} shows a part not explicitly of order $\vec{r}^{\,2}/m^2$ given by

$$-F + 2H + G - 2I \ . \qquad \text{(IV-35)}$$

Using equation (IV-22), we can write

$$F(\rho_1^2) = F_0 + \mathcal{O}(\vec{r}^{\,2}/m^2) ,$$

with similar expressions for the other invariants. Thus (IV-35) may be written

$$-F_0 + 2H_0 + G_0 - 2I_0 + \mathcal{O}(\vec{r}^{\,2}/m^2) , \qquad \text{(IV-36)}$$

and we see that the behavior of ϕ^{-+} for $\vec{r}^{\,2}/m^2 \ll 1$ is dominated by the term

$$-F_0 + 2H_0 + G_0 - 2I_0 \ . \qquad \text{(IV-37)}$$

In Chapter VI we develop a consistency condition on the dNN vertex function, based on the formal field-theoretical PCAC hypothesis and the assumption that the Austern-model resonance amplitude for pion disintegration of the deuteron, extrapolated off the pion mass shell, gives the correct behavior of the non-pole part of the pion disintegration amplitude in the limit of zero momentum transfer. The consistency condition is

$$F_o - 2H_o = 0 \tag{II-7}$$

and implies that the residual term in Φ^{-+} is

$$G_o - 2I_o \tag{IV-38}$$

Now, we have the very interesting question as to whether or not the symmetric relation,

$$G_o - 2I_o \doteq 0 \tag{II-8}$$

also holds. This question is important, as the vanishing or non-vanishing of (IV-38) makes a difference of a factor of order $\vec{r}^{\,2}/m^2$ in the relative contributions of Φ^{++} and Φ^{-+} to the relativistic deuteron wave function Φ_d given in equation (IV-2), and thus has direct bearing on the importance of anti-nucleon contributions to deuteron processes near the mass shell.

As an alternative to Gross' prescription (IV-31) – (IV-34), we speculate that equation (II-8) is valid, and we make the approximate assignments

$$H = \frac{F}{2} \; , \; I = \frac{G}{2} \tag{IV-39}$$

where we commit an error no worse than of order $\vec{r}^{\,2}/m^2$ in H and I, and hence no worse than of order $\vec{r}^{\,4}/m^4$ in the dNN vertex function. Using

(IV-39) we obtain the identifications for F and G given by

$$F = \sqrt{8\pi}\,(\vec{r}^{\,2}+\alpha^2)\left(1+\frac{3\vec{r}^{\,2}}{4m^2}+\frac{\alpha^2}{m^2}\right)\left[u_0(r)-\frac{1}{\sqrt{2}}W_2(r)\right] , \qquad \text{(IV-40)}$$

and

$$G = \frac{3m^2(\vec{r}^{\,2}+\alpha^2)\sqrt{8\pi}}{\sqrt{2}\,\vec{r}^{\,2}}\left(1+\frac{\vec{r}^{\,2}+\alpha^2}{2m^2}\right)W_2(r)+\frac{F}{2} \qquad \text{(IV-41)}$$

Comparing our prescription (IV-39) - (IV-41) to Gross', (IV-31)-(IV-34), we see that F and G are virtually the same while H is very different, with ours consistent with PCAC, and I is apparently different. We say apparently different because examination of equations (II-5) and (II-6) shows that for a ρ of three percent we have the relation

$$\frac{G_0}{F_0} \cong 25 \qquad \text{(IV-42)}$$

Consequently, for $\vec{r}^{\,2}/m^2 \ll 1$, we expect G to be much larger than F, and this implies that Gross' expression for I and ours are quantitatively approximately the same. Indeed, in Chapter V, we show that cross sections calculated using the two prescriptions are essentially the same. In that Chapter, we show that the total cross section for pion disintegration is critically dependent on the form chosen for I in that, using either (IV-34) or (IV-39), we obtain a result consistent with experiment, while a different choice for I (I = 0) results in drastic modification of the cross section which is most significant at intermediate energies (see Figure 13). This result indicates that cross sections are sensitive to the form chosen for I, and strengthens our belief in the correctness of (II-8) in that it leads to agreement with experiment, whereas a significant deviation from (II-8) leads to severe disagreement with experiment. Even if this does not conclusively prove (II-8), it at least establishes that G and I are of the same order of magnitude near the mass shell.

We close this section with some practical remarks concerning the use of (IV-31) - (IV-34) or (IV-39) - (IV-41) in scattering calculations. These equations are of the form

$$F(P^2) = f(|\vec{r}|) , \qquad \text{(IV-43)}$$

where the functional form on the left is independent of reference frame by virtue of its invariant argument, while the functional form on the right is dependent on choice of reference frame. In the processes we consider, such as that shown in Figure 3, Chapter II, the restriction $\vec{d} = 0$ in our identifications above implies that (IV-31) - (IV-34) and (IV-39)-(IV-41) hold only in the rest frame of the deuteron, which is usually the laboratory frame. However, the Austern model amplitudes of Chapter III are evaluated in the center of mass frame of the deuteron and the incoming pion or photon, and we would like to perform calculations in this frame. Thus, we need to know how the functional correspondence in (IV-43) changes when we transform to the center-of-mass frame. To do this, we consider the invariant

$$r^2 = r_{LAB}^{o2} - \vec{r}_{LAB}^{\,2} = r_{CM}^{o2} - \vec{r}_{CM}^{\,2} . \qquad \text{(IV-44)}$$

Now, in general

$$r^0 = \frac{d^0}{2} - \left(m^2 + \left[\frac{\vec{d}}{2} - \vec{r}\right]^2\right)^{\frac{1}{2}}$$

so,

$$r^{0\,2} = \frac{M_d^2 + \vec{d}^{\,2}}{4} - \left(M_d^2 + \vec{d}^{\,2}\right)^{\frac{1}{2}}\left(m^2 + \left[\frac{\vec{d}}{2} - \vec{r}\right]^2\right)^{\frac{1}{2}} + m^2 + \left(\frac{\vec{d}}{2} - \vec{r}\right)^2.$$

In the processes we consider, $\vec{d}^{\,2}/m^2 \ll 1$ and $\vec{r}^{\,2}/m^2 \ll 1$ (about 10 percent), so we obtain

$$r^{0\,2} \cong -\frac{\vec{d}^{\,2}}{8m^2}\left(\frac{\vec{d}}{2} - \vec{r}\right)^2. \qquad \text{(IV-45)}$$

Thus, in the lab frame, $r^{0\,2}_{LAB} = 0$, while in the center-of-mass frame for deuteron disintegration, $\vec{d} = -\vec{q}$ and $\vec{r} = \vec{K} - \vec{q}$ where $\vec{K}$ is the relative momentum of the physical outgoing nucleons. Thus (IV-45) becomes

$$r^{0\,2}_{CM} \cong -\frac{\vec{q}^{\,2}\vec{K}^2}{8m^2}$$

and (IV-44) yields

$$\vec{r}^{\,2}_{LAB} = \vec{r}^{\,2}_{CM} + \frac{\vec{q}^{\,2}\vec{K}^2}{8m^2}$$

However, $\vec{q}^{\,2}\vec{K}^2/8m^2 \ll \vec{r}^{\,2}_{CM}$ for the processes we consider (about one percent), and we can use

$$F(P^2) = f(|\vec{r}_{CM}|) \qquad \text{(IV-46)}$$

without appreciable error.

CHAPTER V

PION AND PHOTODISINTEGRATION OF THE DEUTERON

In this Chapter we examine the background amplitudes for pion and photodisintegration of the deuteron, and present the total and differential cross sections for both processes, using both George's parametric procedure, and the phenomenological method discussed in Chapter IV. This method appears to have been over-looked by other authors, and to our knowledge, this is the first application of this method to deuteron disintegration. The procedure used to calculate the cross sections is discussed in Appendix A. The diagrams corresponding to the background amplitudes in the George model are given in Figures 11 and 12.

Pion Disintegration of the Deuteron

The amplitude corresponding to the first diagram in Figure 11 is

$$i\sqrt{2}\, g_{N\pi}\, \bar{u}(P_1)\, \gamma_5 \frac{(\not{P}_1 - \not{q} + m)}{D(t)} \times \tag{V-1}$$

$$\left\{ F(t)\not{U} - \frac{G(t)}{m} U\cdot(P_1 - q) + \frac{(\not{P}_1 - \not{q} - m)}{m}\left[H(t)\not{U} - \frac{I(t)}{m} U\cdot(P_1 - q)\right]\right\} C\,\bar{u}^T(P_2),$$

where we have used (I-10) and defined $D(t) = t - m^2$. The reduction of (V-1) proceeds with the elimination of $\not{P}_1$, using the Dirac equation. It is then grouped into elementary terms which are easily expressed in terms of the amplitudes of Table 1, and the antisymmetrized amplitude is formed

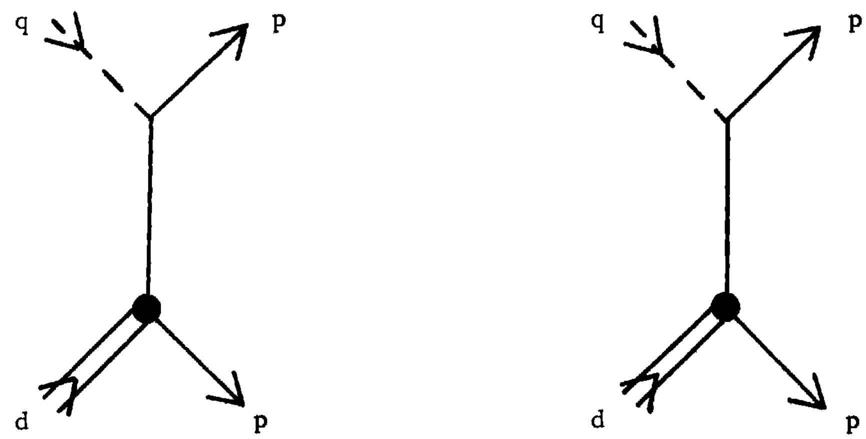

Figure 11. Background Amplitudes for Pion Disintegration of the Deuteron

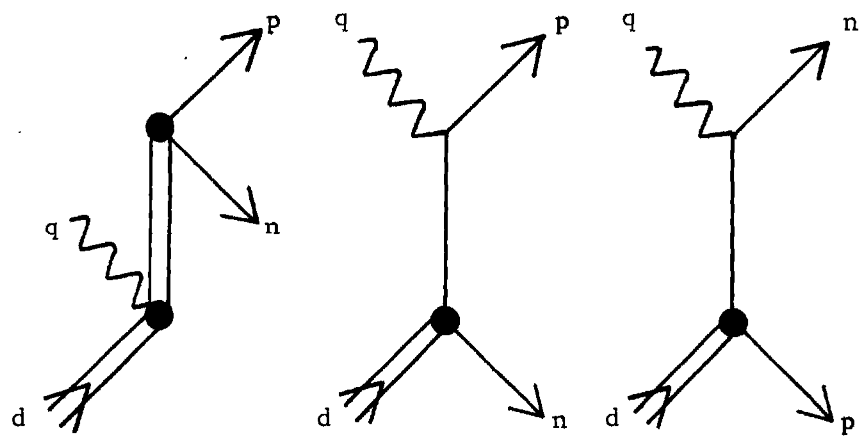

Figure 12. Background Amplitudes for Photodisintegration of the Deuteron

using equation (I-27). The resulting coefficients are given in Table 11.

Cross Section Using George's Background

George used the dNN vertex function given by equations (II-9) and (II-10), with F_0 and G_0 evaluated using the representations given by (II-5) and (II-6). As discussed in Chapter II, the value of the asymptotic d-to-s ratio ρ, as determined from low energy nucleon scattering, is approximately three percent. George found that with a ρ of three percent, the cross section calculated using the background terms alone exceeded the experimental cross section at the resonant peak. His procedure was to use ρ, in the background amplitudes of Table 11, and Λ, appearing in the resonant amplitudes of Table 8, as adjustable parameters. He also found it necessary to adjust m^* from its accepted value of 1236 MeV, as determined from pion-nucleon scattering. Since we found some algebraic discrepancies in George's resonant amplitudes, we have recalculated his total cross section and find the result shown as the curve labeled GEORGE in Figure 13, corresponding to $\Lambda = 4.13\alpha$, $\rho = 0.6$, and m^* = 1210 MeV. This curve represents an improvement over George's reported result in that his curve does not fit the data at high energies, and the value of 1210 MeV for m* is closer to the accepted value than his reported 1190 MeV. Again we emphasize that this is just the result of a numerical re-analysis of George's work, and contains nothing new. The corresponding differential cross sections for center-of-mass pion kinetic energies of 40, 76, 140, and 180 MeV are given by the curves labeled GEORGE, in Figures 14, 15, 16, and 17.

---

*See the footnote on page 37.

Table 11. Invariant Coefficients for the Background Amplitude in Pion Disintegration of the Deuteron

i	$B_i^\pi = g_{N\pi}\left[\mathcal{C}_i^\pi(s,t,u) - \varepsilon_i \mathcal{C}_i^\pi(s,u,t)\right]$
1	$-i\,2\sqrt{2}\,m\,g_{N\pi}\left[\frac{F(t)}{D(t)} + \frac{F(u)}{D(u)} - \frac{I(t)+I(u)}{2m^2}\right]$
2	$-i\sqrt{2}\,g_{N\pi}\left[\frac{I(t)-I(u)}{m}\right]$
3	$i\sqrt{2}\,g_{N\pi}\left[\frac{H(t)+H(u)}{m}\right]$
4	$-i\sqrt{2}\,m\,g_{N\pi}\left[\frac{F(t)}{D(t)} - \frac{F(u)}{D(u)}\right]$
5	$-i\sqrt{2}\,m\,g_{N\pi}\left[\frac{G(t)}{D(t)} + \frac{G(u)}{D(u)}\right]$
6	$i\sqrt{2}\,m\,g_{N\pi}\left[\frac{G(t)}{D(t)} - \frac{G(u)}{D(u)}\right]$

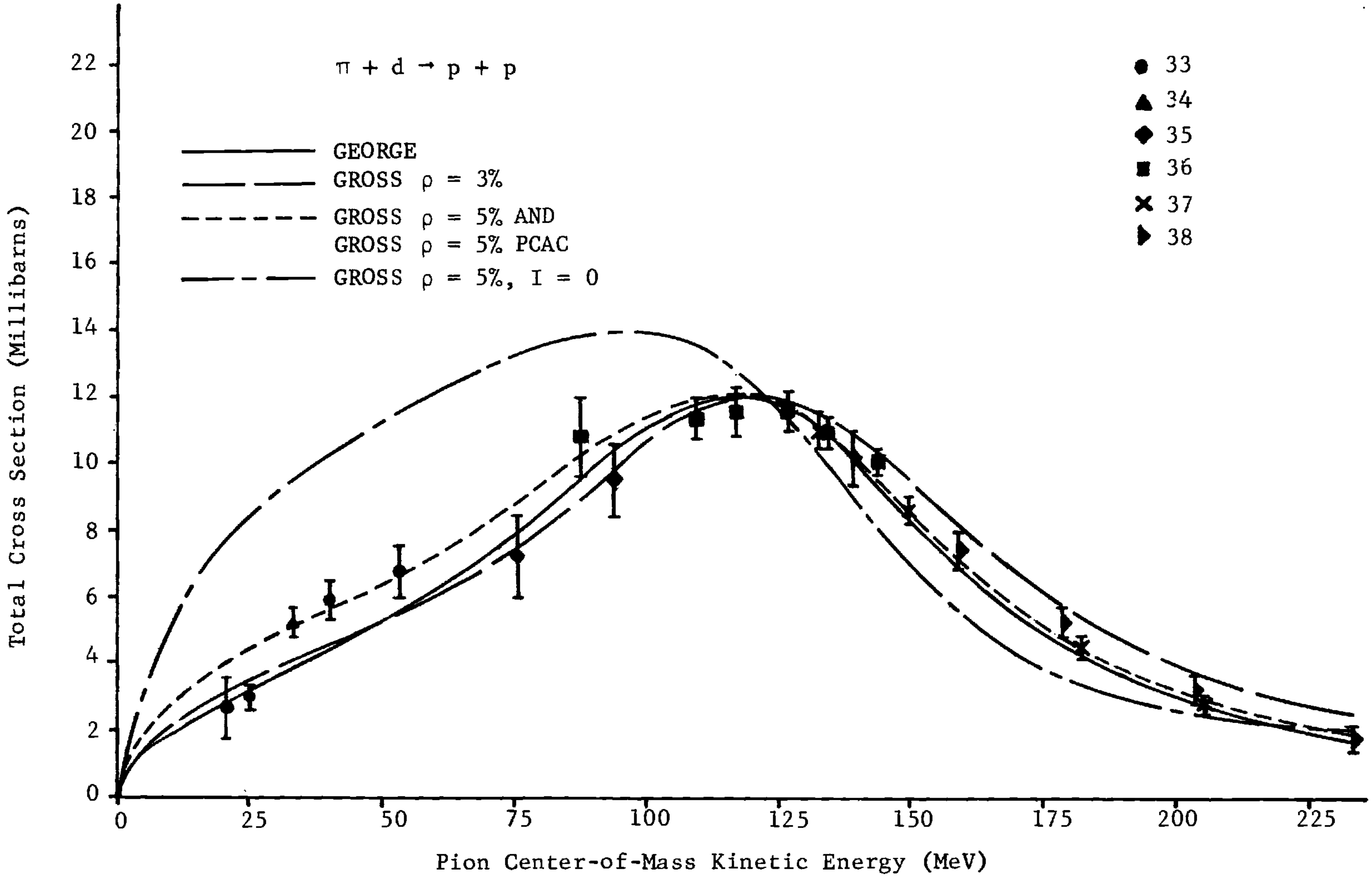

Figure 13. Total Cross Section for Pion Disintegration of the Deuteron

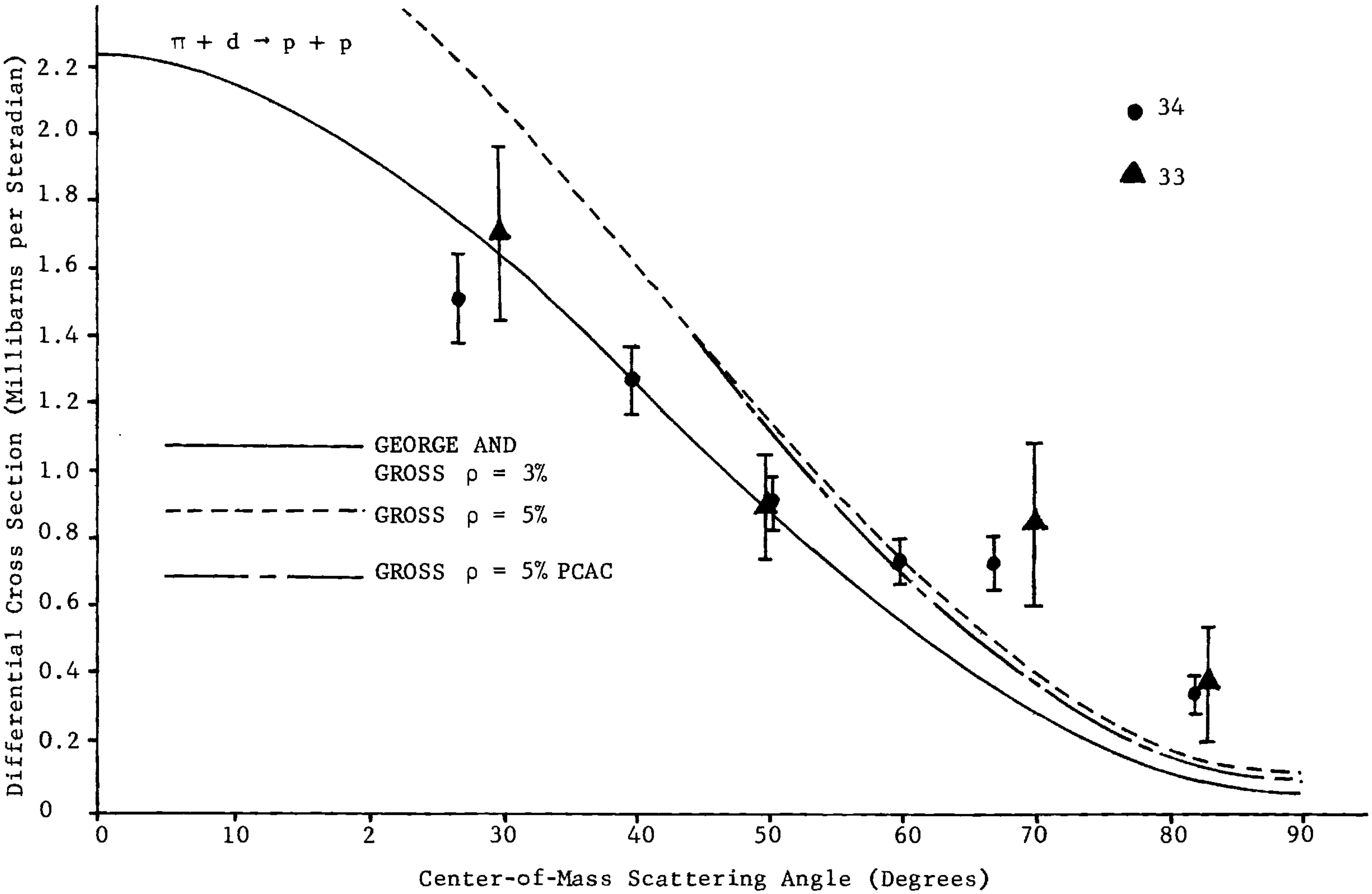

Figure 14. Center-of-Mass Differential Cross Section for T_{CM} = 40 MeV

Cross Section Using the Phenomenological Vertex Invariants

In Appendix B we give a discussion of phenomenological deuteron s and d state wave functions determined by selecting general Hulthen forms and adjusting the associated parameters to be consistent with the observed properties of the deuteron.[45] To allow an additional degree of freedom in fitting the nucleon-nucleon triplet scattering data at higher energies, a hard core radius is also introduced.

The most significant physical properties affecting the resulting wave functions are the hard core radius x_c, and the asymptotic d-to-s admixture ratio ρ. Wave functions corresponding to hard core radii of 0.0 f, 0.432 f, and 0.561 f, and values of ρ of three, four, and five percent were considered for the present analysis. Using the forms given in Appendix B to construct the invariants given in Chapter IV, we found that a nonzero hard-core radius gives much too large a result for the high-energy total cross section. Consequently, we have chosen $X_c = 0$ and have determined the total and differential cross sections for the three values of ρ. These are displayed with the label GROSS for ρ = three and five percent in Figures 13 - 17. The curves for ρ = four percent are intermediate between the other two, and we have omitted them for clarity. We note that, for a center-of-mass pion kinetic energy T_π = 140 MeV, the differential cross sections produced by George's method, and using the ρ = three percent Gross invariants are indistinguishable, but separate at higher energies. We also note that the modification of Gross' identification procedure suggested at the end of Chapter IV produces insignificant changes in the total cross section and the low-energy differential cross section, but begins to show a slight effect in the differen-

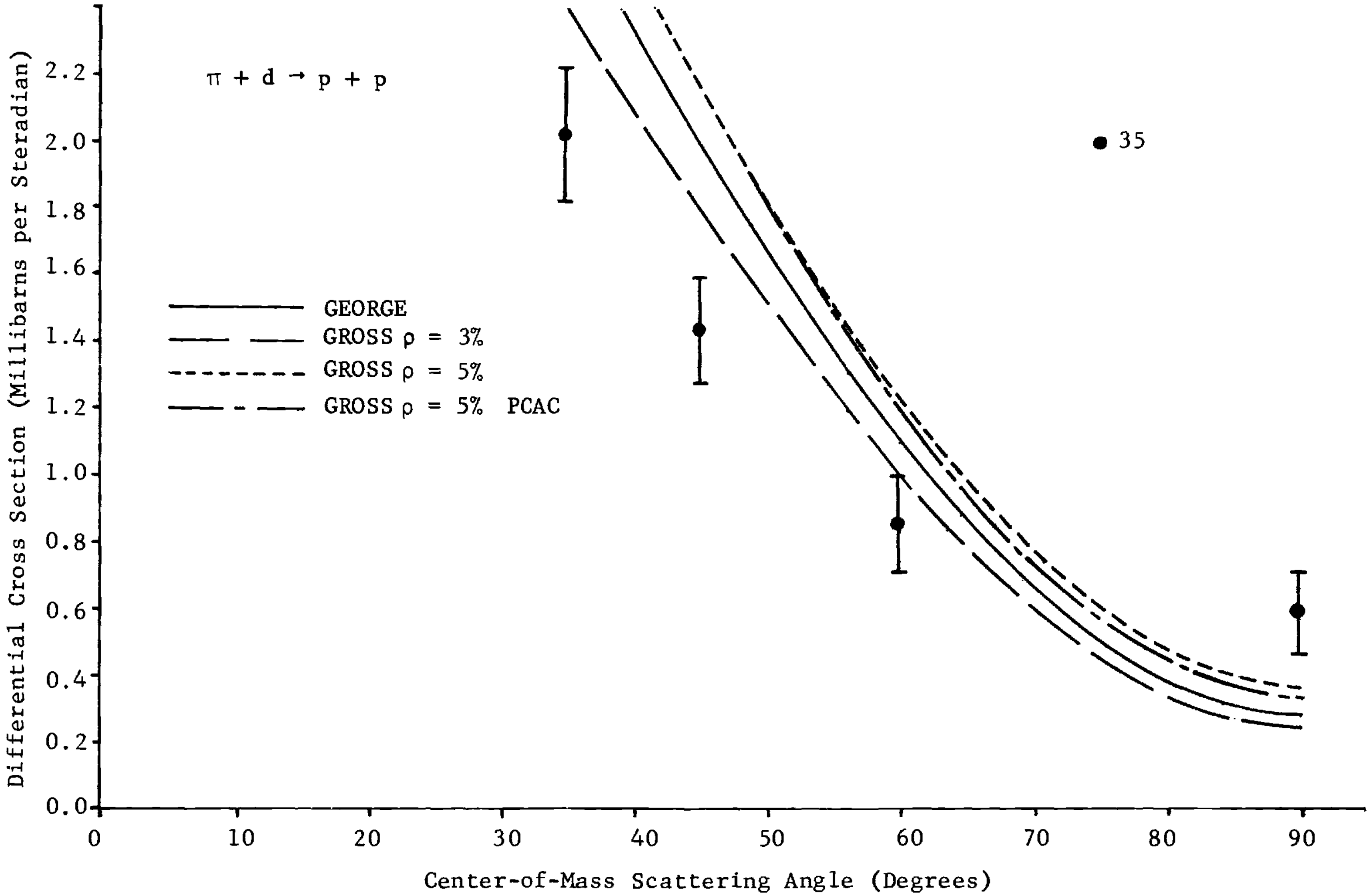

Figure 15. Center-of-Mass Differential Cross Section for T_{CM} = 76 MeV

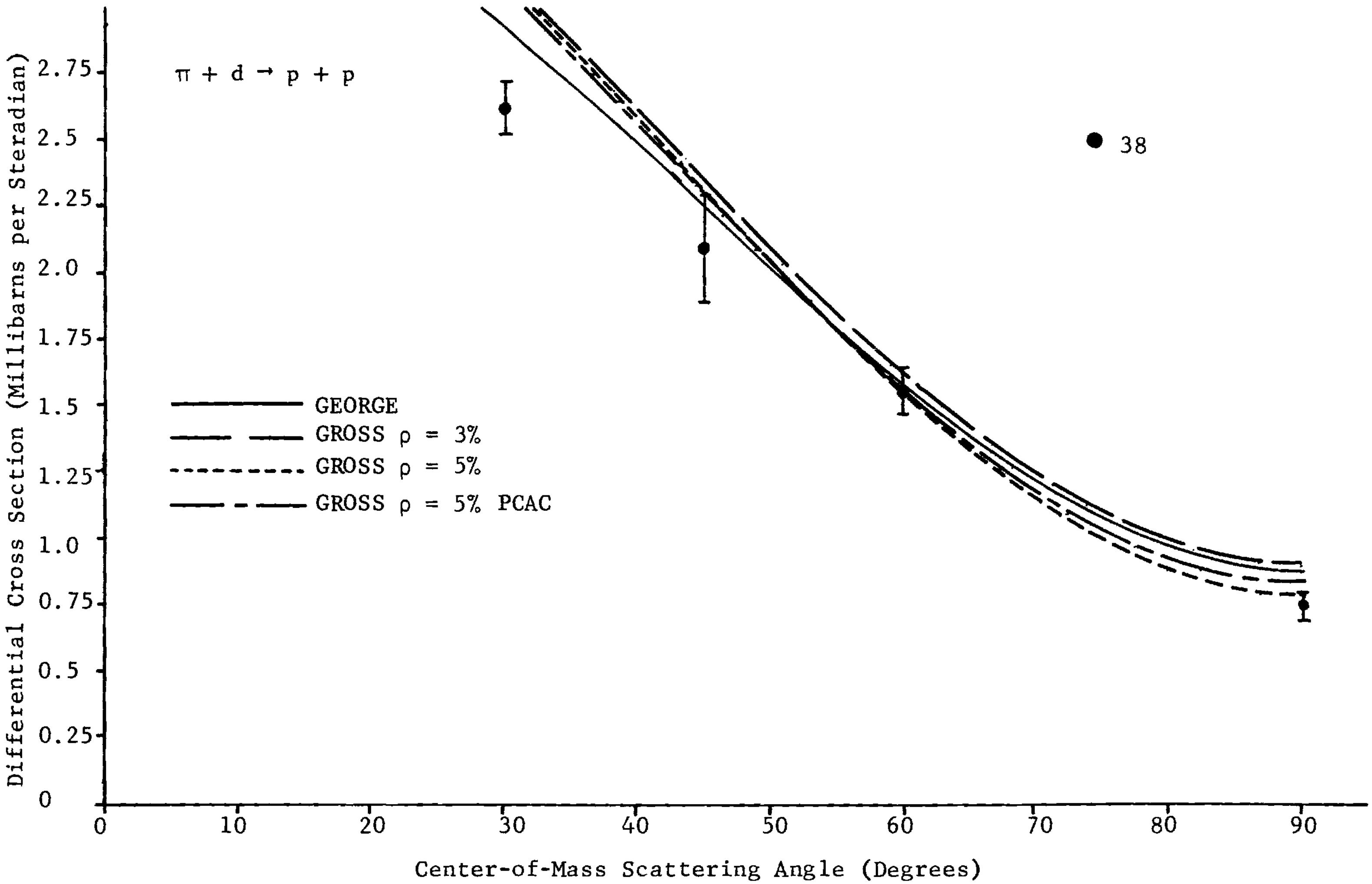

Figure 16. Center-of-Mass Differential Cross Section for T_{CM} = 140 MeV

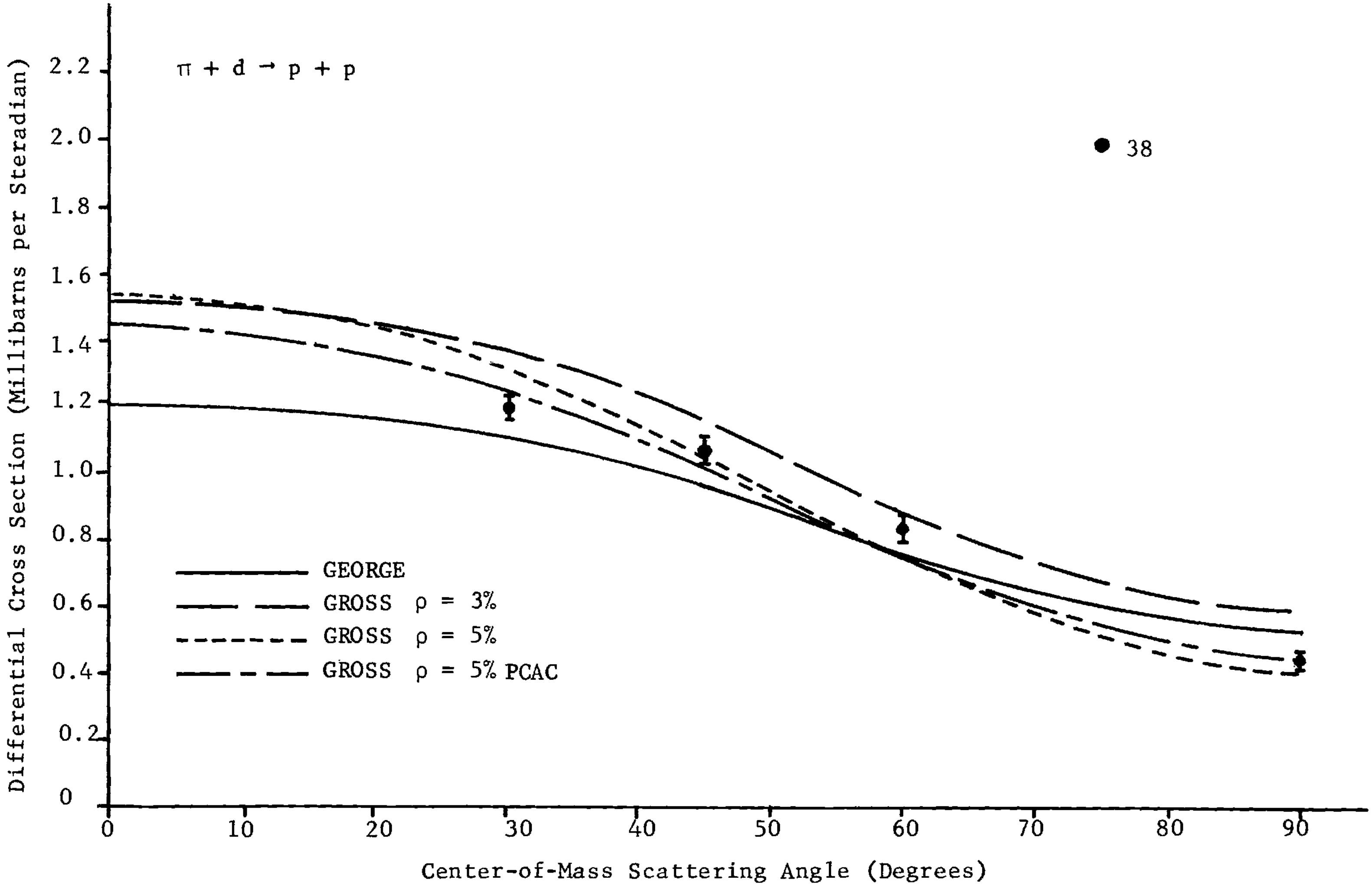

Figure 17. Center-of-Mass Differential Cross Section for T_{CM} = 180 MeV

tial cross section at higher energies. These curves are labeled GROSS PCAC in Figures 13 - 17. We have also considered the effect of neglecting I in the phenomenological dNN vertex function to estimate how critically the cross section depends on the form chosen for this function. The result is shown in the curve labeled GROSS I = 0 in Figure 13.

To summarize the results for pion disintegration of the deuteron, we note that by using either George's method, or Gross' invariants, the total cross section is adequately reproduced at the peak and at higher energies. At lower energies, the Gross or Gross PCAC invariants with $\rho =$ five percent seem to give the best fit, although there is sufficient scatter in the experimental data to make this conclusion questionable. For the differential cross section, both methods give acceptable results, and there is no basis for selecting one over the other, except that the GROSS PCAC result for $\rho =$ five percent seems to give the best fit at high energies.

We have shown that, for pion disintegration of the deuteron, the background amplitude may be systematically constructed from triplet nucleon scattering data using a method presumably generally applicable to any process involving the deuteron at comparable energies, and have obtained results equal or superior to George's essentially mathematical treatment of this amplitude.

Photodisintegration of the Deuteron

The Nucleon-Pole Amplitude

The amplitude corresponding to the nucleon-pole diagrams in Figure 12 is given by

$$e\,\bar{u}(p_1)\left[\not\epsilon + \frac{\chi_p}{2m}\not q\not\epsilon\right]\frac{(\not p_1-\not q+m)}{D(t)}\times \tag{V-2}$$

$$\left\{F(t)\not U - \frac{G(t)}{m}U\cdot(p_1-q) + \left(\frac{\not p_1-\not q-m}{m}\right)\left[H(t)\not U - \frac{I(t)}{m}U\cdot(p_1-q)\right]\right\}C\bar{u}^T(p_2)$$

$$+e\,\bar{u}(p_2)\frac{\chi_n}{2m}\not q\not\epsilon\,\frac{(\not p_2-\not q+m)}{D(u)}\times$$

$$\left\{F(u)\not U - \frac{G(u)}{m}U\cdot(p_2-q) + (\not p_2-\not q-m)\left[H(u)\not U - \frac{I(u)}{m}U\cdot(p_2-q)\right]\right\}C\bar{u}^T(p_1)\,,$$

where $\chi_p = 1.793$ and $\chi_n = -1.913$ are the anomolous magnetic moments of the proton and neutron, in units of the Bohr nuclear magneton $e/2m$, and determine the Pauli coupling of the photon to the nucleon.

The reduction of (V-2) proceeds by eliminating $\not p_1$ and $\not p_2$ using the Dirac equation. The second term is then transposed, and the resulting amplitude is grouped into elementary forms which are then reduced to invariant coefficients multiplying the invariant amplitudes of Table 4. The reduction is accomplished using the prescription given in Table 9, and the isoscalar and isovector amplitudes are constructed using equations (I-31) and (I-32). Using the convention $S = +1$ for isoscalar and -1 for isovector, the amplitudes for Dirac coupling are given in Table 12, and the amplitudes for Pauli coupling are given in Table 13. We note that the F and G terms in the coefficients agree with George except for a relative sign in the second Dirac coefficient and the overall sign of the twelfth Dirac and Pauli coefficients.

The Deuteron-Pole Amplitude

This amplitude involves the dNN vertex function with the deuteron

Table 12. Dirac Nucleon-Pole Invariant Coefficients for Photodisintegration of the Deuteron. $\mathcal{S} = +1$ for Isoscalar and -1 for Isovector Amplitudes.

i	$\left(\frac{e}{2}\right)\left[C_i^{\tau}(s,t,u) + \mathcal{S}\,\varepsilon_i C_i(s,u,t)\right]$
1	$me\left\{\frac{G(t)}{D(t)} + \mathcal{S}\frac{G(u)}{D(u)} + \frac{H(t)+\mathcal{S}H(u)}{q\cdot Q}\right\}$
2	$me\left\{\frac{q\cdot k}{q\cdot Q}\left[\frac{G(t)}{D(t)} + \mathcal{S}\frac{G(u)}{D(u)}\right] + \frac{H(t)-\mathcal{S}H(u)}{q\cdot Q} + \frac{I(t)-\mathcal{S}I(u)}{2q\cdot Q}\right\}$
3	$me\left\{\frac{-m^2}{q\cdot Q}\left[\frac{G(t)}{D(t)} - \mathcal{S}\frac{G(u)}{D(u)}\right]\right\}$
4	$me\left\{\frac{m^2}{q\cdot Q}\left[\frac{F(t)}{D(t)} - \mathcal{S}\frac{F(u)}{D(u)}\right] - \frac{I(t)-\mathcal{S}I(u)}{4q\cdot Q}\right\}$
5	$me\left\{\frac{F(t)}{D(t)} + \mathcal{S}\frac{F(u)}{D(u)}\right\}$
6	0
7	$me\left\{\frac{I(t)-\mathcal{S}I(u)}{4q\cdot Q}\right\}$
8	$me\left\{-\frac{1}{2}\left[\frac{G(t)}{D(t)} + \mathcal{S}\frac{G(u)}{D(u)}\right] + \frac{1}{4m^2}\left[1 - \frac{2Q^2}{q\cdot Q}\right]\left[I(t)+\mathcal{S}I(u)\right]\right\}$
9	$me\left\{\frac{1}{2}\left[\frac{G(t)}{D(t)} - \mathcal{S}\frac{G(u)}{D(u)}\right] + \frac{I(t)-\mathcal{S}I(u)}{4q\cdot Q} - \frac{q\cdot k}{4m^2 q\cdot Q}\left[I(t)+\mathcal{S}I(u)\right]\right\}$
10	$me\left\{\frac{I(t)-\mathcal{S}I(u)}{4q\cdot Q} - \frac{q\cdot k}{4m^2 q\cdot Q}\left[I(t)+\mathcal{S}I(u)\right]\right\}$
11	$me\left\{-\frac{H(t)+\mathcal{S}H(u)}{2q\cdot Q} + \frac{I(t)+\mathcal{S}I(u)}{4m^2}\right\}$
12	$me\left\{\frac{F(t)}{D(t)} - \mathcal{S}\frac{F(u)}{D(u)} + \frac{k^2}{2m^2 q\cdot Q}\left[I(t)-\mathcal{S}I(u)\right] - \frac{q\cdot k}{2m^2 q\cdot Q}\left[I(t)+\mathcal{S}I(u)\right]\right\}$

Table 13. Pauli Nucleon-Pole Invariant Coefficients for Photodisintegration of the Deuteron. $\mathcal{S} = +1$ for Isoscalar and -1 for Isovector Amplitudes

i	$\left(\frac{e}{2}\right)\left[C_i^r(s,t,u) + \mathcal{S}\,\mathcal{E}_i\, C_i(s,u,t)\right]$
1	0
2	$me(\mathcal{K}_p + \mathcal{S}\mathcal{K}_n)\left\{-\frac{G(t)}{D(t)} + \frac{\mathcal{S}\,G(u)}{D(u)}\right\}$
3	0
4	$me(\mathcal{K}_p + \mathcal{S}\mathcal{K}_n)\left\{\frac{1}{2}\left[\frac{G(t)}{D(t)} - \mathcal{S}\frac{G(u)}{D(u)}\right]\right\}$
5	$me(\mathcal{K}_p + \mathcal{S}\mathcal{K}_n)\left\{\frac{F(t)}{D(t)} + \mathcal{S}\frac{F(u)}{D(u)} + \frac{H(t)+\mathcal{S}H(u)}{2m^2}\right\}$
6	$me(\mathcal{K}_p + \mathcal{S}\mathcal{K}_n)\left\{\frac{1}{2}\left[\frac{G(t)}{D(t)} + \mathcal{S}\frac{G(u)}{D(u)}\right]\right\}$
7	0
8	$me(\mathcal{K}_p + \mathcal{S}\mathcal{K}_n)\left\{-\frac{1}{2}\left[\frac{G(t)}{D(t)} + \mathcal{S}\frac{G(u)}{D(u)}\right] - \frac{I(t)+\mathcal{S}I(u)}{4m^2}\right\}$
9	$me(\mathcal{K}_p + \mathcal{S}\mathcal{K}_n)\left\{\frac{I(t)-\mathcal{S}I(u)}{4m^2}\right\}$
10	$me(\mathcal{K}_p + \mathcal{S}\mathcal{K}_n)\left\{\frac{1}{2}\left[\frac{F(t)}{D(t)} - \mathcal{S}\frac{F(u)}{D(u)}\right] - \frac{1}{2}\left[\frac{G(t)}{D(t)} - \mathcal{S}\frac{G(u)}{D(u)}\right]\right\}$
11	$\frac{me(\mathcal{K}_p + \mathcal{S}\mathcal{K}_n)}{2}\left\{\frac{F(t)}{D(t)} + \mathcal{S}\frac{F(u)}{D(u)}\right\}$
12	$me(\mathcal{K}_p + \mathcal{S}\mathcal{K}_n)\left\{\frac{F(t)}{D(t)} - \mathcal{S}\frac{F(u)}{D(u)} - \frac{K^2}{m^2}\left[\frac{G(t)}{D(t)} - \mathcal{S}\frac{G(u)}{D(u)}\right] + \frac{H(t)-\mathcal{S}H(u)}{2m^2}\right\}$

off the mass shell, and the $d\gamma d$ vertex function with the deuteron off the mass shell. The dNN vertex function was described in Chapter II and the form appropriate to an off-shell deuteron was given in equation (II-3), which we repeat here for reference

$$\Gamma_{dNN}(d'^2) = A'(d'^2)\,U'\cdot d' + F(d'^2)\not{U}' - \frac{G(d'^2)}{m}\,U'\cdot p \;, \tag{II-3}$$

and again we emphasize that nothing is known about the d' dependence of the vertex invariants F and G or the function A'.

We can determine the general form of the $d\gamma d$ vertex function using invariance arguments. The diagram for the vertex is shown in Figure 18. The conditions on the vertex are

$$\epsilon\cdot q = U\cdot d = 0 \;,\quad q^2 = 0 \;,\quad d^2 = M_d^2 \;, \tag{V-3}$$

and

$$q + d = d' \;. \tag{V-4}$$

Equation (V-4) implies that there are only two independent momenta associated with the vertex, and we choose the pair

$$q = d' - d \;,\quad X = d' + d \;. \tag{V-5}$$

The available scalars are

$$q^2 = d'^2 - 2\,d'\cdot d + M_d^2 = 0 \;, \tag{V-6}$$

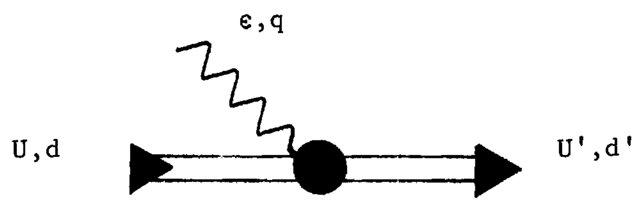

Figure 18. Diagram for the drd Vertex Function

$$q \cdot X = d'^2 - M_d^2 , \tag{V-7}$$

and

$$X^2 = d'^2 + 2\, d \cdot d' + M_d^2 \;, \tag{V-8}$$

where we have used (V-3). It is clear from (V-6)--(V-8) that there is only one independent scalar variable, and we choose d'^2. Lorentz invariance requires that the $d\gamma d$ vertex function be a scalar. It must be linear in ϵ, U and U' and it can be composed of the independent momentum vectors associated with the vertex, and the metric tensor $g_{\mu\nu}$. The general form is

$$\epsilon^{\alpha} U^{\beta} U'^{\beta'} T_{\alpha\beta\beta'} \;, \tag{V-9}$$

and the possible forms composing T are

$$\begin{gathered} q_\alpha\, q_\beta\, q_{\beta'} \;,\quad X_\alpha X_\beta X_{\beta'} \;,\quad q_\alpha\, q_\beta\, X_{\beta'} \;, \\ q_\alpha\, X_\beta\, q_{\beta'} \;,\quad X_\alpha\, q_\beta\, q_{\beta'} \;,\quad q_\alpha\, X_\beta\, X_{\beta'} \;, \\ X_\alpha\, q_\beta\, X_{\beta'} \;,\quad X_\alpha\, X_\beta\, q_{\beta'} \;,\quad g_{\alpha\beta}\, q_{\beta'} \;, \\ g_{\alpha\beta'}\, q_\beta \;,\quad g_{\beta\beta'}\, q_\alpha \;,\quad g_{\alpha\beta}\, X_{\beta'} \;, \\ g_{\alpha\beta'}\, X_\beta \;,\quad g_{\beta\beta'}\, X_\alpha \,. \end{gathered}$$

The Lorentz conditions in (V-3) and the definitions in (V-5) show that the terms involving q_α are not present, and the terms in q_β and X_β are equivalent. With this, the general form for the vertex function is

$$\Gamma_{d\gamma d} = \epsilon^{\alpha} U^{\beta} U'^{\beta'} \left(\alpha_1 X_\alpha q_\beta q_{\beta'} + \alpha_2 X_\alpha X_\beta X_{\beta'} + \alpha_3\, g_{\alpha\beta} q_{\beta'} + \alpha_4\, g_{\alpha\beta'} q_\beta + \alpha_5\, g_{\alpha\beta} X_{\beta'} + \alpha_6\, g_{\beta\beta'} X_\alpha \right) \tag{V-10}$$

As with the dNN vertex, the scalar functions in (V-10) are unknown. When d' is on the mass shell, $U' \cdot d' = 0$, and we can use (V-4) to show

$$U \cdot X \rightarrow U \cdot q \quad , \quad U' \cdot X \longrightarrow U' \cdot q \; ,$$

and (V-10) becomes

$$\Gamma_{d\gamma d} = \alpha \, \epsilon \cdot X \, U \cdot q \, U' \cdot q + \beta \, \epsilon \cdot U \, U' \cdot q \tag{V-11}$$

$$+ \gamma \, \epsilon \cdot U' \, U \cdot q + \delta \, U \cdot U' \, \epsilon \cdot X \; .$$

Applying gauge invariance, and noting that (V-7) implies $q \cdot X = 0$, we conclude $\gamma = -\beta$, and the mass-shell vertex function is

$$\Gamma_{d\gamma d} = \alpha \, \epsilon \cdot X \, U \cdot q \, U' \cdot q + \beta \left(\epsilon \cdot U \, U' \cdot q - \epsilon \cdot U' \, U \cdot q \right) + \delta \, U \cdot U' \, \epsilon \cdot X \tag{V-12}$$

The form (V-12) has been obtained by Sakita[13] who shows by non-relativistic identification that

$$\delta = -e \; , \quad \beta = -2 e \mu_d \; , \quad \alpha = -\frac{e \, Q}{2\sqrt{10}} \; ,$$

where $\mu_d = 0.8576$ is the magnetic moment of the deuteron in nuclear Bohr magnetons, and Q is the deuteron quadrupole moment.

Lacking any means of specifying the off-shell behavior of the vertex functions, we follow George and others[12,13] and use the mass-shell vertex functions in the deuteron-pole amplitude. This is certainly incorrect, as we will indicate below, and makes any attempt to calculate photodisintegration cross sections ambiguous. In addition, there is another possible contribution to the background amplitude in photodisintegration which has been ignored in George's model, as we will show in the sequel, but before discussing this contribution, we examine the numerical results that have been obtained using the present (George's) model.

The amplitude for the deuteron pole term is

$$e \sum_{\lambda'} \bar{u}(p_1)\left\{\left[-\epsilon\cdot(d+d')U\cdot q\,U'\cdot q - 2\mu_d\left(\epsilon\cdot U\,q\cdot U' - \epsilon\cdot U'q\cdot U\right)\right]\times \right. \tag{V-13}$$

$$\left. \frac{1}{s-M_d^2}\left[F_0 \not{U}' - \frac{G_0}{m} U'\cdot p_1\right]\right\} C\,\bar{u}^T(p_2)\,,$$

where the sum is over intermediate deuteron polarizations, the quadrupole term has been neglected, the mass-shell form of (II-3) has been used, and s is defined in (I-10). Using equation (I-3) to perform the polarization sum, we get the result

$$e\,\bar{u}(p_1)\left[-F_0\,\epsilon\cdot(d+d')\,U\cdot q\left\{-\not{q} + \frac{q\cdot d'\not{d}'}{M_d^2}\right\}\right. \tag{V-14}$$

$$-2\mu_d F_0\left\{\epsilon\cdot U\left[-\not{q} + \frac{q\cdot d'\not{d}'}{M_d^2}\right] - U\cdot q\left[-\not{\epsilon} + \frac{\epsilon\cdot d'\not{d}'}{M_d^2}\right]\right\}$$

$$+\frac{G_0}{m}\,\epsilon\cdot(d+d')\,U\cdot q\left\{-q\cdot p_1 + \frac{q\cdot d'\,p_1\cdot d'}{M_d^2}\right\}$$

$$\left.+\frac{2\mu_d G_0}{m}\left\{\epsilon\cdot U\left[-q\cdot p_1 + \frac{q\cdot d'\,p_1\cdot d'}{M_d^2}\right] - U\cdot q\left[-\epsilon\cdot p_1 + \frac{\epsilon\cdot d'\,p_1\cdot d'}{M_d^2}\right]\right\}\right]\times$$

$$\frac{1}{s-M_d^2}\,C\,\bar{u}^T(p_2)\,.$$

We are restricting our calculation to the center-of-mass frame and in Chapter III we chose a gauge such that $\epsilon_0 = 0$. Thus we have

$$\epsilon \cdot q = \epsilon \cdot d = \epsilon \cdot d' = 0$$

and (V-14) reduces to

$$e\bar{u}(P_1)\left[\frac{-2\mu_d F_0}{s - M_d^2}\left\{ \epsilon\cdot U\left[-\not{q} + \frac{q\cdot d'\not{d}'}{M_d^2}\right] + U\cdot q\not{\epsilon}\right\}\right. \tag{V-15}$$

$$\left. + \frac{2\mu_d G_0}{m(s - M_d^2)}\left\{\epsilon\cdot U\left[-q\cdot P_1 + \frac{q\cdot d' P_1\cdot d'}{M_d^2}\right] + U\cdot q\,\epsilon\cdot P_1\right\}\right] C\,\bar{u}^T(P_2)\,.$$

Finally, we use the Dirac equation to remove the $\not{d}'$ term, use $\epsilon\cdot P_1 = \epsilon\cdot Q + \epsilon\cdot K = \epsilon\cdot K$ as in Chapter III, and we write

$$-q\cdot P_1 + \frac{q\cdot d' P_1\cdot d'}{M_d^2} = -q\cdot P_1 + \frac{(q\cdot P_1 + q\cdot P_2)(m^2 + P_1\cdot P_2)}{2(m^2 + P_1\cdot P_2)} = -q\cdot K\,.$$

Comparing to the amplitudes in Table 4, we obtain

$$e\,\bar{u}(P_1)\left\{\frac{4m\mu_d}{s - M_d^2}\left[G_0 I_1^\gamma + F_0 I_5^\gamma\right]\right\} C\,\bar{u}^T(P_2)\,. \tag{V-16}$$

Comparison of (V-16) with equations (I-31) and (I-32) shows that it is pure isoscalar, and hence will appear only in photodisintegration of the deuteron.

Numerical Results

George's program for computing the photodisintegration total cross section consists of using the parameter values found in pion disintegration to construct the nucleon-pole and resonance amplitudes for photodisintegration. The deuteron-pole amplitude is then approximated by the static form given in equation (V-16), with F_0 and G_0 evaluated for the parametric value of ρ, 0.6 percent. Our reconstruction of George's total cross section is given in Figure 19 in the curve labeled GEORGE. Here, we have found it necessary to use a value of $m^* = 1190$ MeV rather than the 1210 MeV value we found necessary in pion disintegration. We will have more to say about this difference below. For comparison, we have evaluated the nucleon-pole amplitudes using the PCAC modified prescription given at the end of Chapter IV, and have calculated the total cross section with these replacing George's nucleon-pole amplitudes. The results for ρ = three and five percent are given as the curves labeled GROSS PCAC in Figure 19. It is clear that the ρ = five percent curve is superior to the three percent curve, and both are superior to George's. This was also the case with the pion disintegration total cross section.

The approximation of the deuteron-pole amplitude by the static form of equation (V-16), with F_0 and G_0 evaluated for $\rho = 0.6$ percent, is somewhat arbitrary. The 0.6 percent value for ρ arises in George's calculation as that value necessary to compensate for unknown off-shell nucleon behavior of the nucleon-pole amplitude, and there is no a priori reason to suppose that it will correctly compensate for unknown off-shell deuteron behavior in the deuteron-pole amplitude. However, the effect of the substitution is to reduce the contribution from the static deuteron-pole amplitude at high energies. Examination of the curve GROSS DPT in Figure 19 shows that some such reduction is necessary. This curve results from the static deuteron-pole amplitude with F_0 and G_0 evaluated for a ρ of

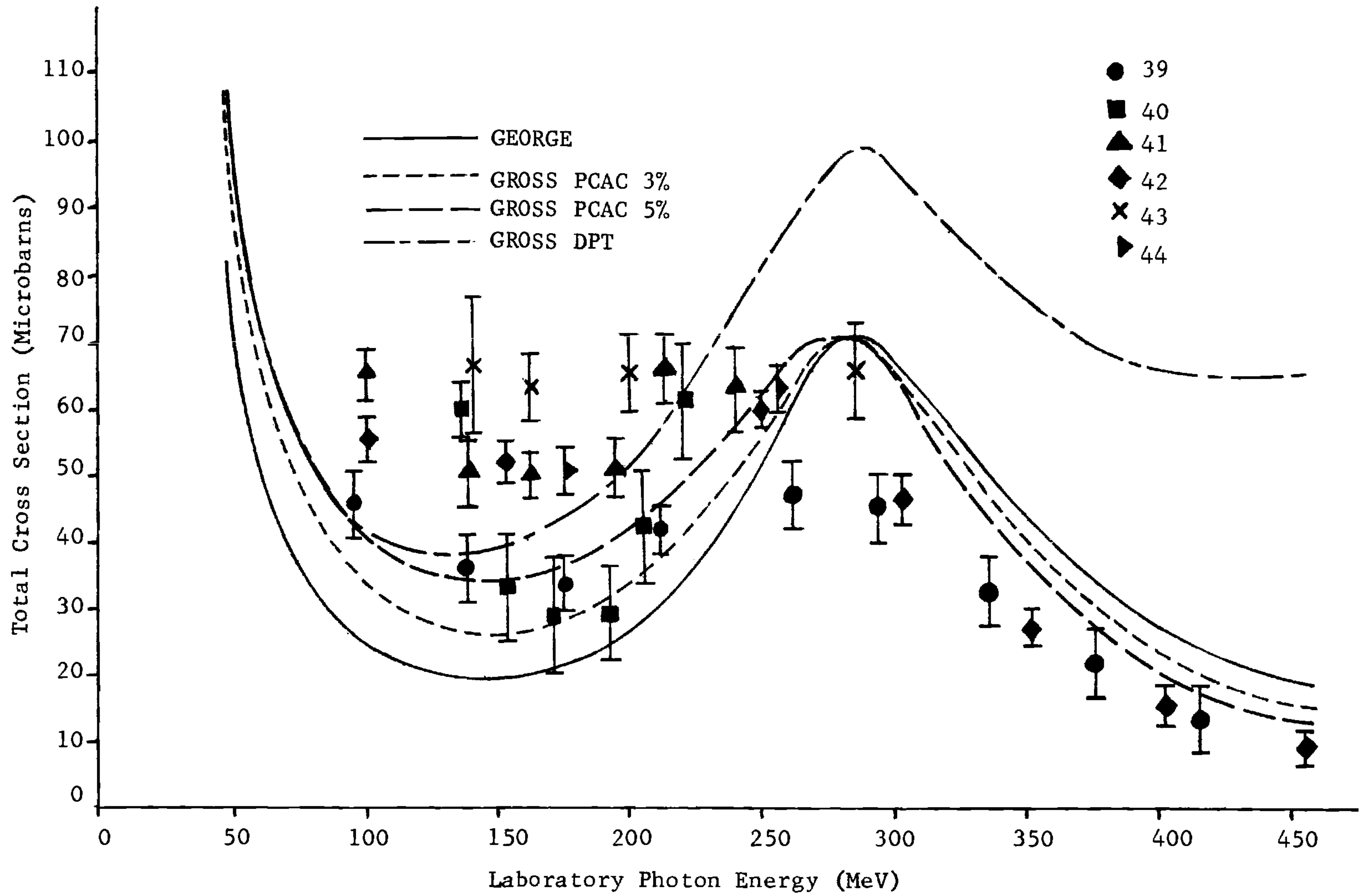

Figure 19. Total Cross Section for Photodisintegration of the Deuteron

three percent, and makes it clear that a correct deuteron-pole amplitude must contain momentum dependent functions which decay with increasing energy transfer.

Of the data available on the photodisintegration total cross section, Kissler's[39] is reported to have been taken with especially careful attention to coincidence elimination of competing events from photodisintegration with charged pion production. As might be expected, Kissler's data falls at the lower fringe of the scattered collective results. In Figure 20, we give the curve which results from our phenomenological $\rho =$ five percent nucleon-pole amplitudes, using the same width ($\Gamma = 120$ MeV) as used in pion disintegration, and with the deuteron-pole amplitude eliminated altogether. This curve differs only a few percent from its counterpart evaluated with the $\rho = 0.6$ percent deuteron-pole amplitude, with the most significant improvement occurring at high energies. It is clear that the curve fits Kissler's data quite well below and above the resonant peak, but is somewhat large in the vicinity of the peak. We find that by adjusting the width of the resonance (this is not the same as adjusting the cut-off parameter) from 120 MeV to 143 MeV, we obtain a total cross section which coincides quite well with Kissler's data.

To summarize our results for pion and photodisintegration, we have: (1) used only nucleon-pole and resonance amplitudes in both processes; (2) constructed the nucleon-pole amplitudes for both processes using the PCAC modified Gross prescription, with the dNN vertex invariants constructed from $\rho =$ five percent phenomenological deuteron wave functions; (3) used a cut-off parameter of $\Lambda = 4.13\alpha$ in the resonance amplitudes for

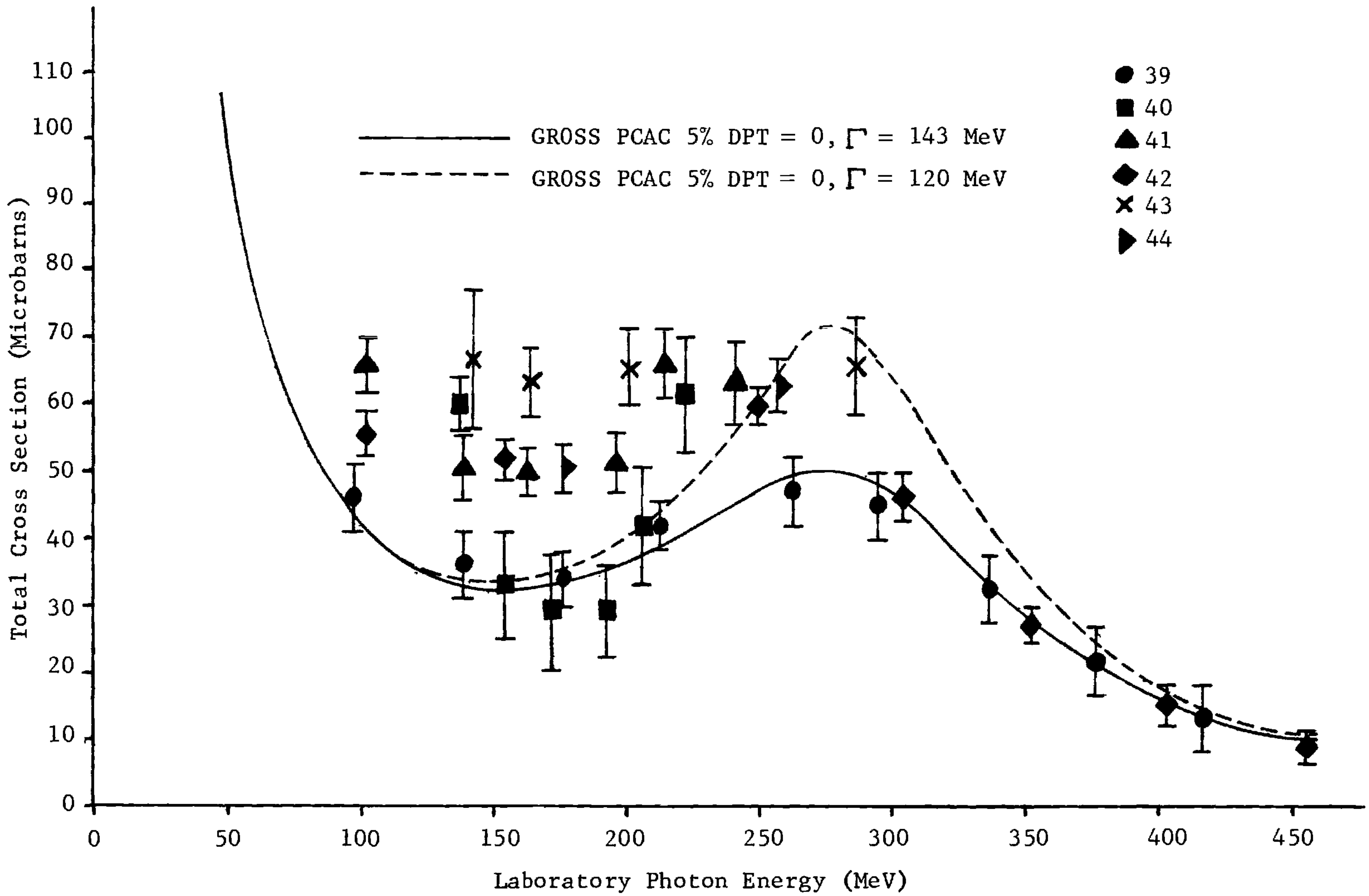

Figure 20. Total Cross Section for Photodisintegration of the Deuteron

both processes; and (4) used a resonance mass and width of 1210 MeV and 120 MeV in pion disintegration and 1190 MeV and 143 MeV in photodisintegration.

At this point, we would like to remark that our calculation of the photodisintegration total cross section has not been in the same spirit as George's. George's intent was to fix the parameters of calculation in pion disintegration, and then obtain a parameter-free theory of photodisintegration. We have already given reasons, in connection with the deuteron-pole term, as to why this procedure may not be realistic, and in subsequent discussion we will strengthen this viewpoint by pointing out an inadequacy in George's model. Consequently, we feel justified in adjusting the resonance mass and width in photodisintegration, and in neglecting the deuteron-pole amplitude, because, in doing so, we can consistently use what we regard to be fundamentally correct nucleon-pole amplitudes in both processes, and obtain excellent results for the photodisintegration total cross section by simple adjustment of the resonance parameters. Our final goal is to obtain an accurate weak-vector amplitude for neutrino disintegration of the deuteron, and in a practical measurement, it will not be possible to examine the behavior of the cross section differential in the outgoing nucleons. Consequently, we have concentrated on an accurate representation of the photodisintegration total cross section.

We close this Chapter with a criticism of George's model for photodisintegration and consequently, of the final form we have chosen for the photodisintegration amplitude. In addition to the lack of knowledge of the correct form for the deuteron-pole amplitude, the model lacks an additional amplitude which may be important at the energies we consider. This is the so-called exchange-current amplitude,[13] illustrated in Figure 21. The analogous amplitude for pion disintegration, shown in Figure 22, does not occur because it violates conservation of G-parity, known to be conserved in strong interactions. To see that the diagram in Figure 22 cannot occur, we note that the G parity of an N pion state is $(-1)^N$. Consequently, G-parity conservation requires that the total number of pions entering and leaving a vertex involving only pions must be even, and this is not satisfied by the $\pi\pi\pi$ vertex.

The missing exchange-current amplitude and the lack of knowledge of the deuteron-pole amplitude indicate that it is quite remarkable that we were successful in obtaining a good representation of the photodisintegration total cross section using only the nucleon-pole amplitudes and the resonance-parameter-adjusted resonance amplitudes. We might take this as an indication that the questionable amplitudes are not important in photodisintegration. However, examination of the differential cross section shows that this is not true. In Figures 23 - 26, we show Kissler's differential cross section data for laboratory photon energies of 140, 260, 300, and 390 MeV, along with our calculated differential cross section. We note that the calculated cross section is very nearly symmetric except for the small asymmetric contribution from the isoscalar part of the nucleon-pole amplitude. In the vicinity of the resonant peak, where the isovector resonant amplitude dominates, the fit to the experimental data is good (Figures 24 and 25). However, below and above the resonant

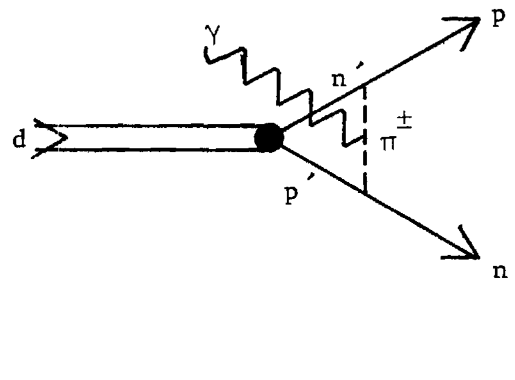

Figure 21. Exchange-Current Amplitude in the Background for Photodisintegration of the Deuteron

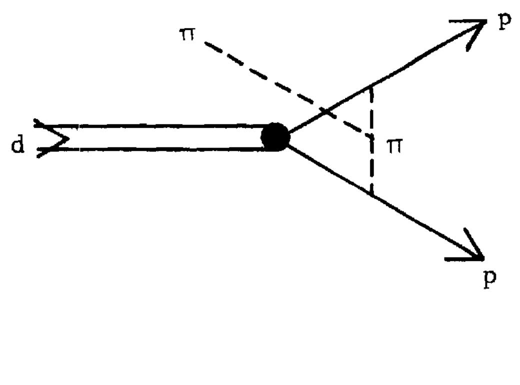

Figure 22. G-Parity-Forbidden Exchange-Current Amplitude for Pion Disintegration of the Deuteron

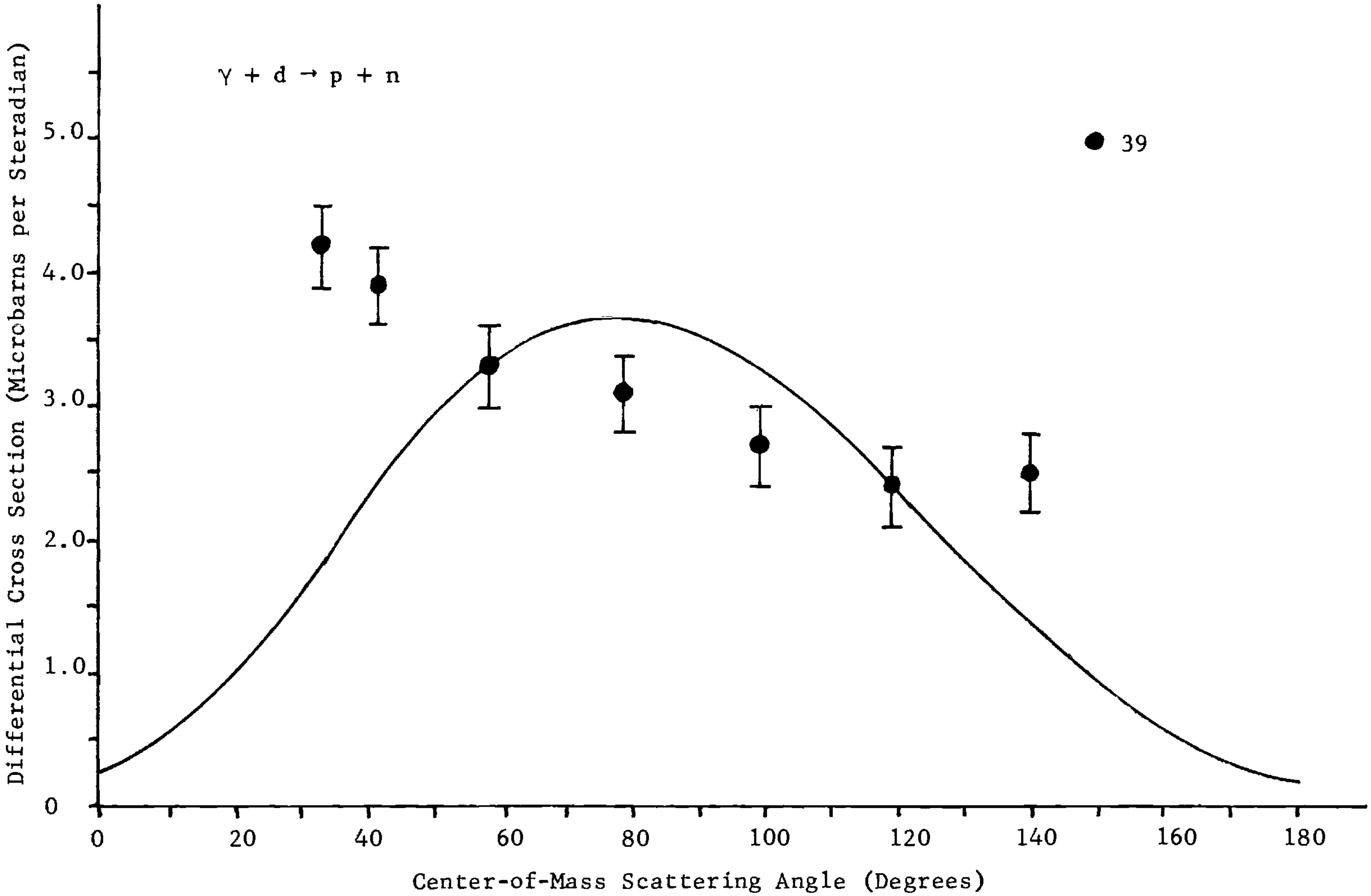

Figure 23. Center-of-Mass Differential Cross Section for E_{LAB} = 140 MeV

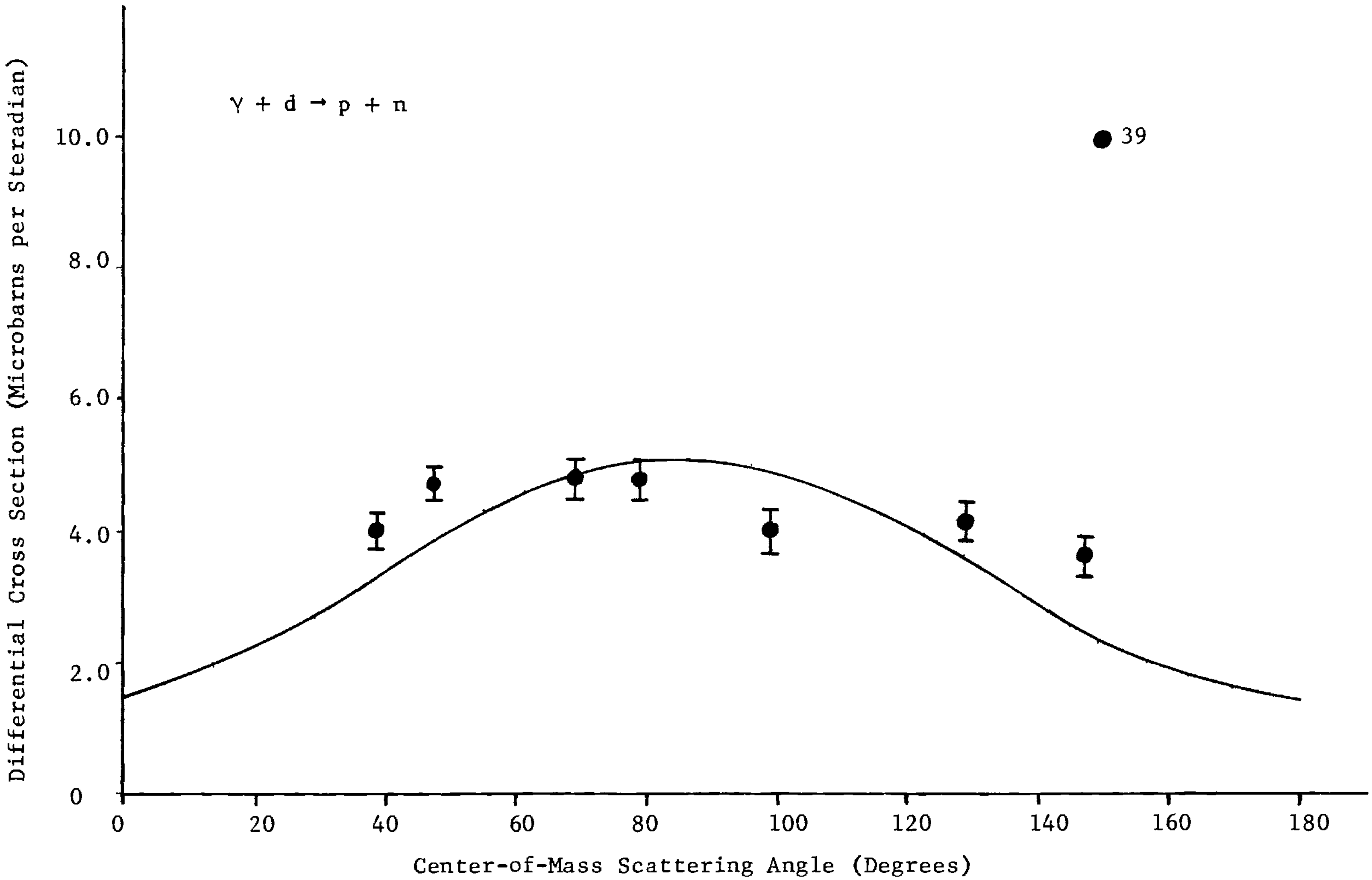

Figure 24. Center-of-Mass Differential Cross Section for $E_{LAB} = 260$ MeV

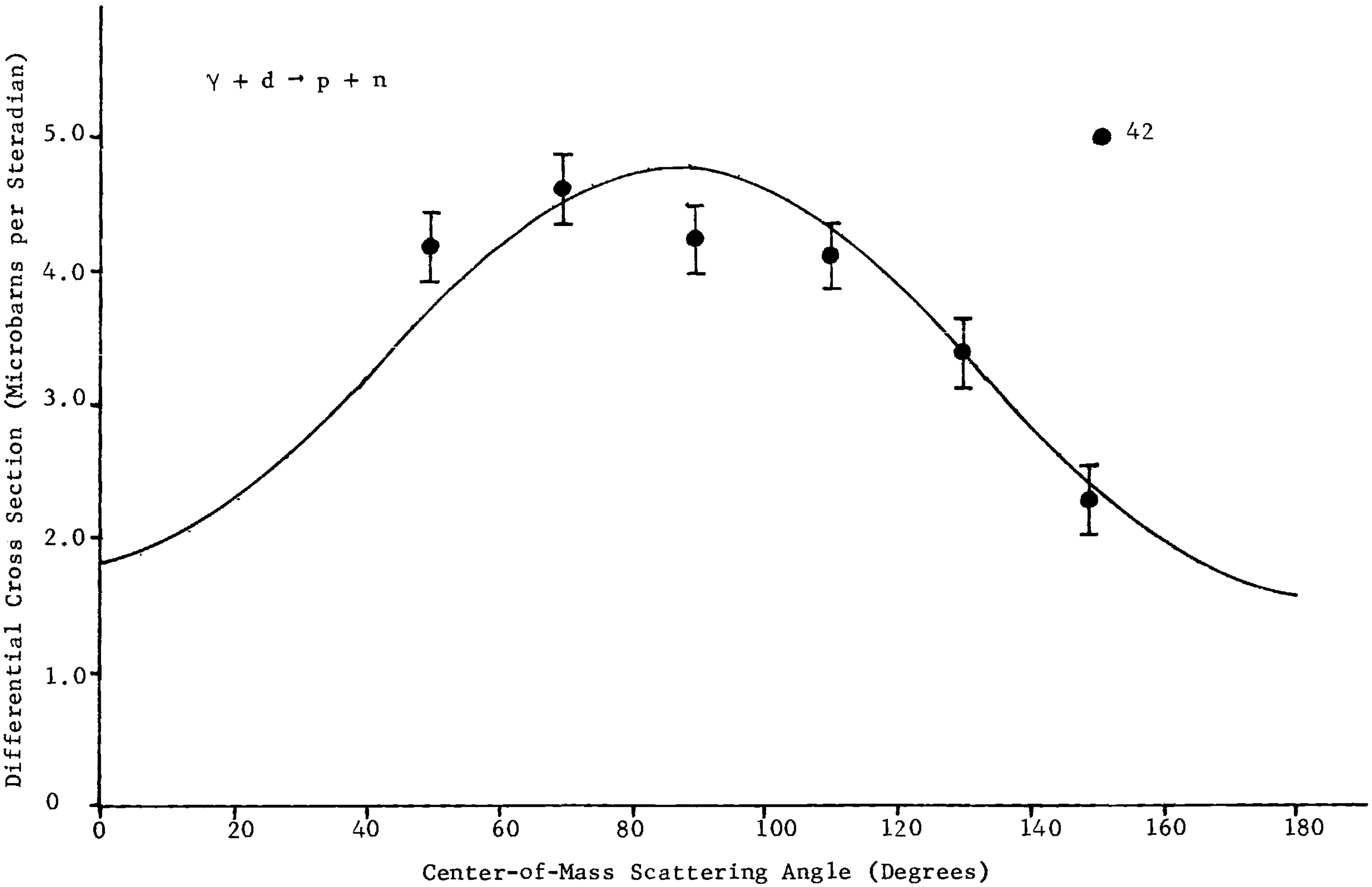

Figure 25. Center-of-Mass Differential Cross Section for E_{LAB} = 300 MeV

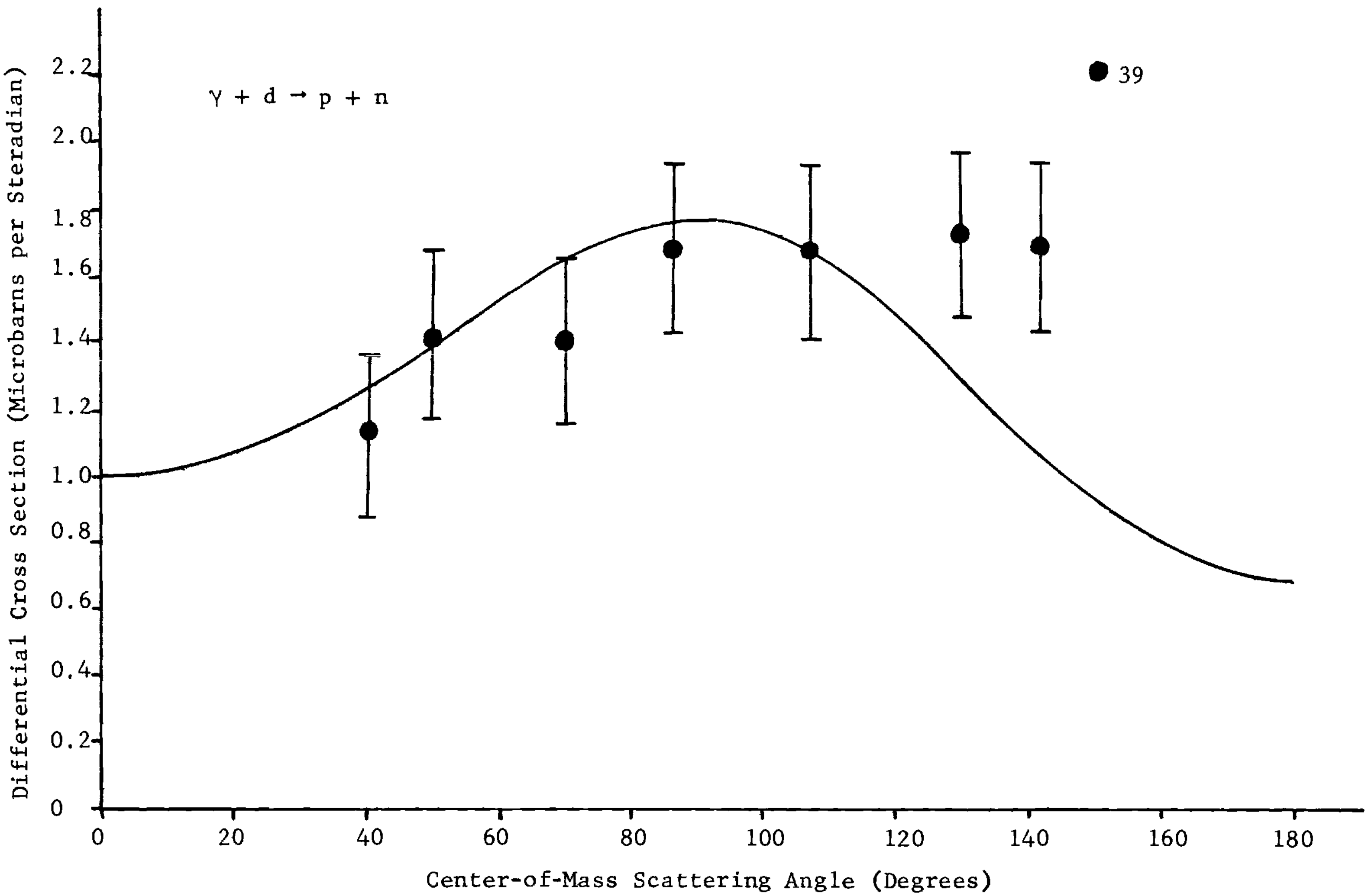

Figure 26. Center-of-Mass Differential Cross Section for E_{LAB} = 390 MeV

peak (Figures 23 and 26) the experimental cross section shows a strong asymmetry, indicating the presence of a significant isoscalar contribution. In both regions, the asymmetry is pronounced, and would probably be accounted for by a correct deuteron-pole amplitude (the deuteron-pole amplitude is pure isoscalar) and probably more important, the isoscalar part of the exchange current amplitude. At the higher energy, the asymmetry presumably is due to residual effects of the deuteron-pole term, and the isoscalar part of the exchange-current amplitude.

We have not attempted to incorporate the exchange-current amplitude into photodisintegration, because it involves the dNN vertex function with both nucleons off the mass shell, given in equation (II-1), as well as a closed-loop momentum integral. A possible approach to the calculation of this amplitude would be to limit the relative momentum at the dNN vertex to values below 370 MeV, use the vertex function appropriate to one off-shell nucleon,[4] and incorporate the Gross phenomenological vertex invariants. However, such a calculation would considerably exceed in complexity the resnance amplitude calculation of Chapter III, and we have not attempted to carry it through.

At very low energies (2.23 – 10 MeV), our calculated cross section compares favorably with the electric-dipole cross section of Blatt and Weiskopf.[24] In the intermediate region (10 – 100 MeV), our calculated cross section is approximately ten percent less than the experimental cross section, presumably due to the omission of the exchange current amplitude.

In the next Chapter, we construct the weak-vector amplitude for neutrino disintegration of the deuteron from the isovector part of the photodisintegration amplitude, using the CVC hypothesis. Even though we do not propose to examine the neutrino cross section differential in the outgoing nucleons, the fact that we have obtained a good representation of the photodisintegration total cross section using amplitudes which are nearly pure isovector leads us to believe that the weak vector amplitude we obtain would be adequate for this purpose.

CHAPTER VI

WEAK DEUTERON DISINTEGRATION AMPLITUDES

In this chapter we give a brief history of the strangeness-conserving weak interaction, including the conserved vector current (CVC) hypothesis[5,25] and the Partially-Conserved Axial-Vector Current (PCAC) hypothesis.[6,7,8,9] We then develop the amplitude for the process $\nu + d \longrightarrow p + p + \ell$ by relating the weak vector amplitude to the isovector amplitude for photodisintegration of the deuteron, and the weak axial-vector amplitude to the amplitude for pion disintegration of the deuteron. The latter relation is obtained by an extension of a technique used by Adler and Dothan,[9] and leads to an interesting consistency condition on the dNN vertex function.

The Strangeness-Conserving Weak Interaction

The earliest evidence for the existence of the weak interaction occurred in nuclear beta decay. The simplest example of this process is the beta decay of the free neutron, $n \longrightarrow p + e^- + \bar{\nu}_e$. In 1934 Fermi[26] proposed a theory to describe beta decay, using electromagnetic interactions as a guide. In Fermi's theory, the nucleons are considered to carry a "weak current" which interacts with the electron-neutrino field at a point, in direct analogy with the coupling of the electromagnetic field with an electric current. In terms of lepton and hadron current operators $\mathcal{L}^\alpha$ and $\mathcal{J}_\alpha^W$, the transition amplitude for beta decay can be written in Fermi's theory as

$$T_{fi} = (2\pi)^4 \delta^4(P_f - P_i) \langle e, \bar{\nu}_e; out | \mathcal{L}^{\alpha}(0) | 0 \rangle \langle p; out | J_{\alpha}^{W}(0) | n; in \rangle . \qquad \text{(VI-1)}$$

The analogous expression for the coupling of the electromagnetic field to the hadronic current is given by

$$T_{fi} = (2\pi)^4 \delta^4(P_f - P_i) N_{\gamma}^{\dagger} \epsilon^{\alpha} \langle p; out | J_{\alpha}^{EM}(0) | p; in \rangle , \qquad \text{(VI-2)}$$

where ϵ is the polarization four-vector for the electromagnetic field. Thus we see the correspondence

$$N_{\gamma} \epsilon^{\alpha} \sim \langle e, \bar{\nu}_e; out | \mathcal{L}^{\alpha}(0) | 0 \rangle . \qquad \text{(VI-3)}$$

There have been some attempts to generalize Fermi's theory by introducing a massive vector boson field to mediate the coupling between leptonic and hadronic weak currents. This would have the effect of giving the weak interaction a nonzero range, and would make the analogy between electromagnetic and weak processes complete. However, the existence of such a boson has not been established experimentally and Fermi's theory appears to be adequate in the range of energies now available to experimenters.

We may factor the spin dependence from the matrix elements in

---

† N is $(m/E)^{\frac{1}{2}}$ for a fermion and $(1/2E)^{\frac{1}{2}}$ for a boson.

equation (VI-1) and write

$$T_{fi} = N_{\bar{\nu}_e} N_e N_p N_n (2\pi)^4 \delta^4(p_f - p_i) \bar{u}(e) L^\alpha v(\bar{\nu}_e) \bar{u}(p) H_\alpha u(n) \,, \qquad \text{(VI-4)}$$

where L^α and H_α are combinations of Dirac gamma matrices and arbitrary scalar functions of the momenta appearing in the process. In neutron beta decay, the energy available to the process is approximately 1.4 MeV and is sufficiently small to assume that the momentum dependence of T_{fi} will be negligible. Thus, we equate the scalar functions to constants. Imposing the requirement of Lorentz invariance on T_{fi} requires that it be either scalar, pseudoscalar, or a mixture of the two. This places restrictions on the possible combinations of gamma matrices that can be incorporated in L^α and H_α. In all, there are five allowable combinations, given in Table 14.

For over twenty years after the introduction of Fermi's theory physicists sought to deduce the specific form of the beta decay interaction by a process of elimination based on experimental observation. The most significant step came in 1956 when Lee and Yang[27] suggested that the weak interaction was not invariant under spatial reflection, and consequently should be a mixture of both scalar and pseudoscalar terms. This suggestion was substantiated by experiments performed by Wu and collaborators,[28] and quickly followed by other experiments[29,30] which specified the precise manner in which parity violation occurs. From these experiments, Marshak and Sudershan[31] were able to specify the precise form of the beta decay amplitude. It is

Table 14. Allowed Combinations of Gamma Matrices and Their Transformation Characteristics

Label	Combination	Transformation Character
S	I	Scalar
V	γ_α	Vector
T	$\gamma_\alpha \gamma_\beta$	Tensor
A	$\gamma_\alpha \gamma_5$	Axial-Vector
P	γ_5	Pseudo-scalar

$$\mathcal{M} = \frac{G}{\sqrt{2}} \bar{u}(e)\gamma^{\alpha}(1-\gamma_5)v(\bar{\nu}_e)\bar{u}(p)\gamma_{\alpha}(1-x\gamma_5)u(n) , \qquad \text{(VI-5)}$$

where X has the value 1.18 and G has the value, in units of the proton Compton wavelength, 1.015×10^{-5}.

<u>The Conserved Vector Current (CVC) Hypothesis</u>

Long before the final elucidation of the interaction form for neutron beta decay, the similar strengths for weak decay of the neutron and the muon lead to speculation on the existence of a universal Fermi interaction governing all weak processes. Following the discovery of parity non-conservation in beta decay in 1957, it was established that the interaction form for muon decay $\mu^- \rightarrow e^- + \bar{\nu}_e + \nu_\mu$ has the form

$$\mathcal{M}' = \frac{G'}{\sqrt{2}} \bar{u}(\nu_\mu)\gamma^{\alpha}(1-\gamma_5)v(\bar{\nu}_e)\bar{u}(e)\gamma_{\alpha}(1-\gamma_5)u(\mu) , \qquad \text{(VI-6)}$$

where G' is equal to the coupling G in neutron beta decay within two percent. The surprising feature of this result is not that the axial-vector coupling in the neutron-proton matrix element is slightly different from that in the electron-muon matrix element, but that the vector couplings are equal.

A fundamental difference between the hadron current in beta decay and the charged lepton current in muon decay is that the hadrons participate in the strong interaction, whereas the electron and muon do not. Because of the strong interaction, the neutron and proton must be viewed as complicated structures surrounded by a "meson cloud." Formally, we can express this by writing the hadronic weak current in terms of "bare" nucleon and pion field operators as

$$J_\alpha^W = \frac{G}{\sqrt{2}} \bar{\Psi}_p \gamma_\alpha \Psi_n + \frac{G''}{\sqrt{2}} (\text{pionic current}) . \qquad \text{(VI-7)}$$

On the other hand, we can write the weak vector current operator for the muon and electron as

$$J_\alpha^{W'} = \frac{G'}{\sqrt{2}} \bar{\Psi}_e \gamma_\alpha \Psi_\mu \quad , \qquad \text{(VI-8)}$$

where no pionic term enters because the electron and muon do not participate in the strong interaction (in both currents we ignore corrections of the order of one percent due to the electromagnetic interaction). Now, if we believe in the existence of a universal Fermi interaction, we might expect the "bare" nucleonic term in the vector hadron current to couple with the same strength as the vector muonic current, and the pionic current would then lead to a correction which would make the observed coupling, that for the "dressed" nucleons, different from that for muon decay. The fact that the observed beta decay coupling is not different leads to the puzzling question of the role of the pionic correction in beta decay.

The question of the equality of vector couplings was resolved by Feynman and Gell-Mann[5] in 1958. They suggested that the pionic term in the weak vector current for the hadrons couples with exactly the same strength (G" = G) as the "bare" nucleons, thus giving the "bare" and "dressed" nucleons the same coupling. An analogous situation exists in electromagnetic interactions wherein all charged particles couple to the electromagnetic field with the same strength, regardless of their other interactions. An important consequence of this equality of couplings is the conservation of the electromagnetic current

$$\partial^{\alpha} J_{\alpha}^{EM}(x) = 0 \; . \tag{VI-9}$$

Feynman and Gell-Mann suggested that an identical conservation equation holds for the weak vector current of the hadrons or,

$$\partial^{\alpha} J_{\alpha}^{W,V}(x) = 0 \; . \tag{VI-10}$$

The CVC hypothesis of Feynman and Gell-Mann entails considerably more than equation (VI-10). The complete statement of their hypothesis also implies a fundamental connection between the weak vector current and the electromagnetic current for hadrons. The charge raising property of the weak vector current operator in beta decay indicates that it can be expressed in terms of isotopic spin operators as

$$J_{\alpha}^{W,V} = \frac{G}{\sqrt{2}} \left(I_{\alpha}^{1} + I_{\alpha}^{2} \right) , \tag{VI-11}$$

where I_{α}^{1} and I_{α}^{2} transform like the 1 and 2 components of an isovector under isospin transformations. On the other hand, in first-order electromagnetic processes, the electromagnetic current is known to have the decomposition in terms of isotopic spin operators given by

$$J_{\alpha}^{em} = e \left(S_{\alpha} + I_{\alpha}^{3\prime} \right) , \tag{VI-12}$$

where S_α is isoscalar and $I_\alpha^{3'}$ is the third component of an isovector. Feynman and Gell-Mann made the conjecture that I_α^1 , I_α^2 , and $I_\alpha^{3'}$ were the components of a single isovector conserved current. One of the implications of this conjecture is that the matrix elements of the isovector part of the electromagnetic current between nucleon states are proportional to nucleonic matrix elements of the weak vector current. This connection is easily established by means of the Wigner-Eckhart theorem.[21] The consequences of the proportionality between electromagnetic and weak vector amplitudes have been thoroughly tested and confirmed, and the CVC hypothesis appears to be well established.

The Partially Conserved Axial-Vector Current Hypothesis

The success of the CVC hypothesis raises the question of the possibility of conservation of the weak axial-vector current. The difference between the axial-vector couplings in beta decay and muon decay is sufficiently small to lead us to wonder if the axial-vector couplings for "bare" and "dressed" nucleons are equal, and the small difference in the two decays attributable to some unknown property of the weak interaction. That this is not the case can be established by a simple calculation. We consider the weak decay of the pion, $\pi^- \rightarrow \mu^- + \bar{\nu}_\mu$ in which the hadronic matrix element is $\langle 0 | J_\alpha^W(0) | \pi \rangle$. This matrix element must be composed of Lorentz vectors or axial vectors associated with the pion. Since the pion is spinless, there is no associated axial vector, and the only vector available is the four-momentum of the pion. Thus, we have

$$N_\pi \langle 0 | J_\alpha^w(0) | \pi \rangle = \frac{G}{\sqrt{2}} f_\pi(q^2) q_\alpha \, , \qquad \text{(VI-13)}$$

where the decaying pion is on the mass shell, $q^2 = m_\pi^2$, and hence f_π is a fixed number. The result obtained in equation (VI-13) implies that $\langle 0|J_\alpha^W(0)|\pi\rangle$ is a Lorentz vector. Since the pion field is pseudo-scalar, this implies that only the axial-vector part of J_α^W can contribute to pion decay. Thus,

$$N_\pi \langle 0|J_\alpha^{W,A}(0)|\pi\rangle = \frac{G}{\sqrt{2}} f_\pi(m_\pi^2) q_\alpha \, . \tag{VI-14}$$

Now, the assumption that the axial-vector current is conserved implies

$$\langle 0|\, \partial^\alpha J_\alpha^{W,A}(x)\,|\pi\rangle = 0 \, . \tag{VI-15}$$

We can write

$$J_\alpha^{W,A}(x) = e^{-iP^\beta x_\beta} J_\alpha^{W,A}(0)\, e^{iP^\beta x_\beta} \, , \tag{VI-16}$$

and use the fact that the vacuum and one-pion states $|0\rangle$ and $|\pi\rangle$ are eigenstates of the momentum operator P^β to obtain

$$\partial^\alpha e^{iq\cdot x}\langle 0|J_\alpha^{W,A}(0)|\pi\rangle = i q^\alpha \langle 0|J_\alpha^{W,A}(0)|\pi\rangle e^{iq\cdot x} = 0 \, . \tag{VI-17}$$

Applying this to equation (VI-14) yields

$$\frac{G}{\sqrt{2}} f_\pi(m_\pi^2) m_\pi^2 = 0 \, , \tag{VI-18}$$

a result which would forbid the observed decay of the pion.

The result in equation (VI-18) suggests that the axial-vector current could be conserved in the limit of vanishing pion mass. To elaborate on this idea we consider the matrix element of the axial-vector current in the process $\nu_\mu + n \rightarrow \mu^- + p^+$. In terms of invariant functions of the momentum transferred to the nucleons, the most general form for this matrix element is

$$N_p N_n \langle p | J_\alpha^{W,A}(0) | n \rangle = \frac{G}{\sqrt{2}} \bar{u}(p) \left[g_A(q^2) \gamma_\alpha \gamma_5 + h(q^2) q_\alpha \gamma_5 \right] u(n), \quad \text{(VI-19)}$$

where $g_A(0) = -1.18$, and $h(q^2)$ is called the induced pseudoscalar form factor. We examine once again the consequence of the assumption $\partial^\alpha J_\alpha^W(x) = 0$. We have

$$N_p N_n q^\alpha \langle p | J_\alpha^{W,A}(0) | n \rangle = \frac{G}{\sqrt{2}} \bar{u}(p) \left[g_A(q^2) \not{q} \gamma_5 + h(q^2) q^2 \gamma_5 \right] u(n) = 0 \,, \quad \text{(VI-20)}$$

where $q = n - p$. We use the Dirac equation to replace $\not{q}$ by $-2m$ and obtain

$$-2m\, g_A(q^2) + h(q^2)\, q^2 = 0 \,, \quad \text{(VI-21)}$$

or

$$h(q^2) = \frac{2m\, g_A(q^2)}{q^2} \,. \quad \text{(VI-22)}$$

We see that the assumption of conservation of the axial-vector current would require that $h(q^2)$ have a pole at $q^2 = 0$, which would suggest that it arises from the exchange of a zero-mass meson. Nambu[7] has suggested that the axial-vector current is "almost" conserved in the sense that $h(q^2)$ can be replaced by

$$h(q^2) = \frac{2m\, h'(q^2)}{q^2 - m_\pi^2} , \tag{VI-23}$$

where $h'(q^2) \cong g_A(q^2)$, and $\lim_{m_\pi \to 0} h'(q^2) = \lim_{m_\pi \to 0} g_A(q^2)$.

Equation (II-23) can be used to establish a connection between the form factors g_A, $g_{N\pi}$, and f_π in the limit of zero momentum transfer. To see this, we expand the induced pseudoscalar part of the axial-vector matrix element in a perturbation series, and exhibit the lowest order term, corresponding to the diagram in Figure 27. We have

$$\frac{G}{\sqrt{2}} \bar{u}(p)\, h(q^2) q_\alpha \gamma_5 u(n) = -\frac{G}{\sqrt{2}} \frac{\sqrt{2}\, g_{N\pi}(q^2) f_\pi(q^2)}{q^2 - m_\pi^2} \bar{u}(p)\, q_\alpha \gamma_5 u(n) \tag{VI-24}$$

$$+ \bar{u}(p)\, \bar{h}(q^2) q_\alpha \gamma_5 u(n),$$

where $\bar{h}(q^2)$ incorporates the contributions from all higher order graphs. If we compare this to Nambu's representation of $h(q^2)$, we have

$$\frac{2m\, g_A(q^2)}{q^2 - m_\pi^2} \cong \frac{\sqrt{2}\, g_{N\pi}(q^2) f_\pi(q^2)}{q^2 - m_\pi^2} + \bar{h}(q^2). \tag{VI-25}$$

If we assume that, in the limit $q^2 \to 0$, $\bar{h}(q^2)$ is negligible compared to the other terms in equation (VI-25), and that $g_{N\pi}(0)$ and $f_\pi(0)$ do not differ appreciably from their physically measured values $g_{N\pi}(m_\pi^2)$ and

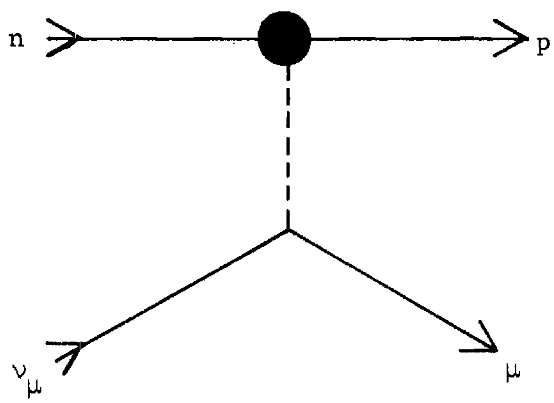

Figure 27. First-Order Diagram in the Expansion of the Induced Pseudoscalar Amplitude

$f_\pi(m_\pi^2)$, we arrive at

$$f_\pi(m_\pi^2) \cong \frac{\sqrt{2}\, m\, g_A(0)}{g_{N\pi}(m_\pi^2)} \; . \qquad \text{(VI-26)}$$

Equation (VI-26) was first derived by Goldberger and Treiman[32] in an approximate dispersion-theoretic analysis, and is called the Goldberger-Treiman (G-T) relation. Using the experimental values $g_{N\pi}(m_\pi^2) \cong 13.5$, $g_A(0) \cong -1.18$, and $f_\pi(m_\pi^2) \cong 0.93\, m_\pi$, we arrive at $0.137 \cong 0.129$ which is satisfied within approximately 10 percent.

The justification for neglecting $\bar{h}(q^2)$ in taking the limit of equation (VI-25) comes from dispersion theory arguments. In forming the spectral decomposition of $h(q^2)$, the pole in the scattering amplitude corresponding to our first order diagram falls at $q^2 = m_\pi^2$, and the next higher pole corresponds to the exchange of three pions, or at $q^2 = 9 m_\pi^2$. Consequently, it is argued that, for $q^2 \ll 9 m_\pi^2$, the single pion pole "dominates" the scattering amplitude.

The above results for the G-T relation and the one-pion exchange picture of the axial-vector current divergence can be derived on the basis of a formal field-theoretic assumption. It is assumed that, at least for small values of the momentum transfer (squared), the axial-vector current and the charged pion field obey the relation

$$\partial^\alpha J_\alpha^{W,A}(x) = C\, m_\pi^2\, \phi(x). \qquad \text{(VI-27)}$$

This equation is called the PCAC hypothesis.[9]

To fix the coefficient C, we form matrix elements as in the example in equation (VI-19):

$$\partial^{\alpha}\langle p|J_{\alpha}^{W,A}(x)|n\rangle = C m_{\pi}^{2}\langle p|\phi(x)|n\rangle . \qquad \text{(VI-28)}$$

Reducing the left-hand side first, we use the steps leading to equation (VI-17) to obtain

$$\partial^{\alpha}\langle p|J_{\alpha}^{W,A}(x)|n\rangle = i\, q^{\alpha}\langle p|J_{\alpha}^{W,A}(0)|n\rangle e^{i\, q\cdot x}, \qquad \text{(VI-29)}$$

with $q = n - p$. As in equation (VI-20), we can reduce equation (VI-29) to

$$N_p N_n \partial^{\alpha}\langle p|J_{\alpha}^{W,A}(x)|n\rangle = i\frac{G}{\sqrt{2}}\bar{u}(p)\left[-2m g_A(q^2)\gamma_5 + h(q^2)q^2\gamma_5\right]u(n)e^{i\, q\cdot x} \qquad \text{(VI-30)}$$

To reduce the right-hand side of equation (VI-28), we write

$$C m_{\pi}^{2}\langle p|\phi(x)|n\rangle = C m_{\pi}^{2}\langle p|\phi_1(x)+i\phi_2(x)|n\rangle = \sqrt{2}\, C m_{\pi}^{2}\langle p|\phi^{+}(x)|n\rangle , \qquad \text{(VI-31)}$$

where $\phi^{+}(x)$ is the pionic isospin raising operator. Next, we use the field equation for the pion field to write

$$\left(-\partial^{\alpha}\partial_{\alpha} + m_{\pi}^{2}\right)\langle p|\phi^{+}(x)|n\rangle = \langle p|J_{\pi}^{+}(x)|n\rangle , \qquad \text{(VI-32)}$$

where $J_{\pi}^{+}(x)$ is the pion source current. We can perform the space-time translation and rewrite equation (VI-32) as

$$(-q^2+m_\pi^2)\langle p|\phi^\dagger(0)|n\rangle e^{iq\cdot x} = \langle p|J_\pi^\dagger(0)|n\rangle e^{iq\cdot x}, \tag{VI-33}$$

or

$$\langle p|\phi^\dagger(x)|n\rangle = -\frac{1}{q^2-m_\pi^2}\langle p|J_\pi^\dagger(0)|n\rangle e^{iq\cdot x}. \tag{VI-34}$$

The most general form for the current matrix element in equation (VI-34) is

$$N_p N_n \langle p|J_\pi^\dagger(0)|n\rangle = i\sqrt{2}\, g_{N\pi}(q^2)\,\bar{u}(p)\gamma_5 u(n). \tag{VI-35}$$

Thus, collecting equations (VI-28), (VI-30), (VI-31), (VI-34), and (VI-35), we obtain

$$i\frac{G}{\sqrt{2}}\,\bar{u}(p)\left[-2m\,g_A(q^2)\gamma_5 + h(q^2)q^2\gamma_5\right]u(n) \tag{VI-36}$$

$$= -\frac{i\,2C\,m_\pi^2\,g_{N\pi}(q^2)}{q^2-m_\pi^2}\,\bar{u}(p)\gamma_5 u(n),$$

or

$$\frac{G}{\sqrt{2}}\left[-2m\,g_A(q^2)+h(q^2)q^2\right] = -\frac{2C\,m_\pi^2\,g_{N\pi}(q^2)}{q^2-m_\pi^2}. \tag{VI-37}$$

Evaluating equation (VI-37) in the limit of zero momentum transfer, we obtain

$$C = -\frac{G}{\sqrt{2}}\,\frac{m\,g_A(0)}{g_{N\pi}(0)}. \tag{VI-38}$$

We emphasize that the foregoing discussion permits us to relate matrix elements of the divergence of the axial-vector current to matrix elements for strong interaction processes involving pions. In this way we will use knowledge of pion disintegration of the deuteron to obtain information about neutrino disintegration of the deuteron. There we will have need for the matrix element of equation (VI-27) between an incoming deuteron state and an outgoing two-proton state. The appropriate equation is

$$q^{\alpha}\langle p_1 p_2 |\, J_{\alpha}^{W,A}(0)\, | d \rangle = \frac{i\, G\, m\, g_A(0)\, m_\pi^2}{g_{N\pi}(0)\,(q^2 - m_\pi^2)} \langle p_1 p_2 |\, J_\pi^{+}(0)\, | d \rangle , \qquad \text{(VI-39)}$$

where $q = p_1 + p_2 - d$.

<u>The Weak Vector Amplitude</u>

Before proceeding to the more complex axial-vector amplitude, we establish the relation between the isovector electromagnetic amplitude and the weak vector amplitude for deuteron disintegration, using the Wigner-Eckhart theorem. Expressing the electromagnetic and weak currents in terms of irreducible isotensors,[21] we obtain

$$J_{\alpha}^{EM} = e\left[I_{\alpha}(00) + I_{\alpha}(10) \right] \qquad \text{(VI-40)}$$

and

$$J_{\alpha}^{W,V} = \frac{G}{\sqrt{2}}\, I_{\alpha}^{+} = -\, G\, I_{\alpha}(11). \qquad \text{(VI-41)}$$

The matrix element of the isovector part of the electromagnetic current is, using equations (I-25), (I-26), and (VI-40)

$$\langle n p |\, J_{\alpha}^{EM,IV}\, | d \rangle$$

$$= \frac{e}{\sqrt{2}} \left(\langle 10| + \langle 00| \right) I_\alpha(10)|00\rangle = \frac{e}{\sqrt{2}} \langle 10| I_\alpha(10)|00\rangle \tag{VI-42}$$

$$= \frac{e}{\sqrt{2}} \langle 10;00|10\rangle \langle 1 \| I(1) \| 0\rangle = \frac{e}{\sqrt{2}} \langle 1 \| I(1) \| 0\rangle \, .$$

For the matrix element of the weak vector current, we use equations (I-23), (I-26), and (VI-41) to obtain

$$\langle pp| J_\alpha^{W,V} |d\rangle = -G \langle 11| I(11)|00\rangle \tag{VI-43}$$

$$= -G \langle 11;00|11\rangle \langle 1 \| I(1) \| 0\rangle = -G \langle 1 \| I(1) \| 0\rangle \, .$$

Thus,

$$\frac{\langle pp| J_\alpha^{W,V} |d\rangle}{\langle np| J_\alpha^{EM,IV} |d\rangle} = -\frac{\sqrt{2}\, G}{e} \tag{VI-44}$$

or

$$\langle pp| J_\alpha^{W,V} |d\rangle = -\frac{2}{e} \frac{G}{\sqrt{2}} \langle np| J_\alpha^{EM,IV} |d\rangle \, . \tag{VI-45}$$

The weak vector amplitude may now be obtained directly from Tables 4, 10, 12, and 13.

<u>The Axial-Vector Amplitude</u>

For energy transfers comparable to those considered in pion and photodisintegration, we assume that the coupling of the axial-vector weak current for the process $\nu + d \rightarrow p + p + \ell$ can be represented by the diagrams shown in Figure 28. The first two diagrams are nucleon-pole diagrams for the direct coupling of the axial-vector current, and are governed by the axial-vector coupling constant $g_A(q^2)$. The third diagram

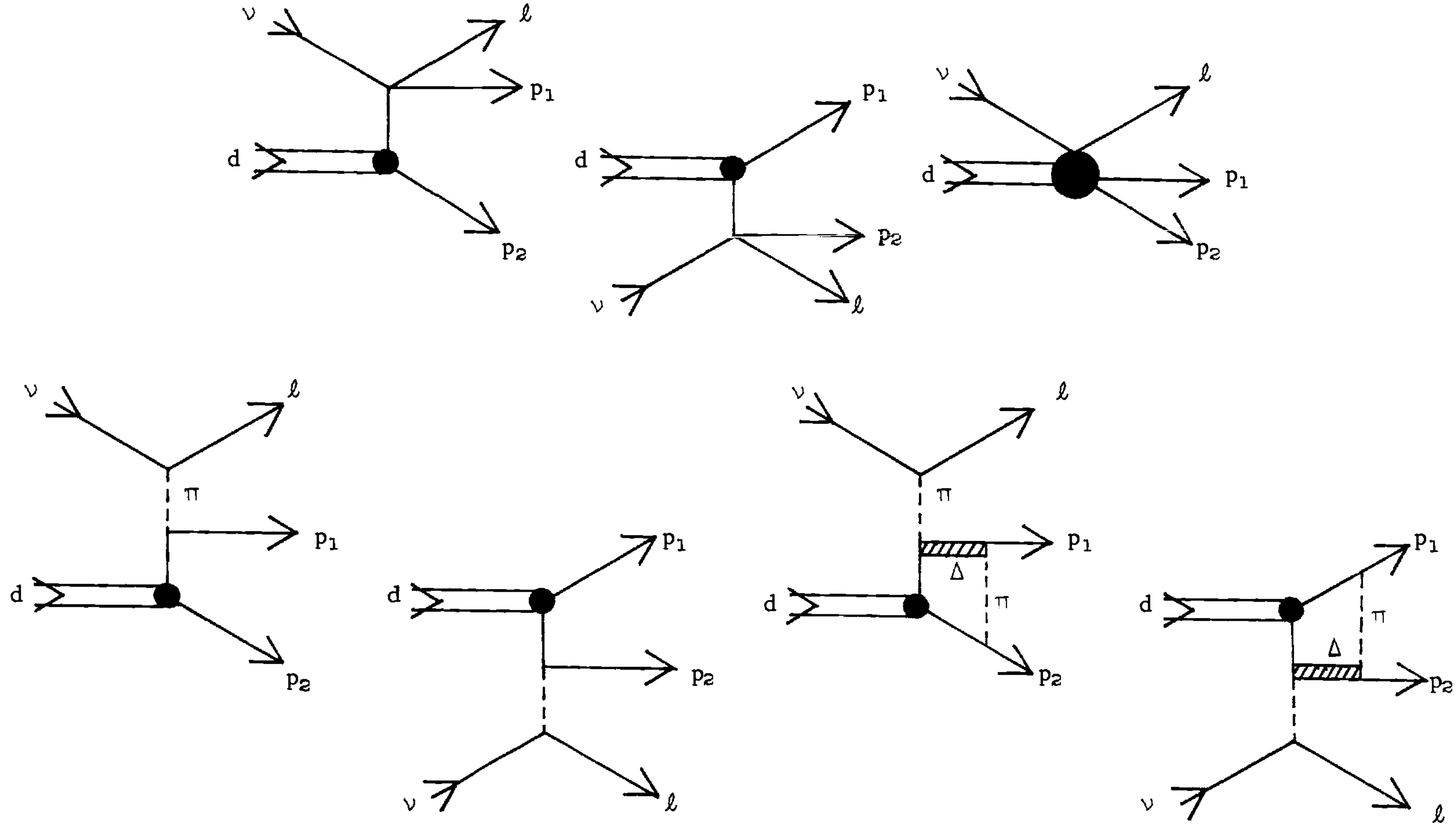

Figure 28. Diagrams for the PCAC Amplitude in Neutrino Disintegration of the Deuteron

represents structure associated with the direct coupling of the axial-vector current, and contains the effects of the Δ resonance. The amplitude associated with this diagram will be determined using the PCAC hypothesis, and explicit knowledge of the other diagrams based on the Austern model and the phenomenological wave function treatment of the dNN vertex function. The remaining four diagrams are constructed on the basis of PCAC single pion exchange, and the Austern-George model for pion disintegration of the deuteron. We note that, in this construction, the momentum transfer is not fixed, and we are extrapolating the pion disintegration amplitudes off the pion mass shell. To estimate the reliability of this extrapolation, we note that the weak vector form factors of the nucleon are the same as the electromagnetic form factors measured in electron-proton scattering, and these do not deviate appreciably from their zero momentum transfer values for momentum transfers $q^2 > -.05\,(\text{BeV})^2$. We will use this value of momentum transfer as a cut-off for our calculations, and assume that $g_A(q^2) \cong g_A(0) = g_A$ and $g_{N\pi}(q^2) \cong g_{N\pi}(m_\pi^2) \cong g_{N\pi}(0) = g_{N\pi}$. However, in the Austern model amplitudes, we will want to estimate the behavior in the limit of zero momentum transfer, and we will replace m_π^2, where appropriate, by q^2.

We write the axial-vector amplitude in the form

$$\frac{G}{\sqrt{2}}\,\mathcal{M}_\alpha = \frac{G}{\sqrt{2}}\left(\mathcal{M}_\alpha^P + \mathcal{M}_\alpha^S + \mathcal{M}_\alpha^\pi\right), \qquad \text{(VI-46)}$$

where $\mathcal{M}_\alpha^P$ corresponds to the first two diagrams in Figure 28, $\mathcal{M}_\alpha^S$ to the third diagram, and $\mathcal{M}_\alpha^\pi$ to the last four diagrams. In the analysis to follow, we find it more convenient to work directly in terms of the antisymmetrized amplitudes rather than perform the antisymmetrization at the end. We will use the shorthand notation

$$\Gamma^1 = F(t)\not{U} - \frac{G(t)}{m} U\cdot(P_1-q) - \left(\frac{m-[\not{P}_1-\not{q}]}{m}\right)\left[H(t)\not{U} - \frac{I(t)}{m} U\cdot(P_1-q)\right], \quad \text{(VI-47)}$$

$$\Gamma^2 = F(u)\not{U} - \frac{G(u)}{m} U\cdot(P_2-q) - \left(\frac{m-[\not{P}_2-\not{q}]}{m}\right)\left[H(u)\not{U} - \frac{I(u)}{m} U\cdot(P_2-q)\right], \quad \text{(VI-48)}$$

where t and u are the mandelstam variables defined in equation (I-10). We will also use the notation

$$D(t) = t - m^2 \quad \text{and} \quad D(u) = u - m^2$$

introduced in Chapter V.

For $\mathcal{M}^P_\alpha$ we have

$$\mathcal{M}^P_\alpha = g_A \bar{u}(P_1)\gamma_\alpha\gamma_5 \left(\frac{\not{P}_1-\not{q}+m}{D(t)}\right)\Gamma^1 C\,\bar{u}^T(P_2) \quad \text{(VI-49)}$$

$$- g_A \bar{u}(P_2)\gamma_\alpha\gamma_5(\not{P}_2-\not{q}+m)\Gamma^2 C\,\bar{u}^T(P_1)$$

$$= g_A \bar{u}(P_1)\left[\gamma_\alpha\gamma_5\left(\frac{\not{P}_1-\not{q}+m}{D(t)}\right)\Gamma^1 - \Gamma^{2C}\left(\frac{\not{P}_2-\not{q}-m}{D(u)}\right)\gamma_\alpha\gamma_5\right]C\,\bar{u}^T(P_2), \quad \text{(VI-50)}$$

where we have transposed the second term in (VI-49) and defined

$$\Gamma^{2C} = C\,\Gamma^{2T} C^{-1}. \quad \text{(VI-51)}$$

Next, we use the G-T relation for the pion decay constant, and perform manipulations as above to obtain

$$\mathcal{M}_\alpha^\pi = \frac{-2mg_A}{q^2-m_\pi^2} q_\alpha \bar{u}(P_1)\left[\gamma_5 \frac{(\not{P}_1-\not{q}+m)}{D(t)}\Gamma^1 - \Gamma^{2c}\frac{(\not{P}_2-\not{q}-m)}{D(u)}\gamma_5 + \frac{T_\pi(q^2)}{i\sqrt{2}\,g_{N\pi}}\right] C\bar{u}^T(P_2)\,, \tag{VI-52}$$

where $T_\pi(q^2)$ is the Austern model resonance amplitude extrapolated off the pion mass shell.

Using equation (VI-39), the divergence condition can be written for the amplitude $\mathcal{M}_\alpha$ as

$$q^\alpha \mathcal{M}_\alpha = -\frac{2g_A m\, m_\pi^2}{q^2-m_\pi^2} \bar{u}(P_1)\left[\gamma_5 \frac{(\not{P}_1-\not{q}+m)}{D(t)}\Gamma^1 - \Gamma^{2c}\frac{(\not{P}_2-\not{q}-m)}{D(u)}\gamma_5 + \frac{T_\pi(q^2)}{i\sqrt{2}\,g_{N\pi}}\right] C\bar{u}^T(P_2)\,. \tag{VI-53}$$

Before writing the divergence expression out in terms of the three amplitudes in (VI-46), we list two useful identities, which are

$$\bar{u}(P_1)\not{q}\gamma_5\frac{(\not{P}_1-\not{q}+m)}{D(t)} = \bar{u}(P_1)\left[\gamma_5 + 2m\gamma_5\frac{(\not{P}_1-\not{q}+m)}{D(t)}\right], \tag{VI-54}$$

and

$$\frac{(\not{P}_2-\not{q}-m)}{D(u)}\not{q}\gamma_5 C\bar{u}^T(P_2) = -\left[\gamma_5 - 2m\frac{(\not{P}_2-\not{q}-m)}{D(u)}\gamma_5\right]C\bar{u}^T(P_2)\,. \tag{VI-55}$$

Now, we take the divergence of (VI-46), use the explicit forms for $\mathcal{M}_\alpha^p$ and $\mathcal{M}_\alpha^\pi$ given in (VI-50) and (VI-52), employ the identities in (VI-54) and (VI-55), and equate the result to (VI-53). We obtain

$$q^{\alpha}\mathcal{M}_{\alpha} = g_A \bar{u}(P_1)\Bigg\{\left[\gamma_5 + 2m\gamma_5\frac{(\not{P}_1 - \not{q} + m)}{D(t)}\right]\Gamma^1$$

$$+\Gamma^{2c}\left[\gamma_5 - 2m\frac{(\not{P}_2 - \not{q} - m)\gamma_5}{D(u)}\right] - \frac{2mq^2}{q^2 - m_\pi^2}\times$$

$$\left[\gamma_5\frac{(\not{P}_1 - \not{q} + m)}{D(t)}\Gamma^1 - \Gamma^{2c}\frac{(\not{P}_2 - \not{q} - m)}{D(u)} + \frac{T_\pi(q^2)}{i\sqrt{2}\,g_{N\pi}}\right]\Bigg\}C\bar{u}^T(P_2)$$

$$+ q^{\alpha}\mathcal{M}_{\alpha}^{s}$$

$$= g_A\bar{u}(P_1)\Bigg\{-\frac{2m\,m_\pi^2}{q^2 - m_\pi^2}\left[\gamma_5\frac{(\not{P}_1 - \not{q} + m)}{D(t)}\Gamma^1\right.$$

$$\left.-\Gamma^{2c}\frac{(\not{P}_2 - \not{q} - m)}{D(u)}\gamma_5 + \frac{T_\pi(q^2)}{i\sqrt{2}\,g_{N\pi}}\right]\Bigg\}C\bar{u}^T(P_2).$$

Combining terms involving the pion propagator, we note that the nucleon propagators in the resulting term will cancel the remaining nucleon propagator terms, and we are left with the simple expression

$$g_A\bar{u}(P_1)\left[\gamma_5\Gamma^1 + \Gamma^{2c}\gamma_5 - \frac{2mT_\pi(q^2)}{i\sqrt{2}\,g_{N\pi}}\right]C\bar{u}^T(P_2) \qquad \text{(VI-56)}$$

$$+ q^{\alpha}\mathcal{M}_{\alpha}^{s} = 0 .$$

Everything is known in (VI-56) except the structure term $\mathcal{M}_{\alpha}^{s}$, and this equation may be used to determine it. First, we note that $\mathcal{M}_{\alpha}^{s}$ is finite as $q \to 0$,[9] and consequently $q^{\alpha}\mathcal{M}_{\alpha}^{s}$ is first order in q. This imposes the consistency condition that the remainder of (VI-56) be first order in q, and any term which is explicitly independent of q must vanish identically. To evaluate $\mathcal{M}_\alpha^S$, we begin with the terms involving Γ^1 and Γ^{2c}. Using (VI-47) and (VI-48), and the Dirac equation to eliminate $\not{p}_1$ and $\not{p}_2$, we have

$$\bar{u}(p_1)\gamma_5\Gamma^1 C\bar{u}^T(p_2) = \bar{u}(p_1)\gamma_5\Big\{F(t)\not{U} \tag{VI-57}$$

$$-\frac{G(t)}{m}U\cdot(p_1-q) - \left(2+\frac{\not{q}}{m}\right)\left[H(t)\not{U} - \frac{I(t)}{m}U\cdot(p_1-q)\right]\Big\}C\bar{u}^T(p_2),$$

and

$$\bar{u}(p_1)\Gamma^{2c}\gamma_5 C\bar{u}^T(p_2) = \bar{u}(p_1)\gamma_5\Big\{F(u)\not{U} \tag{VI-58}$$

$$-\frac{G(u)}{m}U\cdot(p_2-q) - \left[H(u)\not{U} - \frac{I(u)}{m}U\cdot(p_2-q)\right]\left(2+\frac{\not{q}}{m}\right)\Big\}C\bar{u}^T(p_2).$$

Combining terms, we obtain

$$\bar{u}(p_1)\left[\gamma_5\Gamma^1 + \Gamma^{2c}\gamma_5\right]C\bar{u}^T(p_2) = \bar{u}(p_1)\gamma_5 \times \tag{VI-59}$$

$$\Big\{\left[F(t)+F(u)-2\{H(t)+H(u)\}\right]\not{U} - \left[\frac{G(t)}{m} - 2\frac{I(t)}{m}\right]U\cdot(p_1-q)$$

$$-\left[\frac{G(u)}{m} - 2\frac{I(u)}{m}\right]U\cdot(p_2-q) + \left[\frac{I(t)}{m}U\cdot(p_1-q) + \frac{I(u)}{m}U\cdot(p_2-q)\right]\frac{\not{q}}{m}$$

$$-\left[\frac{H(t)}{m}\not{q}\not{U} + \frac{H(u)}{m}\not{U}\not{q}\right]\Big\}C\bar{u}^T(p_2).$$

Next, we use the variables defined in (I-5) to write

$$U\cdot(P_1-q) = U\cdot K - \frac{U\cdot q}{2} ,$$

$$U\cdot(P_2-q) = -U\cdot K - \frac{U\cdot q}{2} ,$$

and we rewrite (VI-59) in the form

$$\bar{u}(P_1)\left[\gamma_5\Gamma^1+\Gamma^{2c}\gamma_5\right]C\bar{u}^T(P_2) = \bar{u}(P_1)\gamma_5 \times \tag{VI-60}$$

$$\Big\{\left[F(t)+F(u)-2\{H(t)+H(u)\}\right]\not{U} - \frac{U\cdot K}{m} \times$$

$$\left[G(t)-G(u)-2\{I(t)-I(u)\}\right] + \frac{U\cdot K}{m^2}\not{q}\left[I(t)-I(u)\right]$$

$$+\frac{U\cdot q}{2m}\left[G(t)+G(u)-2\{I(t)+I(u)\}\right] - \frac{U\cdot q}{2m^2}\not{q}\left[I(t)+I(u)\right]$$

$$-\frac{1}{m}\left[H(t)\not{q}\not{U} + H(u)\not{U}\not{q}\right]\Big\}C\bar{u}^T(P_2).$$

Now we write

$$F(t) = F(m^2) + q^\alpha X_\alpha(t) , \quad G(t) = G(m^2) + q^\alpha Y_\alpha(t), \tag{VI-61}$$

$$H(t) = H(m^2) + q^\alpha Z_\alpha(t) , \quad I(t) = I(m^2) + q^\alpha W_\alpha(t),$$

With similar expressions for the u dependent quantities. To achieve the decompositions shown in (VI-61) we write, e.g.,

$$F(t) = F(m^2) + (t-m^2)\left[\frac{F(t)-F(m^2)}{t-m^2}\right] \quad . \qquad \text{(VI-62)}$$

We note that

$$\lim_{t\to m^2}\left[\frac{F(t)-F(m^2)}{t-m^2}\right] = \left.\frac{dF}{dt}\right|_{t=m^2} . \qquad \text{(VI-63)}$$

In Appendix C we use the wave function representations of the vertex invariants given in Chapter IV, and the explicit forms for $u_0(r)$ and $W_2(r)$ given in Appendix B, to prove that the derivatives of the type (VI-63) exist. Then we can use

$$t - m^2 = (P_1 - q)^2 - m^2 = q^\alpha(q_\alpha - 2P_{1\alpha})$$

to obtain

$$X_\alpha(t) = (q_\alpha - 2P_{1\alpha})\left[\frac{F(t)-F(m^2)}{D(t)}\right] , \qquad \text{(VI-64)}$$

$$X_\alpha(u) = (q_\alpha - 2P_{2\alpha})\left[\frac{F(u)-F(m^2)}{D(u)}\right] , \qquad \text{(VI-65)}$$

and corresponding expressions for Y_α, Z_α, and W_α.

Substituting the forms given in (VI-61) into (VI-60), we can rewrite (VI-56) as

$$q^\alpha \mathcal{M}_\alpha^S = -g_A \bar{u}(P_1)\gamma_5 \Big\{ 2\left[F(m^2) - 2H(m^2)\right]\not{q} - \frac{2mT_\pi(0)}{i\sqrt{2}\, g_{N\pi}} \qquad \text{(VI-66)}$$

(continued)

$$+q^{\alpha}\Big[\{X_\alpha(t)+X_\alpha(u)-2[Z_\alpha(t)+Z_\alpha(u)]\}\not{U}$$

$$-\frac{U\cdot K}{m}\{Y_\alpha(t)-Y_\alpha(u)-2[W_\alpha(t)-W_\alpha(u)]\}$$

$$+\frac{U_\alpha}{2m}\{G(t)+G(u)-2[I(t)+I(u)]\}$$

$$+\gamma_\alpha\left\{\frac{I(t)-I(u)}{m^2}U\cdot K-\frac{I(t)+I(u)}{2m^2}U\cdot q\right\}$$

$$-\frac{H(t)}{m}\gamma_\alpha\not{U}-\frac{H(u)}{m}\not{U}\gamma_\alpha-\frac{2m\overline{T}_{\pi\alpha}}{i\sqrt{2}\,g_{N\pi}}\Big]\Big\}\,C\,\bar{u}^T(P_2)\;,$$

where $q^{\alpha}\overline{T}_{\pi\alpha}$ is that part of the pion disintegration amplitude which is first order in q. In view of the remarks following (VI-56), we have the consistency condition

$$2\left[F(m^2)-2H(m^2)\right]\not{U}-\frac{2mT_\pi(0)}{i\sqrt{2}\,g_{N\pi}}=0\,. \qquad \text{(VI-67)}$$

We assume that the behavior of the non-pole part of the pion disintegration amplitude, $T_\pi(q^2)$, in the limit $q\to 0$, is given by the Austern model amplitude extrapolated off the pion mass shell. To determine the behavior of this amplitude in the limit $q\to 0$, we first note that $1/D'$, given in equation (II-38), is well behaved in this limit. The pion mass appearing explicitly in this expression is associated with the exchanged pion, and is not extrapolated off the mass shell. Thus, the behavior of the Austern model amplitude in the limit $q\to 0$ is governed by the explicit behavior of the invariant amplitudes in Table 1, and the invariant coefficients listed in Table 8. Recalling that $W=-q\cdot K$, and that $\sigma\to q^2$ in the extrapolation, we see that the entire amplitude explicitly vanishes with q except for the y^2 term in the third coefficient R_3^π. To evaluate this term, we recall $y = -K^2$, and we examine

$$K^2 = \frac{(P_1 - P_2)^2}{4} = \frac{m^2}{2} - \frac{P_1 \cdot P_2}{2} \,,$$

$$(q+d)^2 = (P_1 + P_2)^2 = 2m^2 + 2\, P_1 \cdot P_2 \,,$$

and we find

$$K^2 = m^2 - \frac{(q+d)^2}{4} = -\, q^\alpha (q_\alpha + 2 d_\alpha) \,, \qquad \text{(VI-68)}$$

where we have neglected the deuteron binding energy. Thus we conclude

$$T_\pi(0) = 0 \;, \quad F(m^2) = 2\, H(m^2) \,. \qquad \text{(VI-69)}$$

Equation (VI-69) is a new result for deuteron structure. In Chapter IV we used it to speculate on the contribution of negative energy states to the relativistic deuteron wave function, and indicated that the symmetric relation

$$G(m^2) = 2\, I(m^2) \qquad \text{(VI-70)}$$

seems also to hold, but the experimental proof we give in connection with the pion disintegration total cross section (Figure 13) is not conclusive.

To construct the axial-vector amplitude explicitly, we make the assumption that $\mathcal{M}_\alpha^S$ contains no divergenceless part, and assign it the value of the expression within the large square brackets in equation (VI-66). For the part $\overline{T}_{\pi\alpha}$, we examine the resonance amplitude in pion disintegration, which has the form

$$T_{\pi}(q^2) = \gamma_5 \left\{ R_1^{\pi} \frac{U\cdot q}{2m} + R_2^{\pi} \frac{U\cdot K}{m} + R_3^{\pi} \not{U} \right. \tag{VI-71}$$

$$\left. + R_4^{\pi} \frac{[\not{q}, \not{U}]}{2m} + R_5^{\pi} \frac{\not{q}\, U\cdot q}{2m^2} + R_6^{\pi} \frac{\not{q}\, U\cdot K}{m^2} \right\}.$$

We extract a factor of q^{α} to obtain

$$\overline{T}_{\pi\alpha} = \gamma_5 \left\{ \overline{R}_1^{\pi} \frac{U_{\alpha}}{2m} + \overline{R}_{2\alpha}^{\pi} \frac{U\cdot K}{m} + \overline{R}_{3\alpha}^{\pi} \not{U} \right.$$

$$\left. + \overline{R}_{4\alpha}^{\pi} \frac{[\not{q}, \not{U}]}{2m} + \overline{R}_5^{\pi} \frac{\not{q}\, U_{\alpha}}{2m^2} + \overline{R}_{6\alpha}^{\pi} \frac{\not{q}\, U\cdot K}{m^2} \right\}$$

where the $\overline{R}_{\lambda}^{\pi}$ and $\overline{R}_{\lambda\alpha}^{\pi}$ are given in Table 15. Here we write

$$\overline{R}_{3\alpha}^{\pi} = \overline{R}_3^{\pi 1} q_{\alpha} + \overline{R}_3^{\pi 2} K_{\alpha} + \overline{R}_3^{\pi 3} d_{\alpha} .$$

With the resonant part of $\mathcal{M}_{\alpha}^{s}$ specified, we are ready to give the axial-vector amplitude in the form specified by equation (I-29) using the invariant amplitudes specified in Table 5. Using equations (VI-50), (VI-52), (VI-66), and (VI-71), we reduce $\mathcal{M}_{\alpha}^{P}$, $\mathcal{M}_{\alpha}^{\pi}$, and $\mathcal{M}_{\alpha}^{s}$ to elementary forms which are easily rewritten as invariant coefficients times the entries in Table 5. We note that the B_{λ}^{π} and R_{λ}^{π} are taken from Tables 11 and 13, respectively, and $D_{\pi}^{2} = q^{2} - m_{\pi}^{2}$. In Table 16 we give those parts of the coefficients which are independent of resonant structure, while the resonant contributions are given in Table 17. We remark that, although we use equations (II-8) and (IV-39) in the numerical calculations in the next chapter, due to the speculative nature of these equations we have retained the quantities $G_o - 2I_o$ and $G - 2I$ in Table 16.

Table 15. Resonant Coefficients for Direct Coupling of the Axial-Vector Current in Neutrino Disintegration of the Deuteron

---

$$\bar{R}_1^{\pi} = R_1^{\pi}$$

$$\bar{R}_{2\alpha}^{\pi} = \frac{R_2^{\pi} K_\alpha}{q\cdot K}$$

$$\bar{R}_3^{\pi 1} = \frac{i F_0 G_\pi}{D'} \frac{m^5}{3\eta^2}\left[\frac{4\eta^3}{m^2} + \eta^2\left(\frac{2}{m^2} - \frac{7K^2}{2m^4}\right) + \eta\left(-\frac{2}{m^2} + \frac{15K^2}{2m^4}\right) + \frac{3(q\cdot K)^2}{m^6} + \frac{7K^2}{m^4} - \frac{6K^4}{m^6}\right]$$

$$\bar{R}_3^{\pi 2} = \frac{i F_0 G_\pi}{D'} \frac{m^5}{3\eta^2}\left[-\frac{10\eta^2 q\cdot K}{m^4} + \frac{2\eta q\cdot K}{m^4} - \frac{4 q\cdot K K^2}{m^6}\right]$$

$$\bar{R}_3^{\pi 3} = \frac{i F_0 G_\pi}{D'} \frac{m^5}{3\eta^2}\left[\frac{K^2}{m^4}\left(-\eta^2 + \eta + 2\right) - \frac{2K^4}{m^6}\right]$$

$$\bar{R}_{4\alpha}^{\pi} = \frac{R_4^{\pi} K_\alpha}{q\cdot K}$$

$$\bar{R}_5^{\pi} = R_5^{\pi}$$

$$\bar{R}_{6\alpha}^{\pi} = \frac{R_6^{\pi} K_\alpha}{q\cdot K}$$

Table 16. Non-Resonant Coefficients for the Axial-Vector Amplitude in Neutrino Disintegration of the Deuteron

i	B_i^A
1	$g_A\left[-2m\left\{\frac{F(t)}{D(t)}+\frac{F(u)}{D(u)}\right\}-\frac{1}{2m}\left\{G(t)-2I(t)+G(u)-2I(u)\right\}\right]$
2	$-\frac{g_A}{m}\left[\frac{G(t)}{D(t)}-\frac{G(u)}{D(u)}\right]$
3	$-\frac{g_A}{m}\left[\frac{G(t)}{D(t)}+\frac{G(u)}{D(u)}\right]$
4	$\frac{2g_A}{m}\left[\{G_0-2I_0\}\left\{\frac{1}{D(t)}+\frac{1}{D(u)}\right\}+2\left\{\frac{I(t)}{D(t)}+\frac{I(u)}{D(u)}\right\}\right]$
5	$\frac{2g_A}{m}\left[\{G_0-2I_0\}\left\{\frac{1}{D(t)}-\frac{1}{D(u)}\right\}+2\left\{\frac{I(t)}{D(t)}-\frac{I(u)}{D(u)}\right\}\right]$
6	$-4g_A\left[\frac{H(t)}{D(t)}-\frac{H(u)}{D(u)}\right]$
7	$-4g_A\left[\frac{H(t)}{D(t)}+\frac{H(u)}{D(u)}\right]$
8	$-g_A\left[\frac{F(t)}{D(t)}+\frac{F(u)}{D(u)}\right]$
9	$g_A\left[\frac{F(t)}{D(t)}+\frac{F(u)}{D(u)}-\frac{G(t)}{D(t)}-\frac{G(u)}{D(u)}\right]$
10	0
11	0
12	$2g_A\left[\frac{G(t)}{D(t)}-\frac{G(u)}{D(u)}\right]$
13	0

Table 16. (Concluded)

i	B_i^A
14	0
15	$\frac{g_A}{4m}\left[\frac{G(t)}{D(t)} - \frac{G(u)}{D(u)}\right]$
16	$-\frac{g_A}{2m}\left[\frac{G(t)}{D(t)} + \frac{G(u)}{D(u)}\right]$
17	0
18	0
19	$-m g_A\left[\frac{F(t)}{D(t)} - \frac{F(u)}{D(u)}\right]$
20	$-g_A\left[\frac{F(t)}{D(t)} - \frac{F(u)}{D(u)}\right]$
21	$\frac{-2m g_A}{i\sqrt{2}\, g_{N\pi} D_\pi} B_1^\pi + \frac{g_A}{2m}\left[\frac{G(t)}{D(t)} + \frac{G(u)}{D(u)}\right]$
22	$\frac{-2m g_A}{i\sqrt{2}\, g_{N\pi} D_\pi} B_2^\pi - \frac{g_A}{m}\left[\left\{G_0 - 2I_0\right\}\left\{\frac{1}{D(t)} - \frac{1}{D(u)}\right\} + 2\left\{\frac{I(t)}{D(t)} - \frac{I(u)}{D(u)}\right\}\right]$
23	$\frac{-2m g_A}{i\sqrt{2}\, g_{N\pi} D_\pi} B_3^\pi + 2g_A\left[\frac{H(t)}{D(t)} + \frac{H(u)}{D(u)}\right]$
24	$\frac{-2m g_A}{i\sqrt{2}\, g_{N\pi} D_\pi} B_5^\pi$
25	$-\frac{2m g_A}{i\sqrt{2}\, g_{N\pi} D_\pi} B_6^\pi$
26	$\frac{2m g_A}{i\sqrt{2}\, g_{N\pi} D_\pi} B_4^\pi$

Table 17. Resonant Coefficients for the Axial-Vector Amplitude in Neutrino Disintegration of the Deuteron

i	R_i^A
1	0
2	0
3	0
4	$\dfrac{2m\, g_A\, R_2^{\pi}}{i\sqrt{2}\, g_{N\pi}\, q\cdot K}$
5	0
6	$-\dfrac{4m^2 g_A}{i\sqrt{2}\, g_{N\pi}}\, \overline{R}_3^{\pi 2}$
7	$-\dfrac{8m^2 g_A}{i\sqrt{2}\, g_{N\pi}}\, \overline{R}_3^{\pi 3}$
8	$\dfrac{2m\, g_A}{i\sqrt{2}\, g_{N\pi}}\, R_5^{\pi}$
9	0
10	0
11	0
12	0
13	0

Table 17. (Concluded)

i	R_i^A
14	$\frac{2mg_A}{i\sqrt{2}\,g_{N\pi}}\frac{R_6^\pi}{q\cdot K}$
15	0
16	0
17	$\frac{-2mg_A}{i\sqrt{2}\,g_{N\pi}}\frac{R_4^\pi}{q\cdot K}$
18	0
19	0
20	0
21	$\frac{-2mg_A}{i\sqrt{2}\,g_{N\pi}}\frac{R_1^\pi}{D\pi}$
22	$\frac{-2mg_A}{i\sqrt{2}\,g_{N\pi}}\frac{R_2^\pi}{D\pi}$
23	$\frac{-2mg_A}{i\sqrt{2}\,g_{N\pi}}\frac{R_3^\pi}{D\pi} - \frac{4m^2g_A}{i\sqrt{2}\,g_{N\pi}}\left(\bar{R}_3^{\pi 1} - \bar{R}_3^{\pi 2}\right)$
24	$\frac{-2mg_A}{i\sqrt{2}\,g_{N\pi}}\frac{R_5^\pi}{D\pi}$
25	$\frac{-2mg_A}{i\sqrt{2}\,g_{N\pi}}\frac{R_6^\pi}{D\pi}$
26	$\frac{2mg_A}{i\sqrt{2}\,g_{N\pi}}\frac{R_4^\pi}{D\pi}$

CHAPTER VII

NEUTRINO DISINTEGRATION OF THE DEUTERON

In this chapter, we examine the kinematical restriction our theory places on the process of neutrino disintegration of the deuteron with forward lepton scattering. We then examine a theorem due to Adler,[51] based on the CVC hypothesis, which indicates that the axial-vector cross section may be isolated in the type of process we consider. Finally, we evaluate the cross section numerically and compare with Adler's theorem.

Kinematical Analysis

There are a number of considerations to be made in connection with the determination of the laboratory differential cross section for forward lepton scattering. We will examine these in some detail and present the results in the form of kinematical graphs in the plane defined by the laboratory energies E_ν and E_ℓ.

Allowed Momentum Transfers

First, we note that neutrino disintegration of the deuteron occurs with space-like momentum transfers, $q^2 = (p_\nu - p_\ell)^2 < 0$. In terms of laboratory energies with the lepton forward scattered, this is

$$q^2 = m_\ell^2 - 2\, E_\nu^L E_\ell^L + 2\, E_\nu^L \left(E_\ell^{L\,2} - m_\ell^2 \right)^{\frac{1}{2}} < 0 \qquad \text{(VII-1)}$$

We have two important bounds to consider. The first concerns the assumption of constant nucleon vertex functions. If we use electron-proton elastic scattering as a guide, we see that the nucleon form factors first begin to show appreciable deviations for $q^2 < -.05\,(BeV)^2$. The second limitation concerns the PCAC hypothesis. To assure single-pion-exchange dominance, we should require $-m_\pi^2 < q^2 < m_\pi^2$, where $m_\pi^2 \cong .02\,(BeV)^2$. Thus, we examine

$$m_\ell^2 - 2E_\nu^L E_\ell^L + 2E_\nu^L \left(E_\ell^{L\,2} - m_\ell^2\right)^{\frac{1}{2}} < q^2 \qquad \text{(VII-2)}$$

for $q^2 = -.05\,(BeV)^2$ and $-.02\,(BeV)^2$, and plot the results as boundary curves in the E_ν^L, E_ℓ^L plane. This is shown in Figure 29 for the case of an outgoing muon. For an outgoing electron, both curves are essentially vertical lines at the extreme left of the diagram. This merely says that, when the outgoing lepton is an electron, one must go to extremely large energy transfers to probe nucleon structure. Consequently, high energy neutrino experiments involving electrons should be much cleaner and more easily interpreted than analogous experiments with muons.

Energy Transfer

Our analysis of pion and photodisintegration has been limited to pion and photon energies below 450 MeV. Consequently, the same restriction applies to our treatment of neutrino disintegration. This is indicated by the lines $E_\nu^L - E_\mu^L = 0$ and 450 MeV in Figure 29. Here, we have also indicated the neutrino and lepton energies we have chosen for calculations. These are indicated by the horizontal lines at E_ν^L = 600, 800, and 1000 MeV. The three other cases, E_ν^L = 3, 6, and 10 BeV, are not shown.

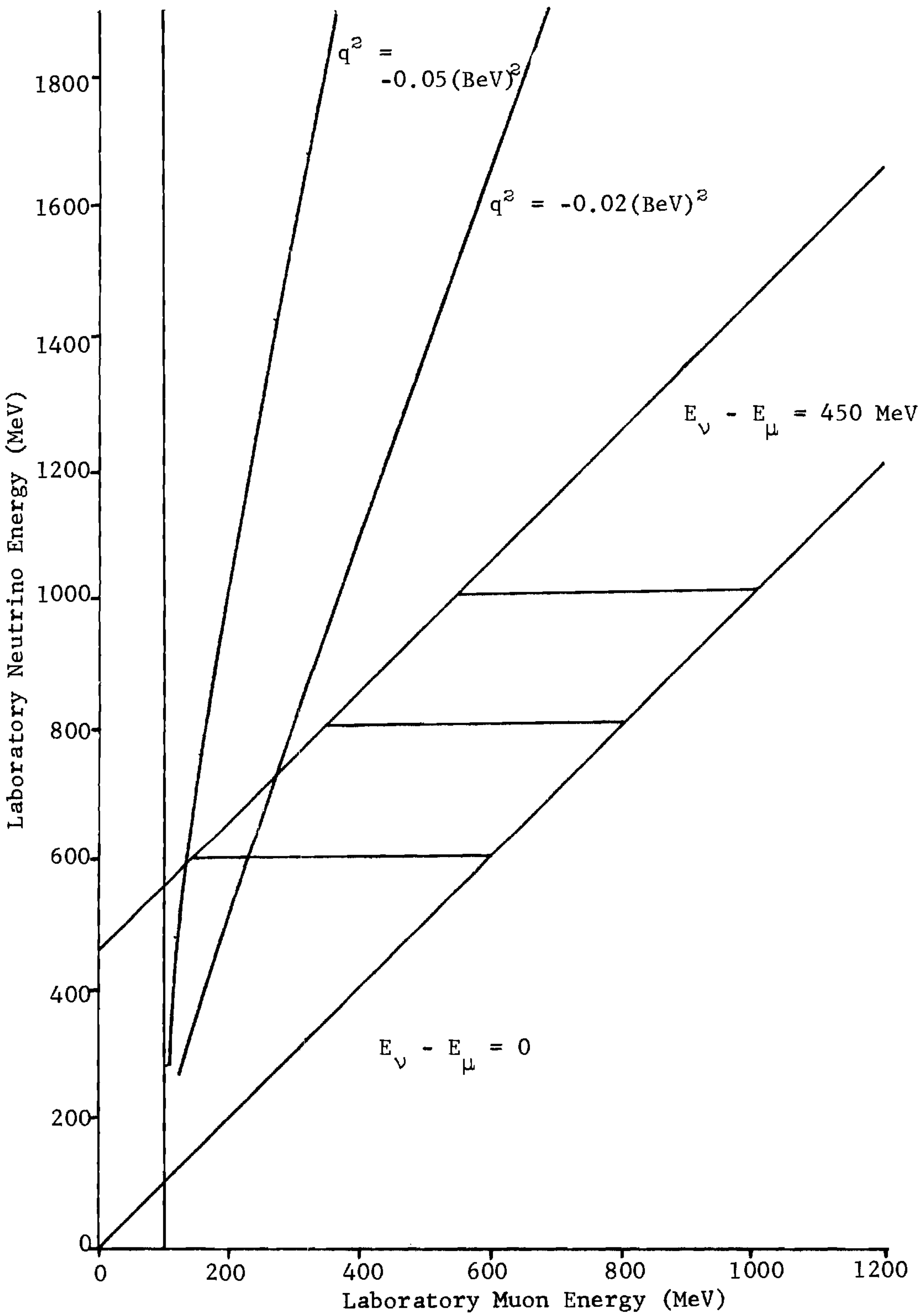

Figure 29. Kinematical Graph for Neutrino Disintegration

Vanishing of the Vector Contribution in High Energy Neutrino Reactions

The following discussion parallels that of Adler.[51] In neutrino processes with an outgoing lepton, the cross section for the process is proportional to

$$T^{\lambda\sigma}\langle\beta|V_\lambda + A_\lambda|\alpha\rangle\langle\beta|V_\sigma + A_\sigma|\alpha\rangle^\dagger , \qquad \text{(VII-3)}$$

where α and β are the initial and final states of the hadronic system, and $T^{\lambda\sigma}$ is given by

$$T^{\lambda\sigma} = \sum_{\substack{\text{lepton}\\ \text{spins}}} \bar{u}(\ell)\gamma^\lambda(1+\gamma_5)u(\nu)\left[\bar{u}(\ell)\gamma^\sigma(1+\gamma_5)u(\nu)\right]^\dagger .$$

Using standard techniques, we can show that

$$T^{\lambda\sigma} \propto \mathrm{Tr}\left\{\gamma^\lambda \not{\ell}\, \gamma^\sigma \not{\nu} - \gamma_5 \gamma^\lambda \not{\ell}\, \gamma^\sigma \not{\nu}\right\} .$$

Now we define $q = \nu - \ell$, and assume that the mass of the outgoing lepton is negligible. Then ℓ, ν and q are null vectors. Next, we assume that the lepton is forward scattered, and that the energy transfer q_0 is nonzero. With this, we have

$$\ell = (\ell_0, 0, 0, \ell_0) \quad , \quad \nu = (\nu_0, 0, 0, \nu_0),$$

and we can write

$$\ell = \frac{\ell_0}{q_0} q \quad , \qquad \nu = \frac{\nu_0}{q_0} q \quad .$$

Then,

$$T^{\lambda\sigma} \propto \frac{\nu_0 \ell_0}{q_0^2} \mathrm{Tr}\left\{\gamma^\lambda \not{q}\, \gamma^\sigma \not{q} - \gamma_5 \gamma^\lambda \not{q}\, \gamma^\sigma \not{q}\right\}.$$

Using the properties of the gamma matrices, it is easy to show that the second term vanishes, and we obtain

$$T^{\lambda\sigma} \propto \frac{\nu_0 \ell_0}{q_0^2}\, q^\lambda q^\sigma . \qquad \text{(VII-4)}$$

Using equations (VII-4) and (VI-16), we can now write (VII-3) as

$$\text{Cross Section} \propto \langle\beta|\,\partial^\lambda V_\lambda + \partial^\lambda A_\lambda|\alpha\rangle\langle\beta|\,\partial^\sigma V_\sigma + \partial^\sigma A_\sigma|\alpha\rangle^\dagger . \qquad \text{(VII-5)}$$

From this, it is clear that, if the weak vector current is conserved, then the vector contribution to the cross section vanishes, and we have

$$\text{Cross Section} \propto \left|\langle\beta|\,\partial^\lambda A_\lambda|\alpha\rangle\right|^2 . \qquad \text{(VII-6)}$$

Application to Neutrino Disintegration of the Deuteron

The theory of neutrino disintegration we have developed is restricted to energy transfers of 0 - 450 MeV for incoming neutrino energies greater than 600 MeV. Consequently, our process satisfies the condition of nonzero energy transfer. Also, since the energy of the outgoing lepton is not less than 150 MeV, it is clear that, for an outgoing electron ($m_e = 0.511$ MeV), the conditions of Adler's theorem are satisfied. However, for an outgoing muon ($m_\mu = 105.7\ MeV$), the lepton mass is not negligible at the lowest neutrino energies, and it will be of interest to see how seriously the cross section deviates from axial-vector dominance. We examine such questions in the next section.

Numerical Results for the Neutrino Disintegration Cross Section

Using the results of Chapter VI, the transition amplitude for the process $\nu + d \longrightarrow p + p + \ell$ takes the form

$$\mathcal{M} = \frac{G}{\sqrt{2}} \mathcal{L}^\alpha U^\beta \bar{u}(P_1)\left\{-\frac{2}{e}\sum_{\lambda=1}^{12}(B_\lambda^{\gamma(V)} + R_\lambda^\gamma) I_{\lambda\alpha\beta}^\gamma + \sum_{\lambda=1}^{26}(B_\lambda^A + R_\lambda^A) I_{\lambda\alpha\beta}^A\right\} C\bar{u}^T(P_2), \quad \text{(VII-7)}$$

where the superscript V denotes the isovector part of the photodisintegration amplitude. In the present section, we use (VII-7) to predict the neutrino disintegration cross section differential in lepton energy and direction, for forward scattering of the lepton in the laboratory.

Using the methods described in Appendix A, we construct the cross section summed over final spins and averaged over initial spins. In Figure 30, we show the cross section for both an outgoing electron and an outgoing muon. The muon cross section is shown resolved into contributions from the vector, interference, and axial-vector parts. The vector and interference contributions remain at this same level up to the highest neutrino energy examined (10 BeV) while the axial-vector contribution increases approximately as the square of the neutrino center-of-mass energy, as would be expected from general considerations.[46] Thus the behavior expected from Adler's theorem is obtained even when the lepton mass is an appreciable fraction of the lepton energy, and the relative importance of

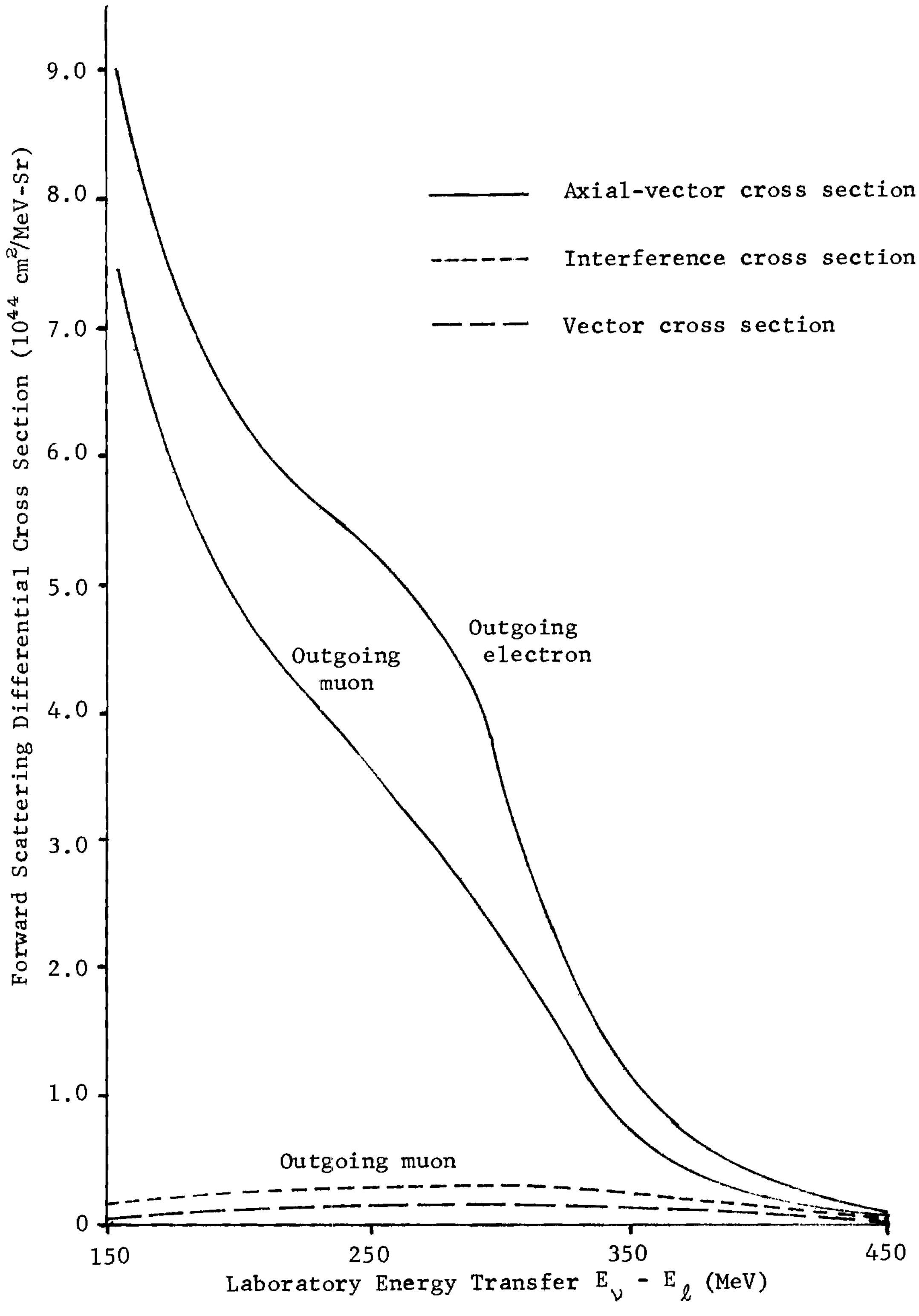

Figure 30. Differential Cross Section for E_ν = 600 MeV

the vector current diminishes rapidly as the lepton energy becomes predominantly kinetic. For an outgoing electron, the vector and interference contributions to the cross section are five orders of magnitude smaller than that shown for the outgoing muon, shown in Figure 30, as was expected on the basis of Adler's theorem. In fact, Adler's theorem serves the corrollary purpose of providing an independent check on the complex spin sums and computer programs required to evaluate the vector and interference cross sections, in that these quantities must vanish for a massless lepton. Because of the close similarity between the vector cross section and the photodisintegration cross section computations, the check serves there as well.

In Figures 31 and 32, we give the neutrino disintegration cross section for both outgoing electron and muon, for neutrino laboratory energies up to 10 BeV. The most notable feature of the cross section, besides its growth with energy, is the fact that the contribution from the Δ resonance becomes more pronounced at higher energies. We remark that the calculation of pion disintegration via the Austern model is quite unambiguous, and fits the experimental data very well. Consequently, the present results for neutrino disintegration, due to the axial-vector dominance, provide a highly characteristic test of the PCAC hypothesis. However, at present, there exists no data for comparison. The weakness of the interaction, together with the limitations on neutrino beam intensities make even total cross section measurements extremely difficult, and our theory applies to the even more restricted case of forward lepton scattering, differential in lepton energy.

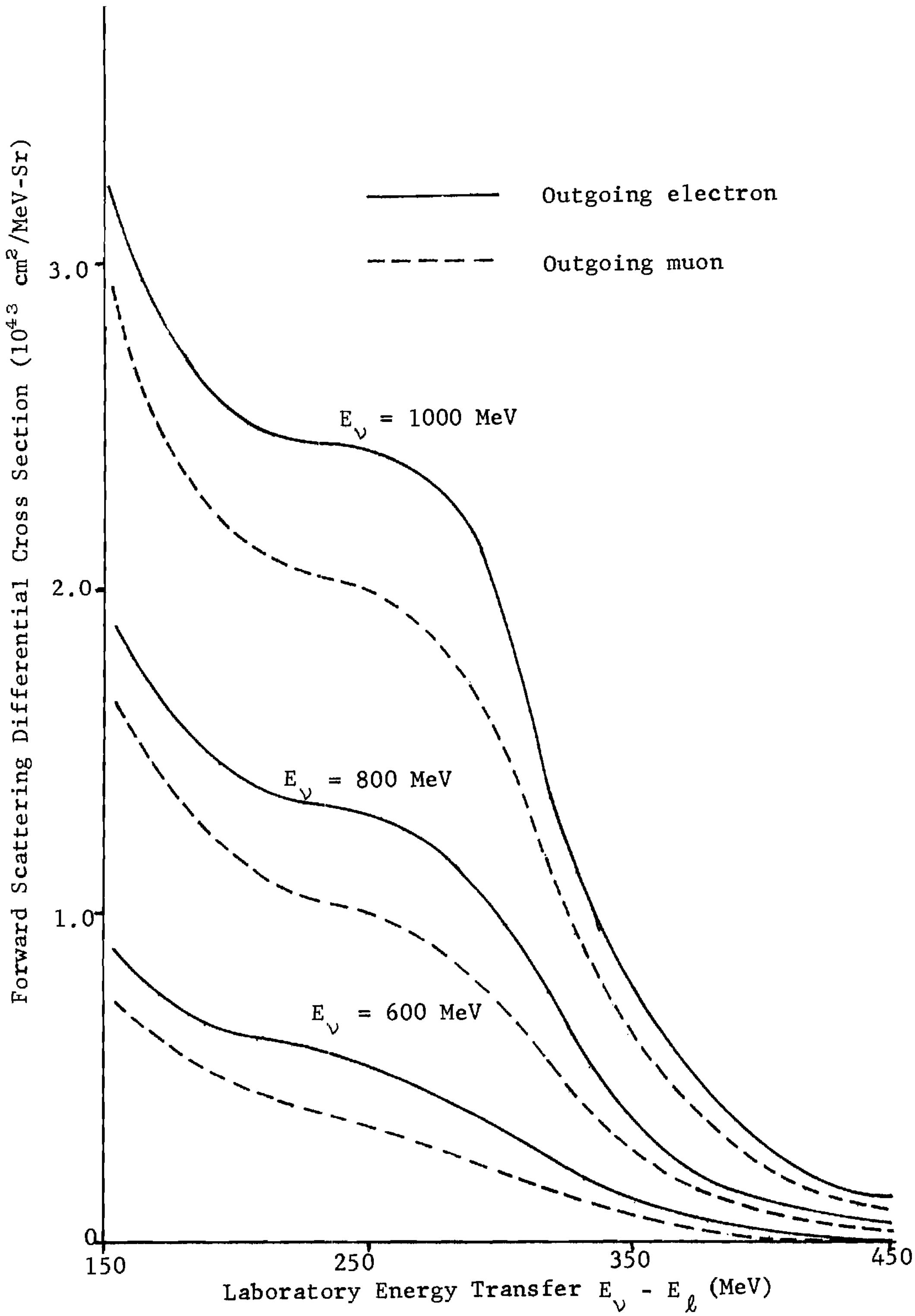

Figure 31. Differential Cross Section for E_ν = 600, 800, and 1000 MeV

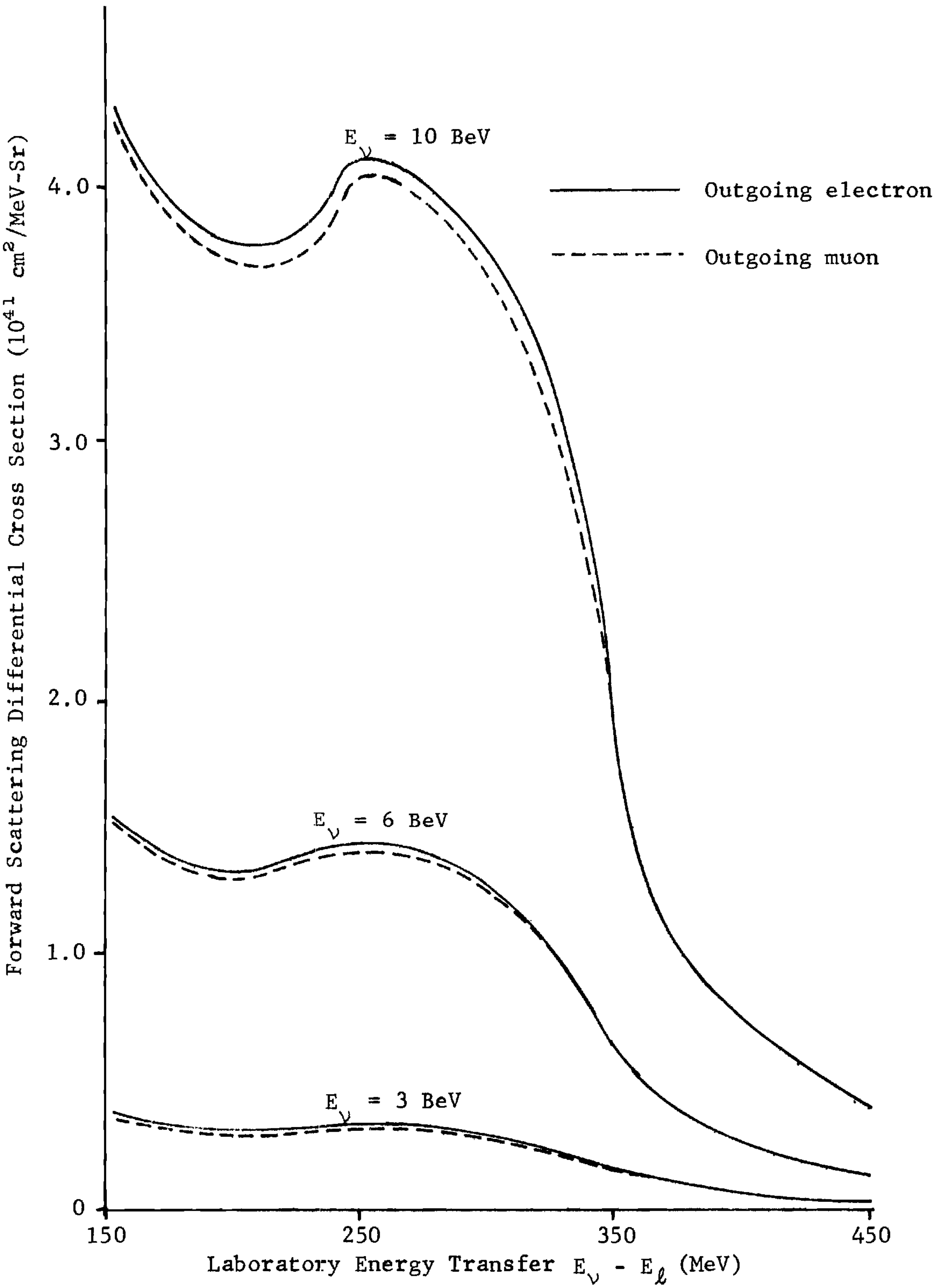

Figure 32. Differential Cross Section for E_ν = 3, 6, and 10 BeV

APPENDIX A

NOTATION, CONVENTIONS, AND CROSS SECTIONS

In this appendix, we list the important conventions used in this work in summary fashion. This is followed by a brief discussion of cross section computations, and a list of the three disintegration cross sections.

Conventions and Notation

Metric

We use the metric tensor

$$g = \begin{pmatrix} 1 & 0 & 0 & 0 \\ 0 & -1 & 0 & 0 \\ 0 & 0 & -1 & 0 \\ 0 & 0 & 0 & -1 \end{pmatrix}$$

Gamma Matrices

The gamma matrices have the anticommutation relations

$$\{\gamma_\alpha, \gamma_\beta\} = 2 g_{\alpha\beta}$$

For an explicit representation we use

$$\gamma_0 = \begin{pmatrix} I & 0 \\ 0 & -I \end{pmatrix} \quad , \quad \vec{\gamma} = \begin{pmatrix} 0 & \vec{\sigma} \\ -\vec{\sigma} & 0 \end{pmatrix} \quad ,$$

where

$$I = \begin{pmatrix} 1 & 0 \\ 0 & 1 \end{pmatrix}$$

and the σ_k are the Pauli spin matrices with explicit representations

$$\sigma_1 = \begin{pmatrix} 0 & 1 \\ 1 & 0 \end{pmatrix} \quad , \quad \sigma_2 = \begin{pmatrix} 0 & -i \\ i & 0 \end{pmatrix} \quad , \quad \sigma_3 = \begin{pmatrix} 1 & 0 \\ 0 & -1 \end{pmatrix} .$$

Slash Notation

We use the Feynman slash notation to represent

$$\gamma \cdot p = \not{p} = \gamma^0 p_0 - \vec{\gamma} \cdot \vec{p} .$$

Then, the momentum space Dirac equations for positive and negative energy free particles having spinors $u(p,s)$, $v(p,s)$ are

$$(\not{p} - m) u(p,s) = 0 = \bar{u}(p,s)(\not{p} - m) ,$$

and

$$(\not{p} + m) v(p,s) = 0 = \bar{v}(p,s)(\not{p} + m) = (\not{p} + m) C \bar{u}^T(p,s) .$$

Here,

$$\bar{u} = u^\dagger \gamma_0 \ , \ \bar{v} = v^\dagger \gamma_0 \ ,$$

and $\dagger$ denotes her metian adjoint.

Spinor Properties

The spinors are normalized according to

$$\bar{u}(p,s)\,u(p,s) = 1 = -\bar{v}(p,s)\,v(p,s) \ ,$$

and may be used to construct positive and negative energy projection operators via

$$\sum_{\pm s} u(p,s) \otimes \bar{u}(p,s) = \frac{\not{p}+m}{2m} \ ,$$

and

$$\sum_{\pm s} v(p,s) \otimes \bar{v}(p,s) = \frac{\not{p}-m}{2m} \ .$$

Cross Sections

The differential cross section for the scattering of two initial particles a and b to N final particles is given by

$$d\sigma = \frac{1}{|\vec{V}_a - \vec{V}_b|} N_a N_b \, |\mathcal{M}|^2 \prod_{i=1}^{N} \left\{ \frac{N_i \, d^3 p_i}{(2\pi)^3} \right\} (2\pi)^4 \, \delta^4\!\left(P_a + P_b - \sum_{i=1}^{N} P_i\right) . \qquad \text{(A-1)}$$

Here $|\vec{V}_a - \vec{V}_b|$ is the relative speed of the incoming particles, N denotes a kinematical normalization factor which is 1/2E for a boson and $(m/E)^{\frac{1}{2}}$ for a fermion, and $\mathcal{M}$ is the invariant Feynman amplitude for the process. In our case, $|\mathcal{M}|^2$ is the squared modulus of the quantity we have called the disintegration amplitude, summed over final particle spin states and averaged over initial particle spin states. We define the disintegration amplitudes in equations (I-1) and (I-6).

Pion Disintegration

For Pion disintegration we have, in the center-of-mass frame $\vec{V}_\pi = \vec{q}/q_0$ and $\vec{V}_d = \vec{d}/d_0$. Using $\vec{d} = -\vec{q}$, we then obtain

$$d\sigma = \frac{1}{16\pi^2}\frac{1}{(q_0+d_0)|\vec{q}|}|\mathcal{M}|^2 \frac{d^3P_1}{E_1}\frac{d^3P_2}{E_2}\,\delta^4(P_1+P_2-q-d). \qquad \text{(A-2)}$$

Integrating (A-2) over $\vec{P}_2$ results in the restriction $\vec{P}_1 = \vec{P}$, $\vec{P}_2 = -\vec{P}$, and integration over E_1 then requires $E_1 = E_2 = E = (q_0 + d_0)/2$. Using Tables 8 and 11 to construct the disintegration amplitude, and averaging over the three deuteron polarization states, we obtain

$$\left(\frac{d\sigma}{d\Omega_P}\right)_{CM} = \frac{m^2}{64\pi^2}\frac{|\vec{P}|}{E^2|\vec{q}|}\left\{\frac{1}{3}\sum_{\lambda}\sum_{\pm s_1}\sum_{\pm s_2}\left|\bar{u}(P_1)\sum_{i=1}^{6}\left(B_i^\pi + R_i^\pi\right)I_i^\pi C\,\bar{u}^T(P_2)\right|^2\right\}. \qquad \text{(A-3)}$$

The total cross section is then obtained as

$$\sigma_{CM} = \frac{1}{2}\int\left(\frac{d\sigma}{d\Omega_P}\right)_{CM} d\Omega_P \quad , \qquad \text{(A-4)}$$

where the factor of 1/2 is inserted because we have two identical final state particles. In general, the total cross section contains a factor of $1/m!$ for each set of m identical final state particles.

Photodisintegration

Here, the construction of the cross section is identical to that for pion disintegration, except for the photon polarization. Defining B_i^γ as the sum of the entries in Tables 12 and 13 (for both values of δ) and the appropriate term in V-16 when $i = 1$ or 5, and obtaining R_i^γ from Table 10, the differential cross section is

$$\left(\frac{d\sigma}{d\Omega_p}\right)_{CM} = \frac{m^2}{64\pi^2}\frac{|\vec{P}|}{E^2|\vec{q}|}\left\{\frac{1}{6}\sum_{\pm\rho}\sum_{\lambda}\sum_{\pm S_1 \pm S_2}\left|\bar{u}(P_1)\sum_{i=1}^{12}(B_i^{\tau}+R_i^{\tau})I_i^{\tau}C\bar{u}^T(P_2)\right|^2\right\}, \quad \text{(A-5)}$$

where ρ denotes photon polarization. The total cross section is then

$$\sigma_{CM} = \int\left(\frac{d\sigma}{d\Omega_p}\right)_{CM} d\Omega_p \quad , \qquad \text{(A-6)}$$

where there is no statistical factor for photodisintegration, since the neutron and proton are distinguishable. In this connection, we note that the differential cross section for pion disintegration will be symmetric about the center-of-mass scattering angle of 90 degrees, whereas the photodisintegration differential cross section will be asymmetric, in general.

Neutrino Disintegration

In this case $\vec{V}_\nu^c = \vec{P}_\nu^c/E_\nu^c$, $\vec{V}_d^c = \vec{d}^c/E_d^c$, and $\vec{d}^c = -\vec{q}^c = -(\vec{P}_\nu^c - \vec{P}_\ell^c)$. Then

$$\frac{1}{|\vec{V}_\nu^c - \vec{V}_d^c|} = \frac{E_d^c\, E_\nu^c}{|(E_d^c + E_\nu^c)\vec{P}_\nu^c - E_\nu^c \vec{P}_\ell^c|} = \frac{E_d^c}{E_d^c + E_\nu^c - |\vec{P}_\ell|} \qquad \text{(A-7)}$$

for forward scattering of the lepton, where we have used $E_\nu^c = |\vec{P}_\nu^c|$. Then we have

$$d\sigma = \frac{m^2 m_\nu m_\ell\, |\mathcal{M}|^2}{64\pi^5 E_\nu^c E_\ell^c (E_d^c + E_\nu^c - |\vec{P}_\ell^c|)} \frac{d^3P_1}{E_1}\frac{d^3P_2}{E_2} d^3P_\ell\ \delta^4(P_\nu + d - P_\ell - P_1 - P_2) . \qquad \text{(A-8)}$$

Integrating over $\vec{P}_2$ and E_1 , we get $\vec{P}_1 = \vec{P}$, $\vec{P}_2 = -\vec{P}$, and $E_1 = E_2 = E$, where $2E = E_\nu^c + E_d^c - E_\ell^c$. Integrating over the solid angle of the outgoing protons, introducing the statistical factor of 1/2, and using the symmetry of the disintegration amplitude about 90 degrees center-of-mass proton scattering angle, we obtain the cross section differential in muon momentum

$$d\sigma = \frac{m^2 m_\nu m_\ell}{32\pi^4 E_\nu^c E_\ell^c} \frac{|\vec{P}|\, d^3 P_\ell}{(E_d^c + E_\nu^c - |\vec{P}_\ell^c|)(E_d^c + E_\nu^c - E_\ell^c)} \int_0^1 |\mathcal{M}|^2 d\cos\theta_p \; . \qquad \text{(A-9)}$$

Then, using (VII-1), and

$$d^3 P_\ell^c = |\vec{P}_\ell^c|^2 d|\vec{P}_\ell^c|\, d\Omega_\ell^c = E_\ell^c\, |\vec{P}_\ell^c|\, dE_\ell^c\, d\Omega_\ell^c \; ,$$

we obtain

$$\left(\frac{d\sigma}{dE_\ell\, d\Omega_\ell}\right)_{cm} = \frac{m^2 m_\nu m_\ell}{32\pi^4 E_\nu^c} \frac{|\vec{P}|\,|\vec{P}_\ell^c|}{(E_d^c + E_\nu^c - |\vec{P}_\ell^c|)(E_d^c + E_\nu^c - E_\ell^c)} \times \qquad \text{(A-10)}$$

$$\int_0^1 \frac{1}{6} \sum_\lambda \sum_{\substack{\pm s_\nu, s_\lambda, \\ s_1, s_2}} \frac{G^2}{2} \Bigg| \mathcal{L}^\alpha U^\beta \bar{u}(P_1) \Bigg\{ -\frac{2}{e} \sum_{i=1}^{12} \left(B_i^{\gamma(V)} + R_i^{\gamma(V)}\right) I_{i\alpha\beta}^{\gamma}$$

$$+ \sum_{i=1}^{26} \left(B_i^A + R_i^A\right) I_{i\alpha\beta}^A \Bigg\} C\, \bar{u}^T(P_2) \Bigg|^2 d\cos\theta_p \; .$$

We remark that we have used the artifice of assigning the neutrino a nonzero mass m_ν . Then in the evaluation of the spin sums in (A-10), the factor $\mathcal{L}^\alpha = \bar{u}(P_\ell, S_\ell)\gamma^\alpha(1+\gamma_5)\, u(P_\nu, S_\nu)$ will lead to a projection operator

$$\frac{P_\nu - m_\nu}{2m_\nu}$$

and m_ν will not appear explicitly in the final result.

The transformation from the nucleon center-of-mass frame to the laboratory frame deserves comment. Following Hagedorn,[53] we write

$$\frac{\partial^2\sigma^L}{\partial E_\ell^L\partial\Omega_\ell^L} = \frac{\partial(E_\ell^c,\Omega_\ell^c)}{\partial(P_\ell^c,\Omega_\ell^c)}\frac{\partial(P_\ell^c,\Omega_\ell^c)}{\partial(P_\ell^c,\theta_\ell^c,\phi_\ell^c)}\frac{\partial(P_\ell^c,\theta_\ell^c,\phi_\ell^c)}{\partial(P_{1\ell}^c,P_{2\ell}^c,P_{3\ell}^c)}\frac{\partial(P_{1\ell}^c,P_{2\ell}^c,P_{3\ell}^c)}{\partial(P_{1\ell}^L,P_{2\ell}^L,P_{3\ell}^L)}\times \tag{A-11}$$

$$\frac{\partial(P_{1\ell}^L,P_{2\ell}^L,P_{3\ell}^L)}{\partial(P_\ell^L,\theta_\ell^L,\phi_\ell^L)}\frac{\partial(P_\ell^L,\theta_\ell^L,\phi_\ell^L)}{\partial(P_\ell^L,\Omega_\ell^L)}\frac{\partial(P_\ell^L,\Omega_\ell^L)}{\partial(E_\ell^L,\Omega_\ell^L)}\frac{\partial^2\sigma^c}{\partial E_\ell^c\partial\Omega_\ell^c}.$$

Here we use the Jacobian notation

$$\frac{\partial(x,y)}{\partial(u,v)} = \det\begin{pmatrix}\frac{\partial x}{\partial u} & \frac{\partial x}{\partial v}\\ \frac{\partial y}{\partial u} & \frac{\partial y}{\partial v}\end{pmatrix}$$

We have

$$\frac{\partial(E,\Omega)}{\partial(P,\Omega)} = \frac{P}{E} = 1\Big/\frac{\partial(P,\Omega)}{\partial(E,\Omega)} \tag{A-12}$$

$$\frac{\partial(P,\Omega)}{\partial(P,\theta,\phi)} = \sin\theta = 1\Big/\frac{\partial(P,\theta,\phi)}{\partial(P,\Omega)}$$

and

$$\frac{\partial(P_1,P_2,P_3)}{\partial(P,\theta,\phi)} = P^2\sin\theta = 1\Big/\frac{\partial(P,\theta,\phi)}{\partial(P_1,P_2,P_3)}.$$

For the Lorentz transformation, we define the total energy and momentum of the nucleon system by $\mathcal{E}$ and $\mathcal{P}$, where, in the laboratory,

$$\mathcal{E}^L = E_\nu^L + M_d - E_\ell^L\,,\quad \mathcal{P}^L = E_\nu^L - P_\ell^L\,, \tag{A-13}$$

and we introduce

$$\beta = \frac{\mathcal{P}^L}{\mathcal{E}^L} \quad , \quad \Upsilon = \frac{\mathcal{E}^L}{(\mathcal{E}^{L2} - \mathcal{P}^{L2})^{\frac{1}{2}}} \, . \qquad \text{(A-14)}$$

Then, for forward lepton scattering

$$P^c_{1\ell} = P^L_{1\ell} \, , \quad P^L_{2\ell} = P^c_{2\ell} \, , \quad P^c_{3\ell} = \Upsilon (P^L_{3\ell} - \beta E^L_\ell) .$$

Thus

$$\frac{\partial(P^c_{1\ell}, P^c_{2\ell}, P^c_{3\ell})}{\partial(P^L_{1\ell}, P^L_{2\ell}, P^L_{3\ell})} = \frac{\partial P^c_{3\ell}}{\partial P^L_{3\ell}} = \frac{\partial P^c_\ell}{\partial P^L_\ell} = \Upsilon \left[1 - \beta \frac{P^L_\ell}{E^L_\ell} \right] \cdot \qquad \text{(A-15)}$$

Then, combining (A-12) and (A-15), (A-11) becomes

$$\frac{\partial^2 \sigma^L}{\partial E^L_\ell \, \partial \Omega^L_\ell} = \frac{E^L_\ell \, P^L_\ell}{E^c_\ell \, P^c_\ell} \, \Upsilon \left(1 - \beta \frac{P^L_\ell}{E^L_\ell} \right) \frac{\partial^2 \sigma^c}{\partial E^c_\ell \, \partial \Omega^c_\ell} \quad , \qquad \text{(A-16)}$$

where Υ and β are defined in (A-13) and (A-14).

APPENDIX B

PHENOMENOLOGICAL WAVE FUNCTIONS FOR THE DEUTERON s AND d STATES

In reference 45, the deuteron s and d states are assigned the general forms

$$U(x) = N \cos \xi \left[1 - e^{-\beta\alpha(x-x_c)}\right] e^{-\alpha x}, \tag{B-1}$$

and

$$W(x) = N \sin \xi \left[1 - e^{-\gamma\alpha(x-x_c)}\right]^2 e^{-\alpha x} \cdot \tag{B-2}$$

$$\left[1 + 3\frac{(1-e^{-\gamma\alpha x})}{\alpha x} + 3\frac{(1-e^{-\gamma\alpha x})^2}{\alpha^2 x^2}\right],$$

where $x \geq x_c$. Here, the input parameters are the deuteron binding energy B, the triplet effective range r_e , the deuteron quadrupole moment Q, the deuteron magnetic moment μ , and a hard core radius x_c . The hard core radius is provided to allow an extra degree of freedom in fitting the triplet scattering data at higher energies. These physical parameters occur in (B-1) and (B-2) both directly and indirectly. The binding energy occurs in $\alpha = (mB)^{\frac{1}{2}}$. The triplet effective range appears in

$$N = \left(\frac{2\alpha}{1-\alpha r_e}\right)^{\frac{1}{2}} .$$

The magnetic moment is indirectly related to the d-state probability, and thus determines the angle ξ . Finally, for a given X_c , the quadrupole moment and overall normalization determine the parameters β and γ .

The deuteron binding energy is well determined at 2.226 MeV. There is an ambiguity in the triplet effective range, and in the determination of (B-1) and (B-2) two values are used, 1.704×10^{-13} cm and 1.734×10^{-13} cm. Ambiguity also occurs in the determination of P_d from μ , and provisions are made to examine the three possibilities $P_d = 3\%, 4\%$, and 5% . The measured quadrupole moment is $Q = 2.738 \times 10^{-27}$ cm^2, and three values for X_c are examined, $X_c = 0$, 0.4316×10^{-13} cm, and 0.5610×10^{-13} cm. The resulting parameter values are tabulated in Table B-1.

Of the input parameters which are given multiple values, the hard-core radius and the d-state probability have the most pronounced effect on the form of $u(x)$ and $W(X)$, the difference associated with the two values of r_e being insignificant.

Using the conversion $1/\alpha = 4.316 \times 10^{-13}$ cm, we can write (B-1) and (B-2) in the dimensionless form

$$u(y) = N \cos\xi \left[1 - e^{-\beta(y-y_c)}\right] e^{-y}, \tag{B-3}$$

and

$$W(y) = N \sin\xi \left[1 - e^{-\gamma(y-y_c)}\right]^2 e^{-y} \cdot \tag{B-4}$$

$$\left[1 + 3\frac{(1 - e^{-\gamma y})}{y} + 3\frac{(1 - e^{-\gamma y})^2}{y^2}\right],$$

where $y = \alpha x$. Introducing $s = r/\alpha$, where r is a momentum, we can write equations (IV-6) and (IV-7) as

Table B-1. Parameter Values for Deuteron s- and d-State Wave Functions

X_c (cm)	r_e (cm)	P_d(%)	β	γ	Sin ϵ	Cos ϵ
0	1.704×10^{-13}	3	4.860	2.494	.03232	.99948
		4	4.751	2.922	.02928	.99957
		5	4.647	3.275	.02754	.99962
	1.734×10^{-13}	3	4.741	2.505	.03192	.99949
		4	4.637	2.936	.02891	.99958
		5	4.536	3.289	.02720	.99963
0.4316×10^{-13}	1.704×10^{-13}	3	8.237	3.155	.02942	.99957
		4	7.961	3.798	.02666	.99965
		5	7.699	4.346	.02514	.99968
	1.734×10^{-13}	3	7.933	3.175	.02901	.99958
		4	7.675	3.814	.02634	.99965
		5	7.431	4.364	.02487	.99969
0.5610×10^{-13}	1.704×10^{-13}	3	10.223	3.413	.02873	.99958
		4	9.814	4.144	.02611	.99966
		5	9.433	4.771	.02471	.99970
	1.734×10^{-13}	3	9.774	3.436	.02832	.99960
		4	9.397	4.170	.02577	.99967
		5	9.045	4.799	.02438	.99970

$$U_0(S) = \frac{1}{\alpha^2}\int_{Y_c}^{\infty} u(Y)\, j_0(SY)\, Y\, dY \ , \tag{B-5}$$

and

$$W_2(S) = \frac{1}{\alpha^2}\int_{Y_c}^{\infty} W(Y)\, j_2(SY)\, Y\, dY \tag{B-6}$$

Using the definition given in (IV-8), we can apply the transformations (B-5) and (B-6) to the wave functions given in (B-3) and (B-4). We obtain

$$U_0(r) = \frac{N\cos\xi\, e^{-Y_c}}{\alpha^2 S}\Big\{ \sin(SY_c)\Big[\frac{1}{1+S^2} - \frac{1+\beta}{(1+\beta)^2+S^2}\Big] \tag{B-7}$$

$$+ S\cos(SY_c)\Big[\frac{1}{1+S^2} - \frac{1}{(1+\beta)^2+S^2}\Big]\Big\} \ ,$$

and

$$W_2(S) = \frac{N\sin\xi}{\alpha^2}\Big\{ e^{-Y_c}\Big[\frac{\sin(SY_c)}{S}\Big(-\frac{1}{1+S^2} + \frac{2(1+\gamma)}{S^2+(1+\gamma)^2} \tag{B-8}$$

$$-\frac{1+2\gamma}{S^2+(1+2\gamma)^2} + \frac{3\gamma^2}{S^2 Y_c}(1-e^{-\gamma Y_c})^2\Big) + \cos(SY_c)\Big(-\frac{1}{1+S^2}$$

$$+\frac{2}{S^2+(1+\gamma)^2} - \frac{1}{S^2+(1+2\gamma)^2}\Big)\Big] + g(1+\gamma,1)\Big[\frac{3}{S^3}(1+\gamma)^3$$

$$-\frac{9}{2S^3}(1+\gamma)^2 + \frac{3}{S}(1+\gamma) - \frac{3}{2S} + e^{\gamma Y_c}\Big(\frac{3}{S^3}(1+\gamma)^3$$

$$-\frac{9}{S^3}(1+\gamma)^2 + \frac{6}{S^3}(1+\gamma) + \frac{3}{S}(1+\gamma) - \frac{3}{S}\Big)\Big] + g(1+2\gamma,1)\times$$

$$\Big[-\frac{3}{2S^3}(1+2\gamma)^3 - \frac{3}{2S}(1+2\gamma) + e^{\gamma Y_c}\Big(-\frac{6}{S^3}(1+2\gamma)^3 + \cdots$$

(continued)

$$+ \frac{9}{S^3}(1+2\gamma)^2 - \frac{6}{S}(1+2\gamma) + \frac{3}{S}\Big) + e^{2\gamma y_c}\Big(-\frac{3}{2S^3}(1+2\gamma)^3$$

$$+ \frac{9}{2S^3}(1+2\gamma)^2 - \frac{3}{S^3}(1+2\gamma) - \frac{3}{2S}(1+2\gamma) + \frac{3}{2S}\Big)\Big]$$

$$+ g(1+3\gamma, 1)\Big[\Big(\frac{3}{S^3}(1+3\gamma)^3 + \frac{3}{S}(1+3\gamma)\Big)e^{\gamma y_c}$$

$$+\Big(\frac{3}{S^3}(1+3\gamma)^3 - \frac{9}{2S^3}(1+3\gamma)^2 + \frac{3}{S}(1+3\gamma) - \frac{3}{2S}\Big)e^{2\gamma y_c}\Big]$$

$$+ g(1+4\gamma, 1)\Big(-\frac{3}{2S^3}(1+4\gamma)^3 - \frac{3}{2S}(1+4\gamma)\Big)e^{2\gamma y_c}\Big\} ,$$

where

$$g(a,1) = \int_{y_c}^{\infty} \frac{e^{-ay}\sin(Sy)\,dy}{y} . \tag{B-9}$$

In the limit $y_c \to 0$, we have

$$\underset{(y_c=0)}{U_0(S)} = \frac{N\cos\xi}{\alpha^2}\left[\frac{1}{1+S^2} - \frac{1}{(1+\beta)^2+S^2}\right] , \tag{B-10}$$

and

$$\underset{(y_c=0)}{W_2(S)} = \frac{N\sin\xi}{\alpha^2}\Big\{-\frac{1}{S^2+1} + \frac{2}{S^2+(1+\gamma)^2} - \frac{1}{S^2+(1+2\gamma)^2} \tag{B-11}$$

$$+\tan^{-1}\Big(\frac{S}{1+\gamma}\Big)\Big[\frac{6}{S^3}(1+\gamma)^3 - \frac{27}{2S^3}(1+\gamma)^2 + \frac{6}{S^3}(1+\gamma) + \frac{6}{S}(1+\gamma) - \frac{9}{2S}\Big]$$

$$+\tan^{-1}\Big(\frac{S}{1+2\gamma}\Big)\Big[-\frac{9}{S^3}(1+2\gamma)^3 + \frac{27}{2S^3}(1+2\gamma)^2 - \frac{3}{S^3}(1+2\gamma) - \frac{9}{S}(1+2\gamma + \frac{9}{2S}\Big] + \cdots$$

(continued)

$$+ \mathrm{Tan}^{-1}\left(\frac{S}{1+3\gamma}\right)\left[\frac{6}{S^3}(1+3\gamma)^3 - \frac{9}{2S^3}(1+3\gamma)^2 + \frac{6}{S}(1+3\gamma) - \frac{3}{2S}\right]$$

$$+ \mathrm{Tan}^{-1}\left(\frac{S}{1+4\gamma}\right)\left[-\frac{3}{2S^3}(1+4\gamma)^3 - \frac{3}{2S}(1+4\gamma)\right]\Bigg\} .$$

APPENDIX C

BEHAVIOR OF THE DERIVATIVES OF THE dNN VERTEX INVARIANTS NEAR THE MASS SHELL

We begin by considering the relation between the variables t and $\vec{r}$. At the dNN vertex the deuteron enters with momentum d and the two nucleons leave with momenta p and p' , and we take p to be off the mass shell, and $t = p^2$. We have

$$d = p + p' \quad , \quad r = \frac{p - p'}{2} \tag{C-1}$$

and thus,

$$d^2 = M_d^2 = p^2 + 2\,p\cdot p' + m^2 \ , \tag{C-2}$$

and

$$4r^2 = p^2 - 2\,p\cdot p' + m^2 . \tag{C-3}$$

Thus, we obtain

$$t = 2r^2 + \frac{M_d^2}{2} - m^2 . \tag{C-4}$$

Now,

$$r_0 = \frac{M_d}{2} - (m^2 + \vec{r}^{\,2})^{\frac{1}{2}} \ , \tag{C-5}$$

$$r_0^2 = \frac{M_d^2}{4} - M_d\,(m^2+\vec{r}^{\,2})^{\frac{1}{2}} + m^2 + \vec{r}^{\,2}\,, \tag{C-6}$$

and

$$r^2 = r_0^2 - \vec{r}^{\,2} = \frac{M_d^2}{4} - M_d\,(m^2+\vec{r}^{\,2})^{\frac{1}{2}} + m^2. \tag{C-7}$$

Thus, we can use (C-7) to rewrite (C-4) as

$$t = M_d^2 + m^2 - 2M_d\,(m^2+\vec{r}^{\,2})^{\frac{1}{2}}\,. \tag{C-8}$$

Then, on the mass shell, $t = m^2$ and

$$M_d^2 - 2M_d\,(m^2+\vec{r}^{\,2})^{\frac{1}{2}} = 0\,. \tag{C-9}$$

To be consistent with the approximations made throughout this work, we expand (C-9) to first order, and obtain

$$\vec{r}^{\,2} + \alpha^2 = 0\,, \quad |\vec{r}| = i\alpha\,. \tag{C-10}$$

To examine the derivatives of the dNN vertex invariants near the mass shell, we use the chain rule to write

$$\frac{dF}{dt} = \frac{dF}{d|\vec{r}|}\,\frac{d|\vec{r}|}{dt}\,. \tag{C-11}$$

We may use (C-8), with $|\vec{r}| = r$, to write

$$\frac{dr}{dt} = -\frac{(m^2+\vec{r}^{\,2})^{\frac{1}{2}}}{2rM_d} \longrightarrow \frac{i\,(m^2-\alpha^2)}{2\alpha M_d} \tag{C-12}$$

on the mass shell. Thus the behavior of dF/dt for $t \to m^2$ is determined by the behavior of dF/dr for $r \to i\alpha$.

Now, examination of equations (B-10) and (B-11) for $U_0(r)$ and $W_2(r)$ shows that, near $r = i\alpha$, they have the forms

$$U_0(r) \longrightarrow \frac{A}{r^2+\alpha^2} \tag{C-13}$$

and

$$W_2(r) \longrightarrow \frac{B}{r^2+\alpha^2} \tag{C-14}$$

and all of the other terms in these functions are analytic (possess derivatives of all orders) at $r = i\alpha$. Thus, near the mass shell, F and G may be written in the form

$$F = N\,(r^2+\alpha^2)(a+br^2)\left(\frac{A-B}{r^2+\alpha^2}\right), \tag{C-15}$$

and

$$G = \frac{N\,(r^2+\alpha^2)}{r^2}\left[1 + C\,(r^2+\alpha^2)\right]\frac{B}{r^2+\alpha^2} + \frac{F}{2}, \tag{C-16}$$

where we have used the prescriptions for F and G given in equations (IV-40) and (IV-41).

From the equations (C-15) and (C-16), it is clear that $dF/dt\,|_{m^2}$

and $dG/dt|_{m^2}$ exist. Then, using either of the prescriptions (IV-34) or (IV-39), it follows that $dH/dt|_{m^2}$ and $dI/dt|_{m^2}$ exist.

BIBLIOGRAPHY*

1. N. Austern, Phys. Rev. 100, 1522 (1955).

2. S. Barshay, Phys. Rev. Lett. 17, 49 (1966).

3. D. J. George, Phys. Rev. 167, 1357 (1968).

4. F. Gross, Phys. Rev. 140, B410 (1965).

5. R. P. Feynman, M. Gell-Mann, Phys. Rev. 109, 193 (1958).

6. M. Gell-Mann, M. Lévy, Nuovo Cimento 16, 705 (1960).

7. Y. Nambu, Phys. Rev. Lett. 4, 380 (1960).

8. K. C. Chou, Zh. Eksperim. i Teor. Fiz. (English Transl.: Soviet Phys. - JETP 12, 492 (1961)).

9. S. L. Adler, Y. Dothan, Phys. Rev. 151, 1267 (1966).

10. J. D. Bjorken, S. D. Drell, Relativistic Quantum Mechanics, McGraw-Hill, New York, 1964.

11. B. Sakita, Phys. Rev. 127, 1800 (1962).

12. M. LeBellac, F. M. Renard, J. Tran Thanh Van, Nuovo Cimento 33, 594 (1964).

13. B. Sakita, C. J. Goebel, Phys. Rev. 127, 1787 (1962).

14. D. J. George, Thesis, Stanford University, Stanford, California, 1967.

15. R. Blankenbecler, L. F. Cook, Jr., Phys. Rev. 119, 1745 (1960).

16. W. Heisenberg, Z. Physik. 77, 1 (1932).

17. R. H. Dalitz, D. G. Sutherland, Phys. Rev. 146, 1180 (1966).

18. G. Mohan, S. C. Agarwal, Nuovo Cimento 37, 431 (1964).

---

*Abbreviations used herein conform to Science Abstracts, Section A, Physics Abstracts.

BIBLIOGRAPHY (Continued)

19. G. Breit, E. Wigner, Phys. Rev. 49, 519 (1936).

20. E. Ferrari, F. Selleri, Nuovo Cimento, Suppl. 24, 453 (1962); Nuovo Cimento 27, 1450 (1963).

21. M. E. Rose, Elementary Theory of Augular Momentum, John Wiley & Sons, Inc., New York, 1957.

22. A. C. Hearn, Comm. Amer. Comp. Machy. 9, 572 (1966).

23. E. E. Salpeter, H. A. Bethe, Phys. Rev. 84, 1232 (1951).

24. J. M. Blatt, V. F. Weisskopf, Theoretical Nuclear Physics, John Wiley & Sons, Inc., New York, 1952.

25. S. S. Gershtein, I. B. Zeldovitch, Zh. Eksperim i Teor. Fiz. (English Transl.: Soviet Phys. - JETP 2, 576 (1956)).

26. E. Fermi, Z. Physik 88, 161 (1934).

27. T. D. Lee, C. N. Yang, Phys. Rev. 104, 354 (1956).

28. C. S. Wu, E. Ambler, R. Hayward D. Hoppes, R. Hudson, Phys. Rev. 105, 1413 (1957).

29. M. Goldhaber, L. Grodzins, A. W. Sunyar, Phys. Rev. 109, 1015 (1958).

30. M. T. Burgy, V. E. Krohn, T. B. Novey, G. R. Ringo, V. L. Telegdi, Phys. Rev. 120, 1827 (1960).

31. R. E. Marshak, Sudershan, Phys. Rev. 109, 1860 (1958).

32. M. L. Goldberger, S. B. Treiman, Phys. Rev. 110, 1178 (1958); Phys. Rev. 111, 354 (1958).

33. R. Durbin, H. Loar, J. Steinberger, Phys. Rev. 84, 581 (1951).

34. A. M. Sachs, H. Winick, B. A. Wooten, Phys. Rev. 109, 1733 (1958).

35. H. L. Stadler, Phys. Rev. 96, 496 (1954).

36. M. G. Meshcheriakov, B. S. Neganov, Dokl. Akad. Nauk. SSSR 100, 617 (1955).

37. C. Richard-Serre, Etude De La Reaction Pour Des Pions D'Energie Comprise Entre 143 Et 264 MeV, CERN - 68 - 40 (December 1968).

BIBLIOGRAPHY (Concluded)

38. B. S. Neganov, L. B. Parfenov, Zh. Eksperim. i Teor. Fiz. (English Transl.: Soviet Phys. - JETP 7, 528 (1958)).

39. K. H. Kissler, R. Kose, W. Paul, K. Stockhorst, Proceedings of the International Symposium on Electron and Photon Interactions at High Energy, Hamburg, 1965 (Unpublished).

40. S. Kikuchi, Phys. Rev. 85, 1062 (1952).

41. E. A. Whalin, B. D. Schriever, A. O. Hanson, Phys. Rev. 101, 377 (1956).

42. J. C. Keck, A. V. Tollestrup, Phys. Rev. 101, 360 (1956).

43. D. R. Dixon, K. C. Pandtel, Phys. Rev. 104, 1730 (1956).

44. J. C. Keck, R. M. Littauer, G. K. O'Neil, A. M. Perry, W. M. Woodward, Phys. Rev. 93, 827 (1954).

45. L. Hulthén, M. Sugawara, Handbuch der Physik 39, 1 (1957).

46. W. R. Frazier, Elementary Particles, Prentice Hall, Inc. Englewood Cliffs, New Jersey, 1966.

47. I. J. McGee, Phys. Rev. 158, 1500 (1967).

48. F. Gross, Phys. Rev. 134, B405 (1964).

49. T. A. Griffy, L. I. Schiff, Pure and Applied Physics 25-1, 341, Academic Press, New York, 1967.

50. G. Barton, Dispersion Techniques in Field Theory, W. A. Benjamin, Inc., New York, 1965.

51. S. L. Adler, Phys. Rev. 135, B963 (1964).

52. K. V. Vasvada, Ann. Phys. 34, 191 (1965).

53. R. Hagedorn, Relativistic Kinematics, W. A. Benjamin, Inc., New York, 1963.

VITA

William Michael Wynn was born in Denison, Texas on June 19, 1939. He is the son of Gerald Dekata and Glenna Joyce Wynn.

He attended public schools in Atlanta, Georgia, and graduated from J. C. Murphy High School in 1957. In 1959 he received an Associate in Science Degree from Southern Technical Institute, graduating With Honor. In 1963, he received the Bachelor of Science Degree in Physics, With Honor, from the Georgia Institute of Technology. He received Honorable Mention for the William K. Pursley Award for the Outstanding Physics Major in his graduating class.

Upon graduation, he entered graduate school at the Georgia Institute of Technology, where he was employed from 1963 to 1970 as a Graduate Teaching Assistant. In 1970, he joined the U. S. Naval Ship Research and Development Laboratory as a Research Physicist.

He married the former Elizabeth Diane Baxter on March 26, 1962. They have two adopted children, Christian Robin and Michael Todd.